1993

Photochemistry of Nitrous Acid and Nitrite Ion

Kathryn E. Shanks '93
Illinois Wesleyan University

PHOTOCHEMISTRY OF NITROUS ACID AND NITRITE ION

Kathryn E. Shanks

Advisor: Timothy R. Rettich

Chemistry 499 Thesis

Illinois Wesleyan University

May 6, 1993

Approval Page

"Photochemistry of Nitrous Acid and Nitrite Ion"

by Kathryn E. Shanks

A paper submitted in partial fulfillment of the requirements for Chemistry 499 and Honors in Chemistry

Approved, Honors Committee:

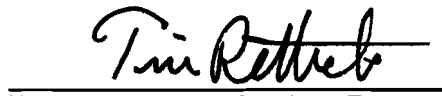

Dr. Timothy R. Rettich, Research Advisor

Dr. David N. Bailey

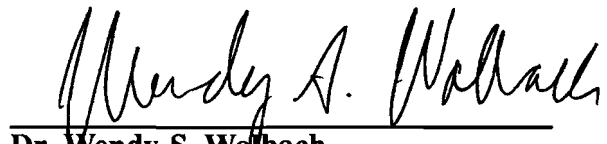

Dr. Wendy S. Wolbach

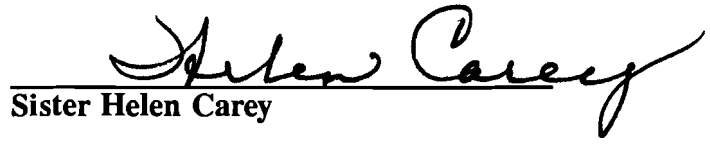

Sister Helen Carey

Illinois Wesleyan University

1993

"I do not know what I may appear to the world; but to myself I seem to have been only like a boy playing on the sea-shore, and diverting myself in now and then finding a smoother pebble or prettier shell than ordinary, whilst the great ocean of truth lay all undiscovered before me."

-Sir Isaac Newton

INDEX

LIST OF FIGURES

LIST OF TABLES

ABSTRACT

Research is currently underway to elucidate the photochemical decomposition mechanism of nitrous acid and nitrite ion in aqueous and non-aqueous media. The quantum yield of the photochemical disappearance of nitrous acid and nitrite, as a function of pH and nitrous acid/nitrite ion concentration ratios, was examined. Spectroscopic studies have been done with nitrite ion in various aprotic organic solvents. Similar work has been started with molecular nitrous acid that was produced in aqueous solution and then extracted into organic solvents. These organic solvents were employed in order to study the quantum yield with respect to NO_2^- and HONO without the complications of the acid dissociation equilibrium seen in aqueous solutions. Other work includes the product analysis of hydroxyl radical scavenging reactions.

INTRODUCTION AND THEORY

The purpose of this research is to investigate the photochemistry of the nitrous acid (HONO)/nitrite ion (NO_2^-) system in both aqueous and non-aqueous (non-equilibrium) media. The quantum yield of the photochemical disappearance of each species (HONO and NO_2^-) is desired. In addition, quantitative analysis of the reaction products by spectroscopic, chromatographic, and other analytical techniques is undertaken.

This research is significant because it adds to the limited chemical knowledge about nitrous acid. Nitrous acid is of interest because it is a known producer of atmospheric hydroxyl radical.[1] Hydroxyl radical, in turn, with hydrogen peroxide and ozone is involved in the photochemical oxidation of sulfur dioxide and hydrocarbons in the atmosphere.[2,3] The oxides of nitrogen, including nitrous acid and nitrite ion, are also well known catalysts in the production of sulfuric acid, the major component of acid rain. So, any additional understanding of nitrous acid chemistry could in fact be the key to solving several interrelated environmental problems including depletion of the ozone layer, formation of smog, and production of acid rain.

Nitrous acid appears to undergo several different types of reactions including thermal reactions and photochemical reactions. Of the thermal reactions, some were studied in the gaseous phase while others were done in the liquid phase. The gas phase reactions of nitrous acid were first studied by Cox and Atkins in 1973.[4] They proposed that nitrous acid is in equilibrium with nitric

oxide and nitrogen dioxide as shown in equation 1:

$$NO(g) + NO_2(g) + H_2O(g) \rightleftharpoons 2HONO(g) \quad (1)$$

In aqueous medium, there are two recognized equilibria, the acid dissociation reaction shown in equation 2:

$$HONO(aq) + H_2O \rightleftharpoons H_3O^+(aq) + NO_2^-(aq) \quad (2)$$

and the dehydration reaction shown in equation 3:

$$2HONO(aq) \rightleftharpoons N_2O_3(aq) + H_2O \quad (3)$$

Another decomposition reaction was actively studied by Ray *et al.*[5] and is shown in equation 4:

$$3HONO(aq) \rightleftharpoons 2NO(aq) + H_3O^+(aq) + NO_3^-(aq) \quad (4)$$

The dehydration and acid dissociation reactions rapidly achieve equilibrium, but the decomposition by reaction 4 has a half life of about 14 hours at 0°C. Therefore, the rate of decomposition is significant and must be accounted for in any photochemical studies.

The first kinetic studies of reaction 4 were performed by Montemartini in 1890.[6] He found the stoichiometry and kinetic order with respect to nitrous acid. He determined that the reaction showed first order kinetics at low nitrous acid concentrations and 2.5 order at high nitrous acid levels. The low concentration work has been reproducible.[5,7,8] The high concentration results, however, have not been confirmed. Reported values for the kinetic order have varied from 2.5 up to

4.[7,8,9]

Two possible decomposition mechanisms for the higher nitrous acid concentrations were proposed by Abel and Schmid in 1928.[9] They are:

$$4HONO(aq) \rightleftharpoons 2NO(aq) + 2H_2O + N_2O_4(aq) \quad (5)$$

$$N_2O_4(aq) + 2H_2O \rightleftharpoons HONO(aq) + H_3O^+(aq) + NO_3^-(aq) \quad (6)$$

and

$$2HONO(aq) \rightleftharpoons N_2O_3(aq) + H_2O \quad (7)$$

$$N_2O_3(aq) \rightleftharpoons NO(aq) + NO_2(aq) \quad (8)$$

$$2NO_2 \rightleftharpoons N_2O_4(aq) \quad (9)$$

$$N_2O_4(aq) + 2H_2O \rightleftharpoons HONO(aq) + H_3O^+(aq) + NO_3^-(aq) \quad (10)$$

Thie proposed another possible mechanism in 1947:[10]

$$2HONO(aq) \rightleftharpoons NO(aq) + NO_2(aq) + H_2O \quad (11)$$

$$2NO_2(aq) \rightleftharpoons N_2O_4(aq) \quad (12)$$

$$N_2O_4(aq) + 2H_2O \rightleftharpoons HONO(aq) + NO_3^-(aq) + H_3O^+(aq) \quad (13)$$

All three of these decomposition mechanisms share the same final step, the hydrolysis of dinitrogen tetroxide. The later studies of Usubillaga[7], Rettich[8], and Park *et al.*[11] fail to distinguish between these mechanisms.

Nitrous acid can also undergo reactions by photochemical means. Again,

studies have been done in both the gaseous and the liquid phases. The gaseous photochemical studies were performed by Cox and Atkins in 1973.[4] They used 330 to 380 nm light and as a result of their work they proposed two primary photodissociations shown in equations 14 and 15:

$$HONO(g) + h\nu \rightarrow NO(g) + OH(g) \quad \textbf{(14)}$$

$$HONO(g) + h\nu \rightarrow H(g) + NO_2(g) \quad \textbf{(15)}$$

Cox and Atkins showed that the total primary quantum yield for these two dissociations is about one and they estimated that the yield for reaction 15 is half that of reaction 14. From this information, Cox[12] proposed a mechanism as follows:

$$HONO(g) + h\nu \rightarrow NO(g) + OH(g) \quad \textbf{(16)}$$

$$OH(g) + NO(g) + M \rightarrow HONO(g) + M \quad \textbf{(17)}$$

$$OH(g) + NO_2 + M \rightarrow HNO_3(g) + M \quad \textbf{(18)}$$

$$OH(g) + HONO(g) \rightarrow H_2O + NO_2(g) \quad \textbf{(19)}$$

From further studies, Cox concluded that reaction 15 contributes less than 10% to the overall reaction and that the primary quantum yield for reaction 14 is 0.92 $\pm$ 0.16.

Nash proposed another gas phase photolysis based solely upon reaction 14 as the initiation step:[13]

$$HONO(g) + h\nu \rightarrow OH(g) + NO(g) \quad (20)$$

$$OH(g) + HONO(g) \rightarrow H_2O + NO_2(g) \quad (21)$$

No further mechanisms for nitrous acid gas phase photolysis have been suggested even though additional studies have been done.

A few aqueous phase photochemical investigations have been performed. Murty and Dhar photolyzed solutions of nitrous acid at wavelengths greater than 445 nm and reported quantum yields up to 15.[14] However, these studies were performed above the region where nitrous acid absorbs readily (400-300 nm).

Rettich[8] suggested that the above decomposition was due to the thermal reaction produced by the heating of the light source. Accounting for factors such as ionic strength, pH, nitrite and nitrous acid concentrations, water source, light source, and reaction vessel geometry, Rettich studied the photochemistry of nitrous acid at 1°C. He discovered that the quantum yield for nitrous acid disappearance showed a linear increase from 0 at zero concentration to 0.14 at 0.14 M nitrous acid. However, for concentrations greater than 0.14 M the quantum yield remained constant at 0.14. Rettich also calculated the quantum yield of escape from the solvent cage as 0.095. The reaction of nitrous acid with the solvent cage is as follows:

$$HONO(aq) + h\nu \rightarrow [HONO^*] \rightarrow [OH + NO] \rightarrow OH(aq) + NO(aq) \quad (22)$$

The significant recombination of the hydroxyl radical and nitric oxide within the solvent cage is responsible for the low primary quantum yield.[8]

Since nitrous acid is in equilibrium with nitrite ion, if nitrous acid is of interest then by inference the reactions of nitrite ion may also be important. Holmes determined in 1926 that nitrite ion undergoes no net photolysis in aqueous solution.[15] This result was also confirmed later by Treinin and Hayon[16] in 1970 using a cadmium lamp(228.8 nm). This reaction is believed to occur by the following primary process:

$$NO_2^- + h\nu \rightarrow NO + O^- \qquad (23)$$

which is analogous to the photochemical reaction of organic nitrites. They proposed the following mechanism under conditions of air saturated solutions with the presence of bromide and carbonate ions:

$$NO_2^- + h\nu \rightarrow NO + O^- \qquad (24)$$

$$O^- + H_2O \rightleftharpoons {}^\bullet OH + OH^- \qquad (25)$$

The bromide and carbonate ions then react with the hydroxyl radical produced in reaction 25 in the manner below:

$$Br^- + {}^\bullet OH \rightarrow Br^\bullet + OH^- \qquad (26)$$

$$Br^\bullet + Br^- \rightleftharpoons Br_2^- \qquad (27)$$

and

$$CO_3^{2-} + {}^\bullet OH \rightarrow {}^\bullet CO_3^- + OH^- \qquad (28)$$

These mechanisms are possible due to the fact that spectra indicate the presence

of the transitory radical species, Br_2^- and CO_3^-.

The $\bullet O^-$ and •OH radicals produced in reactions 24 and 25 can further react with additional nitrite ion in solution or with oxygen gas (O_2) present in the air saturated solutions:

$$\bullet OH + NO_2^- \rightarrow NO_2 + OH^- \quad (29)$$

$$\bullet O^- + NO_2^- + H_2O \rightarrow NO_2 + 2OH^- \quad (30)$$

$$\bullet O^- + O_2 \rightleftharpoons \bullet O_3^- \quad (31)$$

The absence of net photolysis of nitrite ion is attributed to the presence of efficient back reactions.[15] These reactions include the hydrolysis of several possible nitrogen oxide products from reactions 24, 29, and 30. According to Treinin and Hayon, the overall stoichiometry is

$$NO_2 + NO + H_2O \rightleftharpoons 2NO_2^- + 2H^+ \quad (32)$$

Contrary to its nonreactivity in aqueous solution, nitrite ion does show net photolysis in natural (sea) water. In 1981, Zafiriou and McFarland[17] reported that nitrite exhibited the following photolysis with sunlight:

$$NO_2^- + HOH + h\nu \rightleftharpoons NO + \bullet OH + OH^- \quad (33)$$

Zafiriou and Bonneau[18] have since calculated the quantum yield of the reaction in terms of the production of hydroxyl radical. They discovered that the quantum yield was dependent upon wavelength and temperature but independent of pH, trapping agent, O_2 pressure, and ionic strength.

The following mechanism was proposed by Zafiriou for the net photolysis of nitrite where the square brackets indicate species within the solvent cage:[18]

$$NO_2^- + h\nu \rightarrow NO_2^{-*} \quad (34)$$

$$NO_2^{-*} \rightarrow NO_2^- + heat \quad (35)$$

$$NO_2^{-*} \rightarrow [NO, O^-, nH_2O] \quad (36)$$

$$[NO, O^-, nH_2O] \rightarrow NO + O^- + nH_2O \quad (37)$$

$$[NO, O^-, nH_2O] \rightarrow NO_2^- + nH_2O \quad (38)$$

$$[NO, O^-, nH_2O] \rightarrow [NO, OH, OH^-, (n-1)H_2O] \quad (39)$$

$$[NO, OH, OH^-, (n-1)H_2O] \rightarrow HONO + (n-1)H_2O + OH^- \quad (40)$$

$$[NO, OH, OH^-, (n-1)H_2O] \rightarrow NO + OH + OH^- + (n-1)H_2O \quad (41)$$

The quantum yield for the loss of nitrite varied from 2 to 27% per day for different water samples studied. This variation was attributed to 1) sensitized photolysis, 2) direct photolysis with a quantum yield sensitive to pH, oxygen concentration, salinity, temperature, and wavelength, and 3) regeneration of nitrite by secondary reactions of NO.[18]

Hydroxyl radical is of key interest in the reactions of both nitrous acid and nitrite ion, therefore, its pathways of production and destruction are of importance. It is well known that hydrogen peroxide thermally decomposes to

form oxygen gas and water as shown in reaction 42:[19]

$$2H_2O_2 \rightarrow 2H_2O + O_2 \quad (42)$$

Abel proposed a mechanism for the above reaction as follows:[20]

$$H_2O_2 \rightleftharpoons HO_2^- + H^+ \quad (43)$$

$$HO_2^- + H_2O_2 \rightarrow HO_2 + OH^- + {}^\bullet OH \quad (44)$$

$$HO_2 + {}^\bullet OH \rightarrow H_2O + O_2 \quad (45)$$

Hydrogen peroxide forms hydroxyl radicals in the presence of both light and a metal catalyst. In 1952, Hunt and Taube suggested two possible mechanisms for the photochemical dissociation of H_2O_2:[21]

Scheme I:

$$H_2O_2 + h\nu \rightarrow 2HO^\bullet \quad (46)$$

$$HO^\bullet + H_2O_2 \rightleftharpoons HO_2 + H_2O \quad (47)$$

$$2HO_2 \rightleftharpoons H_2O_2 + O_2 \quad (48)$$

Scheme II:

$$H_2O_2 + h\nu \rightarrow H_2O + O \quad (49)$$

$$O + H_2O_2 \rightleftharpoons OH + HO_2 \quad (50)$$

$$OH + H_2O_2 \rightleftharpoons HO_2 + H_2O \quad (51)$$

$$2HO_2 \rightleftharpoons H_2O_2 + O_2 \quad (52)$$

Mansour[22] discovered that the decomposition of hydrogen peroxide was linear with respect to time of photolysis in a general experiment performed with benzene in sunlight. He noted that the decomposition increased with lower pH and high levels of water impurities, particularly metal ions.

In 1934, Haber characterized the decomposition of H_2O_2 in the presence of a metal catalyst.[23] He proposed the following mechanism:

$$M^+ + H_2O_2 \rightarrow M^{2+} + OH^- + \bullet OH \quad (53)$$

$$M^{2+} + HO_2^- \rightarrow M^+ + HO_2 \quad (54)$$

Ferric and cupric ions are the most commonly used catalysts for hydroxyl radical production.

Unlike nitrous acid, hydroxyl radical cannot be determined using standard ultra-violet spectrophotometry. Two reasons are: 1) •OH is a transient species and is unstable in solution and 2) •OH only absorbs in the vacuum UV region, below 200 nm.[24] The presence of hydroxyl radical is therefore detected by its reaction with scavengers such as aromatic or unsaturated organic compounds. The electron rich π bond is homolytically attacked by the hydroxyl radical to produce a new radical. If the double bond is part of an aromatic compound like benzene or toluene, then the resulting radical is more stable (than •OH) due to the stabilization from resonance forms.[19]

As with the reactions of nitrous acid, the gas phase scavenger reactions of hydroxyl radical have been the most widely investigated. In 1975, Davis *et al.* reported that the hydroxyl radical addition to benzene and toluene was pressure dependent, but no product analysis was performed.[25] Sloane characterized the addition of •OH to 1,3,5-trimethylbenzene, toluene, and benzene in 1978.[26] He found the following products:

$$OH + C_6H_{6-n}(CH_3)_n \rightarrow \begin{matrix} C_6H_{6-n}(CH_3)_nOH \\ C_6H_{5-n}(CH_3)_nOH + H \\ C_6H_{5-n}(CH_3)_{n-1}OH + CH_3 \\ C_6H_{6-n}(CH_3)_{n-1}CH_2 + H_2O \end{matrix} \qquad (55)$$

where n = 0, 1, 3

The temperature dependence of the radical addition to aromatic compounds was examined by Perry *et al.*[27] From this work the following reversible mechanism was proposed:[28]

$$\bullet OH + C_6H_6 \rightarrow C_6H_5\bullet + H_2O \rightarrow [C_6H_6OH]^* \qquad (56)$$

$$[C_6H_6OH]^* \rightarrow C_6H_6 + OH\bullet \xrightarrow{\pm M} [C_6H_6OH] \qquad (57)$$

$$[C_6H_6OH] \rightarrow C_6H_6 + \bullet OH \qquad (58)$$

The products of the radical addition of •OH to aromatic compounds like benzene and toluene are phenol and para-nitrosophenol, (PNP). PNP is produced by the further reaction of phenol with nitrous acid.

The first mechanism for the reaction of aqueous benzene and hydroxyl radicals produced from H_2O_2 was suggested by Jacob *et al.*[29] The products include

phenol, α- and ß-hydroxymucondialdehyde, and hydrogen peroxide.

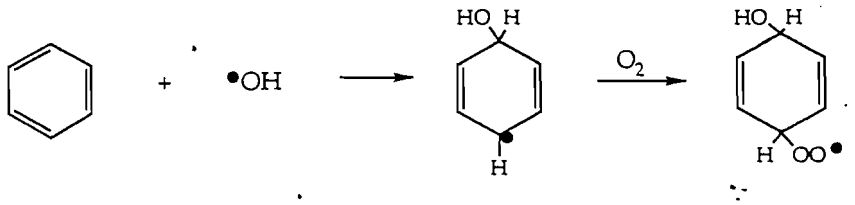

(59)

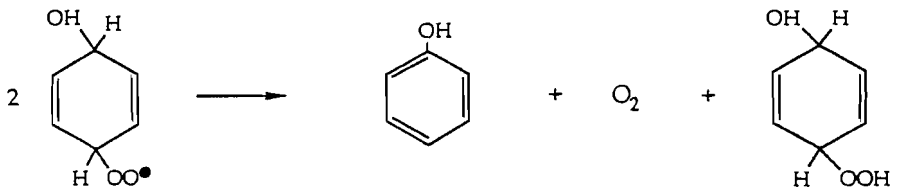

(60)

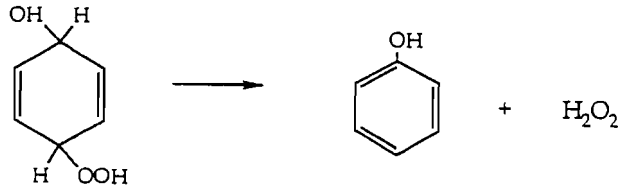

(61)

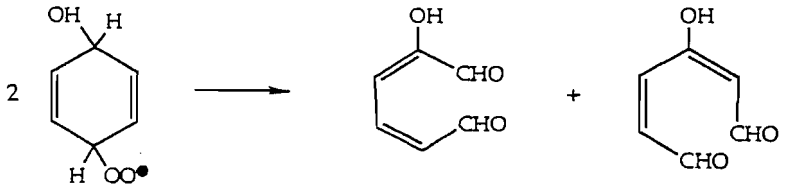

(62)

Eberhardt investigated the hydroxylation mechanism for monosubstituted aromatics.[30]

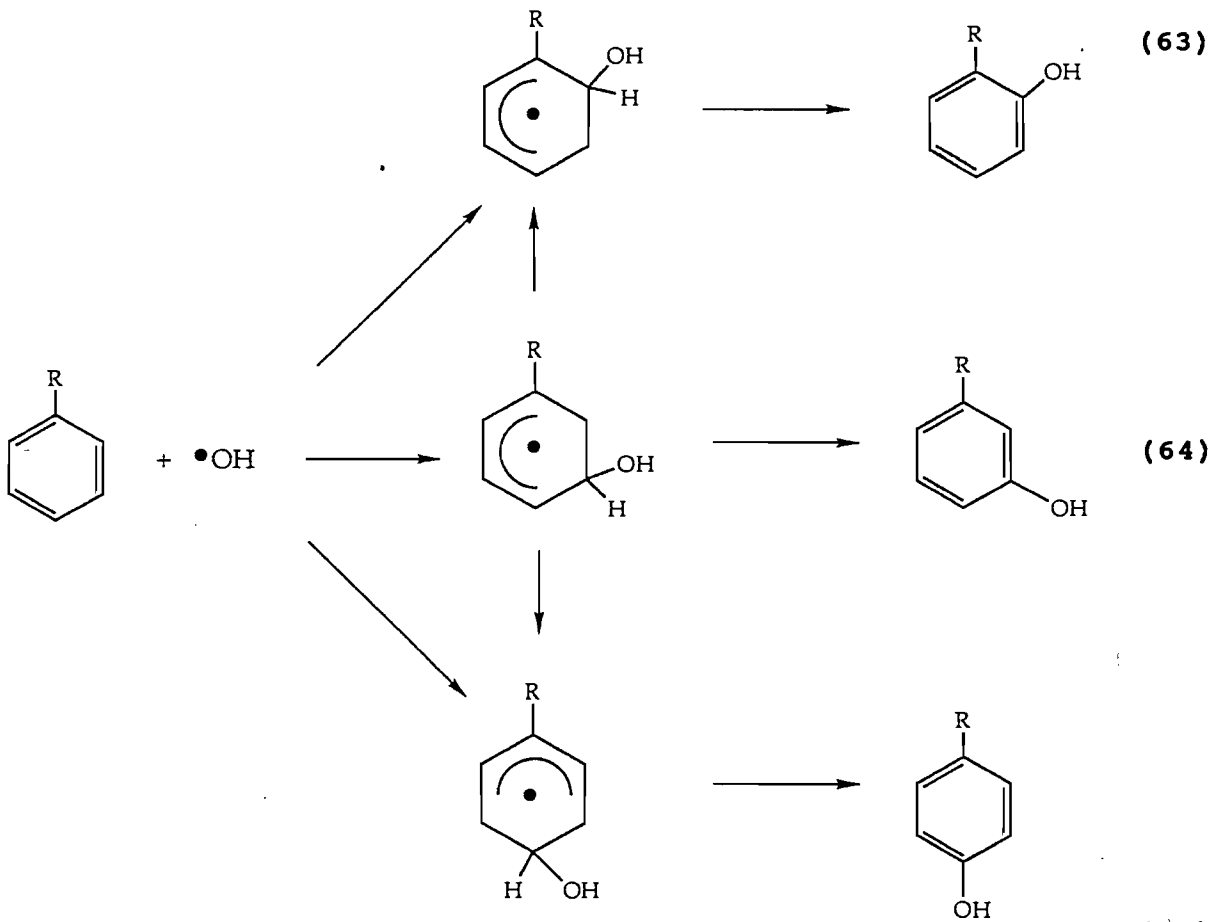

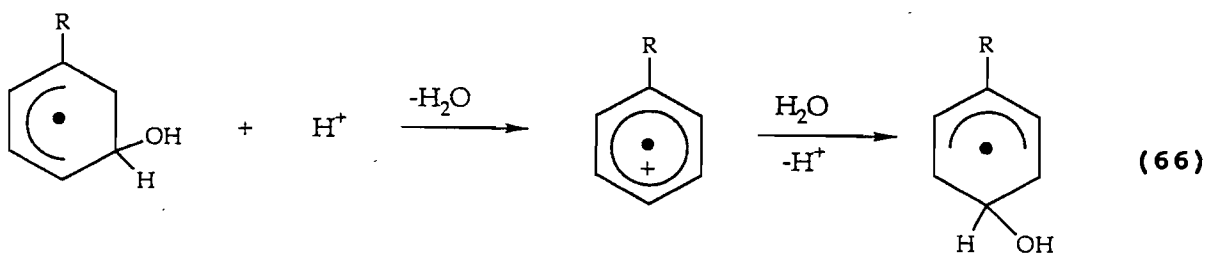

(66)

In his work with nitrous acid, Rettich employed ethylene and benzene as hydroxyl radical scavengers.[8] The mechanism for ethylene is shown in equations 67-71:

$$HONO(aq) + h\nu \rightleftharpoons {}^{\bullet}OH(aq) + NO(aq) \quad (67)$$

$$^{\bullet}OH(aq) + C_2H_4(aq) \rightleftharpoons HOCH_2CH_2{}^{\bullet}(aq) \quad (68)$$

$$HOCH_2CH_2{}^{\bullet}(aq) + NO(aq) \rightleftharpoons HOCH_2CH_2NO(aq) \quad (69)$$

$$HOCH_2CH_2NO(aq) \rightleftharpoons HOCH_2CHNOH(aq) \quad (70)$$

$$HOCH_2CHNOH(aq) + H_2O \rightleftharpoons HOCH_2CHO(aq) + NH_2OH(aq) \quad (71)$$

Glycoaldehyde, the product, decreased in concentration as the concentration of nitrous acid was increased. This trend was ascribed to an increase in competition with ethylene for hydroxyl radical.[8]

Dimethylsulfoxide, DMSO, is useful as an hydroxyl radical probe in biological systems.[31] Norman *et al.* were the first to study •OH reaction with DMSO to give methyl radicals ($^{\bullet}CH_3$).[32] The proposed mechanism, deduced by ESR and radiolysis, is:

$$CH_3-\overset{O}{\overset{|}{S}}-CH_3 + {}^{\cdot}OH \rightarrow CH_3-\overset{HO}{\underset{O}{\overset{|}{\underset{|}{{}^{\cdot}S}}}}-CH_3 \quad (72)$$

$${}^{\cdot}CH_3 + CH_3SOOH \rightarrow CH_4 + CH_3SO_3{}^{\cdot} \quad (74)$$

$$CH_3-\overset{HO}{\underset{O}{\overset{|}{\underset{|}{S}}}}-CH_3 \rightarrow \cdot CH_3 + CH_3SOOH \rightarrow CH_4 + CH_4SO_2\cdot \qquad (73)$$

$$\cdot CH_3 + CH_3-\overset{O}{\underset{\cdot}{S}}-CH_3 \rightarrow CH_4 + \cdot CH_2-\overset{O}{\underset{\cdot}{S}}-CH_3 \qquad (75)$$

$$\cdot CH_3 + \cdot CH_3 \rightarrow CH_3-CH_3 \qquad (76)$$

Challis *et al.* examined the kinetics and the mechanism for the nitrosation reaction of phenol.[33,34] It has been proposed that nitrous acid is in equilibrium with nitrosonium ion (NO^+) in aqueous solution:[35]

$$H^+ + HONO \rightleftharpoons H_2ONO^+ \rightleftharpoons NO^+ + H_2O \qquad (77)$$

Both the nitrosonium ion and its hydrated form can attack the aromatic ring of phenol to form p-nitrosophenol (PNP) by electrophilic substitution. Morrison proposed the following mechanism:[35]

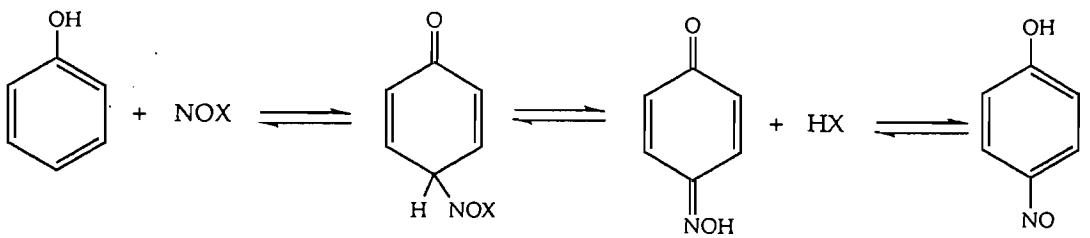

(78)

Many studies indicate that nitrite ion undergoes no net photochemical reaction possibly due to efficient back reactions. Work done by Exstrom[24] with a

Blak-Ray B-100A low pressure mercury lamp did not show net nitrite photolysis. However, additional work by Johnson[36] with higher intensity mercury lamps suggests that, at least in the presence of a hydroxyl radical scavenger like benzene, nitrite displays an obvious photochemical reaction. The proposed products of this reaction are phenol and/or para-nitrosophenol. Previous work by Rettich[8] has indicated that pH does not affect the photochemical decomposition of nitrite. Zafiriou[18] has also stated that nitrite photolysis is independent of pH. More recent work by Hurd[37], however, suggests that the reaction products' concentrations decrease at high pH.

The present study focusses on the photochemistry of nitrite ion in non-aqueous media. The use of aprotic organic solvents allows nitrite to be separated from nitrous acid and its photochemical properties examined independent of those for the conjugate acid. Aprotic solvents do not have the capability to donate a hydrogen ion and thus protonate the nitrite ion to form nitrous acid. Polar solvents are necessary to dissolve significant amounts of the inorganic salts of nitrite. Therefore, various polar, aprotic organic solvents were examined for their usefulness as solvents for the study of nitrite's photochemical properties. Similar work by Gibson[38] is in progress on the photochemistry of the molecular form in aromatic solvents.

EXPERIMENTAL

Apparatus:

The photochemical reactions were performed with a Rayonet photochemical reactor, model #RPR-100. The source of light for all reactions were sixteen mercury lamps banded at 366 $\pm$ 5 nm. Solutions were photolyzed in 20 mL quartz reaction tubes for the times noted. Ultraviolet/visible absorbance measurements were taken with a Perkin-Elmer 559 UV-Vis spectrophotometer using a slit width of 1.0 nm and 1.000 cm quartz cells.

Solvent Suitability Tests:

Solvent suitability tests were done by weighing out 0.02-0.03 g of $NaNO_2$ (Merck, reagent grade) into a 10 mL volumetric flask and solvent was added to volume. If not all of the solid dissolved, the solution was allowed to reach saturation by sitting overnight. The solvents used were dimethylsulfoxide (anhydrous, Aldrich, Gold Label, 99+%), 1,1-dimethoxyethane (Eastman, 99%), 1,2-dimethoxyethane (EM Science, 98%), p-dioxane (Eastman, Scintillation Grade), tetrahydrofuran (Fisher, Histological Grade), dimethylformamide (Baker, Analyzed reagent, 99.0%), and acetonitrile (Baker, Analyzed reagent, 99.5%). Ultraviolet-visible spectrophotometry was used to detect the presence of dissolved nitrite (anticipated λ max = 365 nm). In some cases, spectra indicated the formation of nitrous acid so an attempt was made to dry these solvents and run additional UV-visible spectra of dry solutions. Dimethylformamide was dried over anhydrous magnesium sulfate (Fisher, Certified grade) while 1,2-dimethoxyethane

was dried over anhydrous calcium hydride (Fisher, Purified grade). The p-dioxane was dried by reflux with fresh Na metal and benzophenone (Fisher, Certified grade) until the solution turned blue.

Photolysis of nitrite ion in DMSO:

A 10.0 mL aliquot of 1.0, 0.5, 0.25, or 0.12 M $NaNO_2$ in DMSO was placed in a quartz reaction tube. Up to four reaction tubes could be placed in the merry-go-round apparatus within the Rayonet reactor and photolyzed at one time. Photolysis times were varied from 15 to 60 minutes. Ultraviolet/visible spectrophotometry was used to detect the disappearance of nitrite and the appearance of products.

Thermolysis of DMSO and nitrite ion in DMSO:

A 10.0 mL aliquot of 0.5 or 0.25 M $NaNO_2$ in DMSO was placed in a 20 x 225 mm test tube. This solution was then bubbled with either N_2 (Genex, Dry grade) or O_2 (Genex) gas using a sparging stone for 5 minutes. The test tube was covered with a septum and the headspace was purged with N_2 or O_2 gas for 5 minutes. A similar procedure was followed for tubes of pure DMSO. The tubes were placed in a constant temperature bath held at 60°C for 60 minutes. To prevent problems due to the extreme heating, the tubes were vented to the atmosphere with 22 gauge needles. Ultraviolet/visible spectrophotometry was used to measure the changes, if any, due to thermolysis.

RESULTS

Table 1: Table of Solvent Properties

Solvent	Observations
Dimethyl sulfoxide	Good solubility, Clear nitrite peak
1,2-Dimethoxyethane	Acid peaks seen
p-Dioxane	Acid peaks seen
Tetrahydrofuran	Poor absorbance spectra
Acetonitrile	Poor solubility
Dimethylformamide	Acid peaks seen

Figure 1

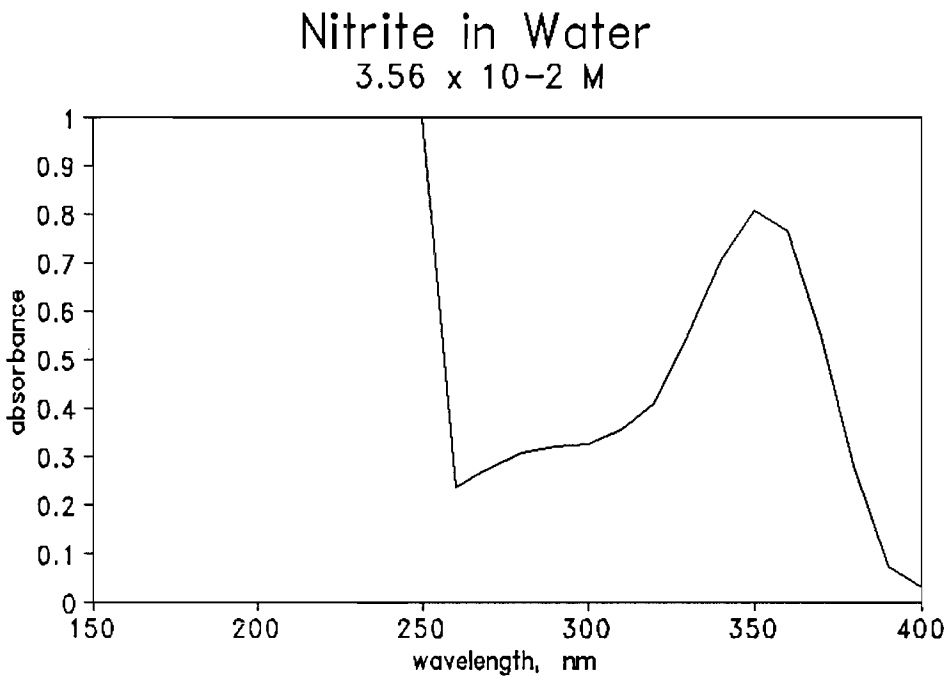
Nitrite in Water
3.56 x 10-2 M
absorbance
1
0.9
0.8
0.7
0.6
0.5
0.4
0.3
0.2
0.1
0
150
200
250
300
350
400
wavelength, nm

Figure 2

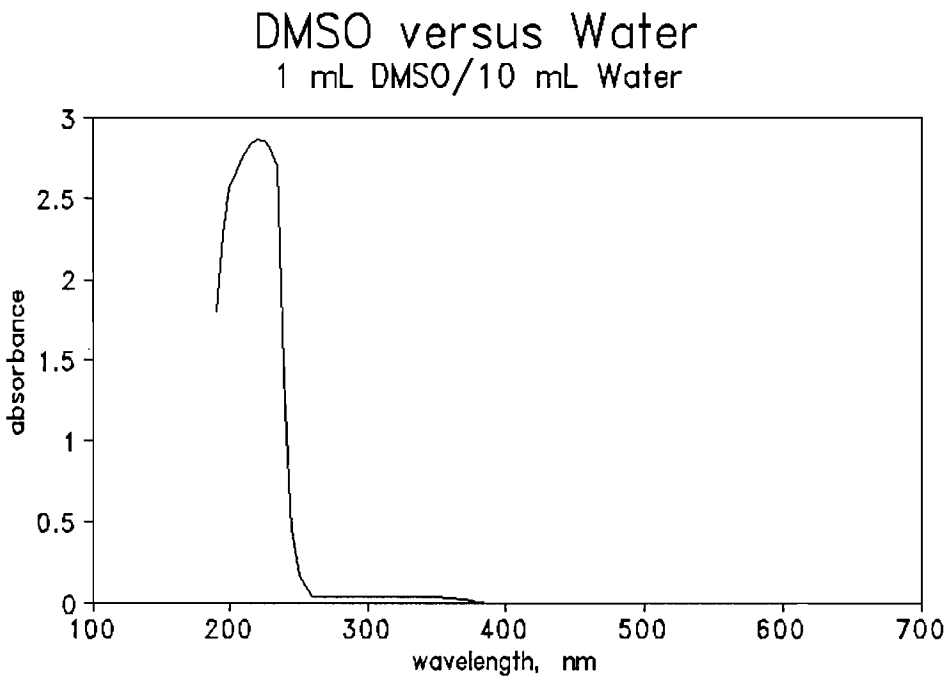
DMSO versus Water
1 mL DMSO/10 mL Water
absorbance
3
2.5
2
1.5
1
0.5
0
100
200
300
400
500
600
700
wavelength, nm

Figure 3

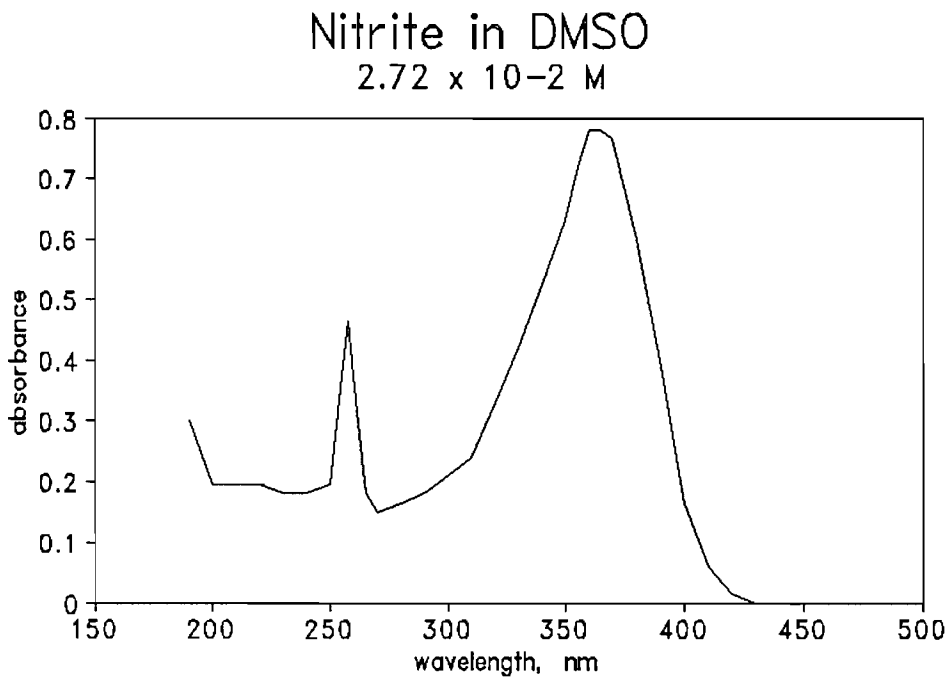
Nitrite in DMSO
2.72 x 10-2 M
absorbance
0.8
0.7
0.6
0.5
0.4
0.3
0.2
0.1
0
150
200
250
300
350
400
450
500
wavelength, nm

Figure 4

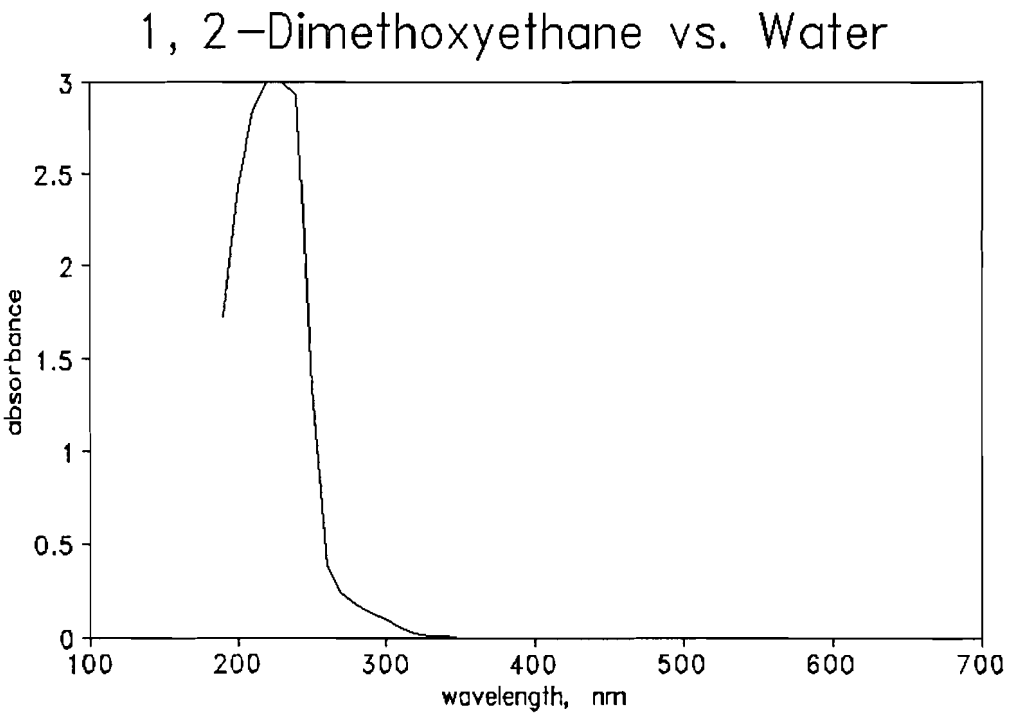
1, 2-Dimethoxyethane vs. Water
absorbance
3
2.5
2
1.5
1
0.5
0
100
200
300
400
500
600
700
wavelength, nm

Figure 5

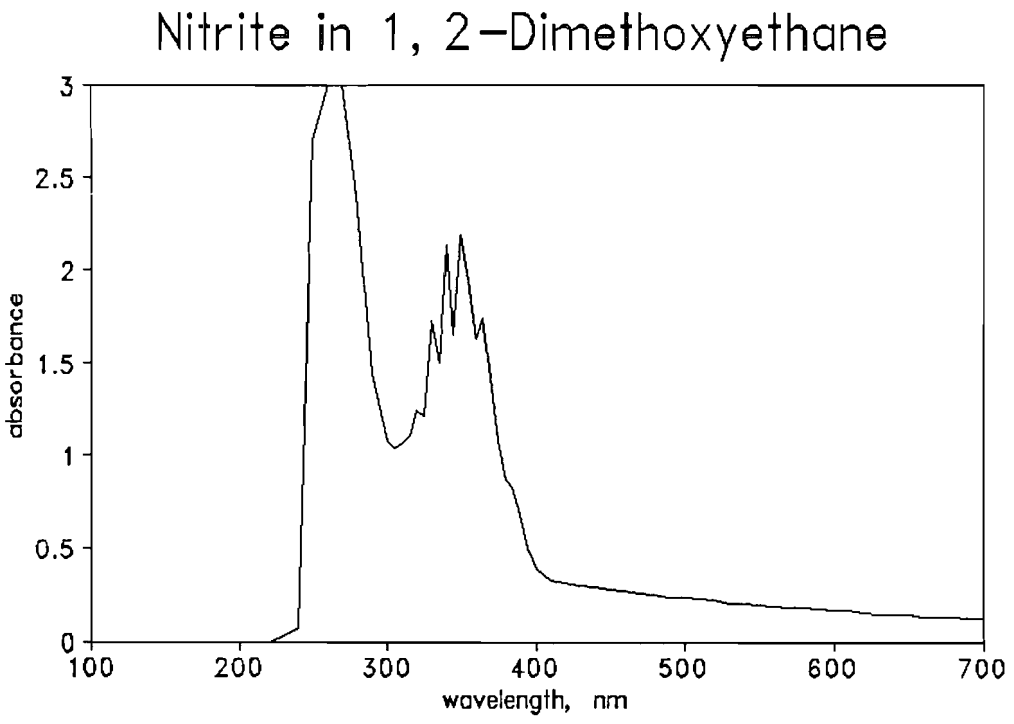
Nitrite in 1, 2-Dimethoxyethane
absorbance
3
2.5
2
1.5
1
0.5
0
100
200
300
400
500
600
700
wavelength, nm

Figure 6

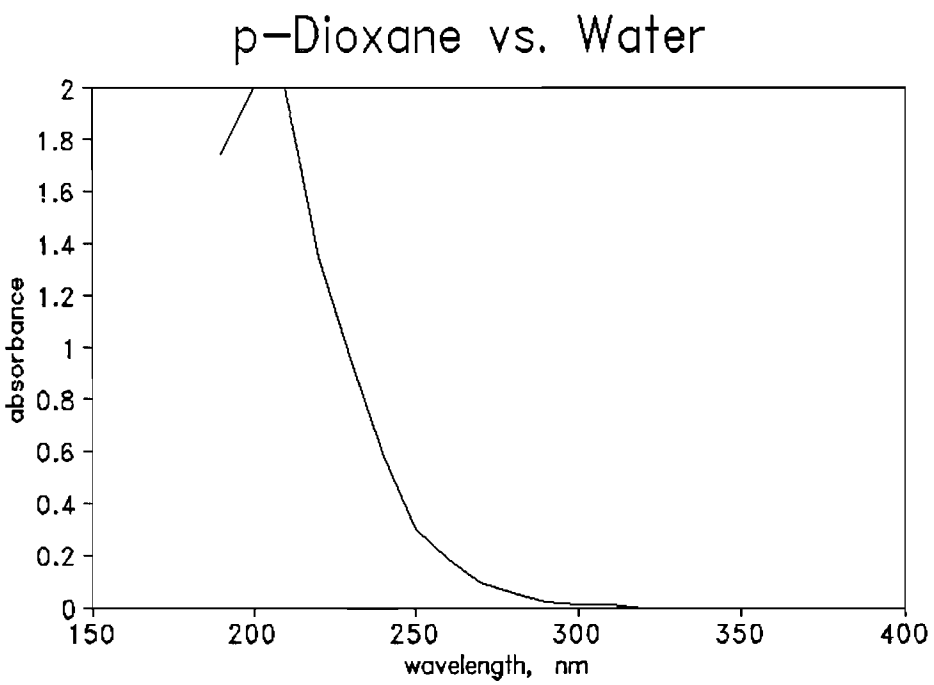
p-Dioxane vs. Water
absorbance
2
1.8
1.6
1.4
1.2
1
0.8
0.6
0.4
0.2
0
150
200
250
300
350
400
wavelength, nm

Figure 7

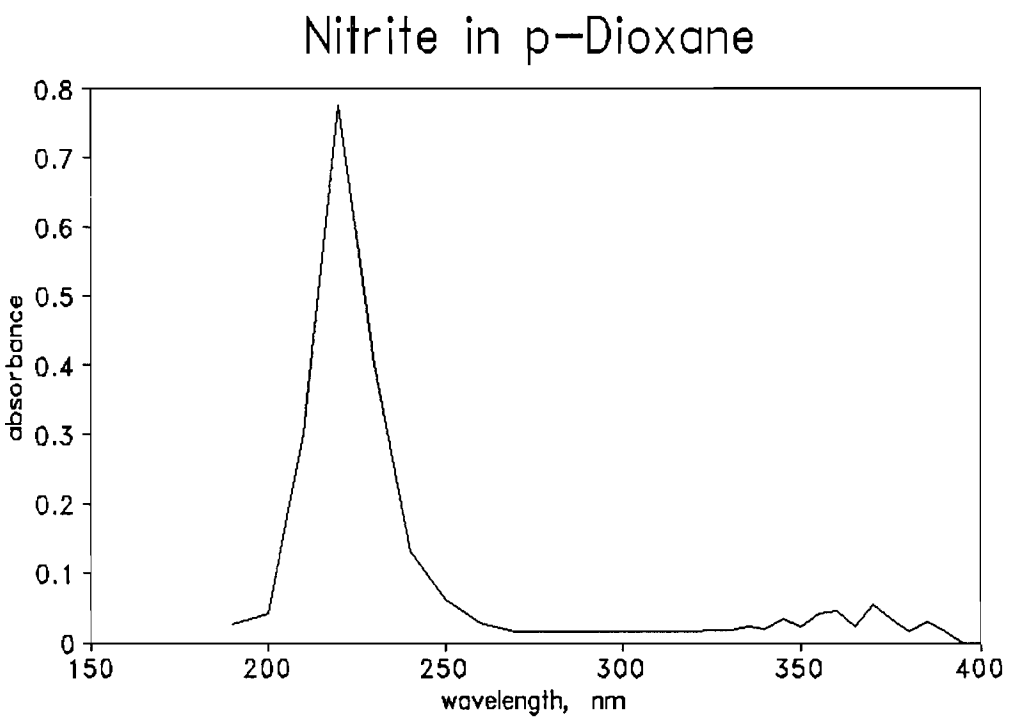
Nitrite in p-Dioxane
absorbance
0.8
0.7
0.6
0.5
0.4
0.3
0.2
0.1
0
150
200
250
300
350
400
wavelength, nm

Figure 8

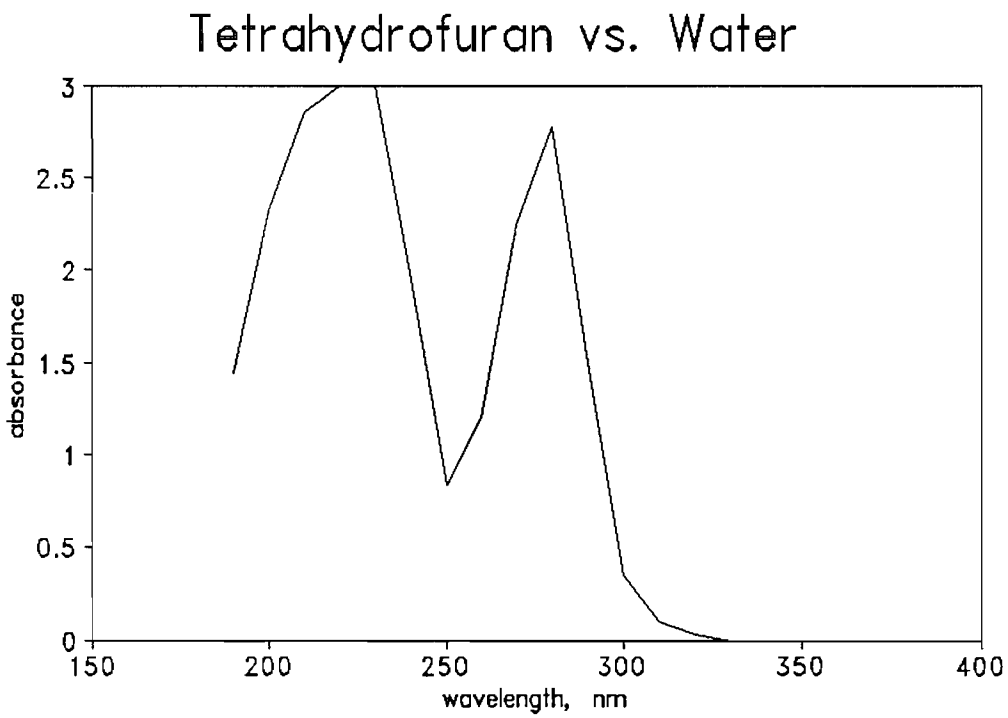
Tetrahydrofuran vs. Water
absorbance
3
2.5
2
1.5
1
0.5
0
150
200
250
300
350
400
wavelength, nm

Figure 9

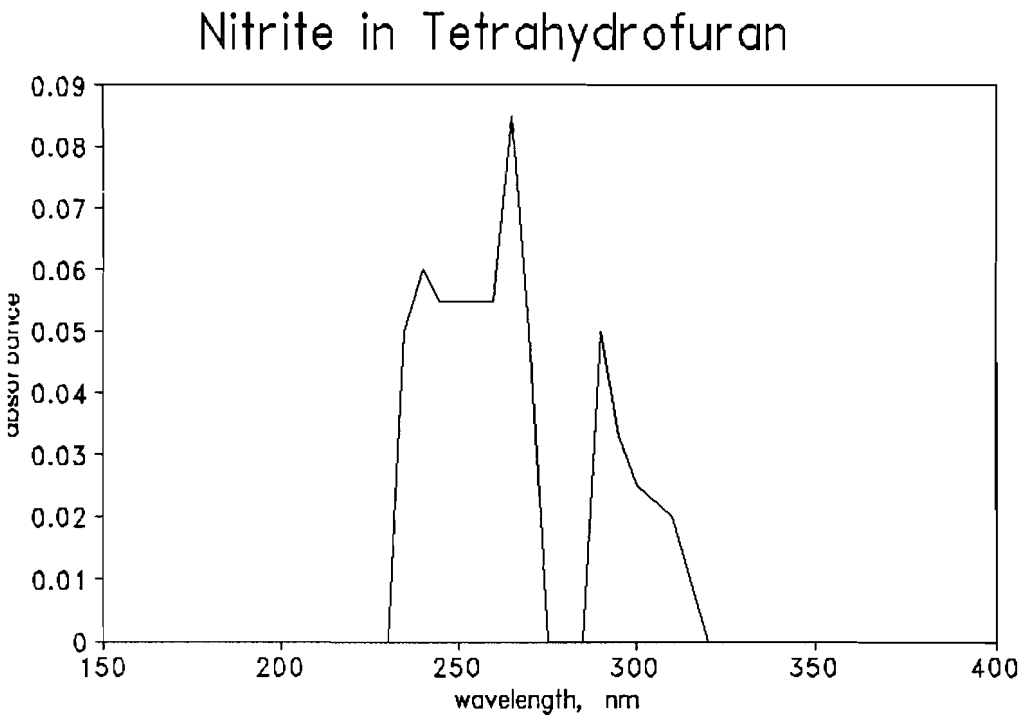
Nitrite in Tetrahydrofuran
0.09
0.08
0.07
0.06
0.05
0.04
0.03
0.02
0.01
0
150
200
250
300
350
400
wavelength, nm

Figure 10

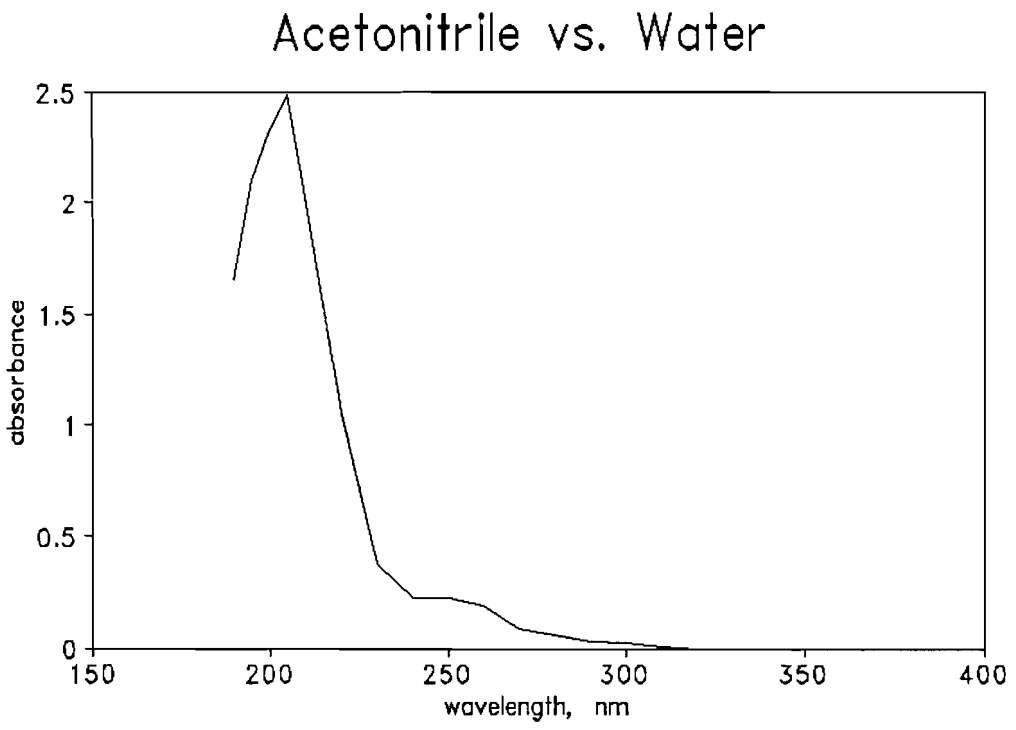
Acetonitrile vs. Water
absorbance
2.5
2
1.5
1
0.5
0
150
200
250
300
350
400
wavelength, nm

Figure 11

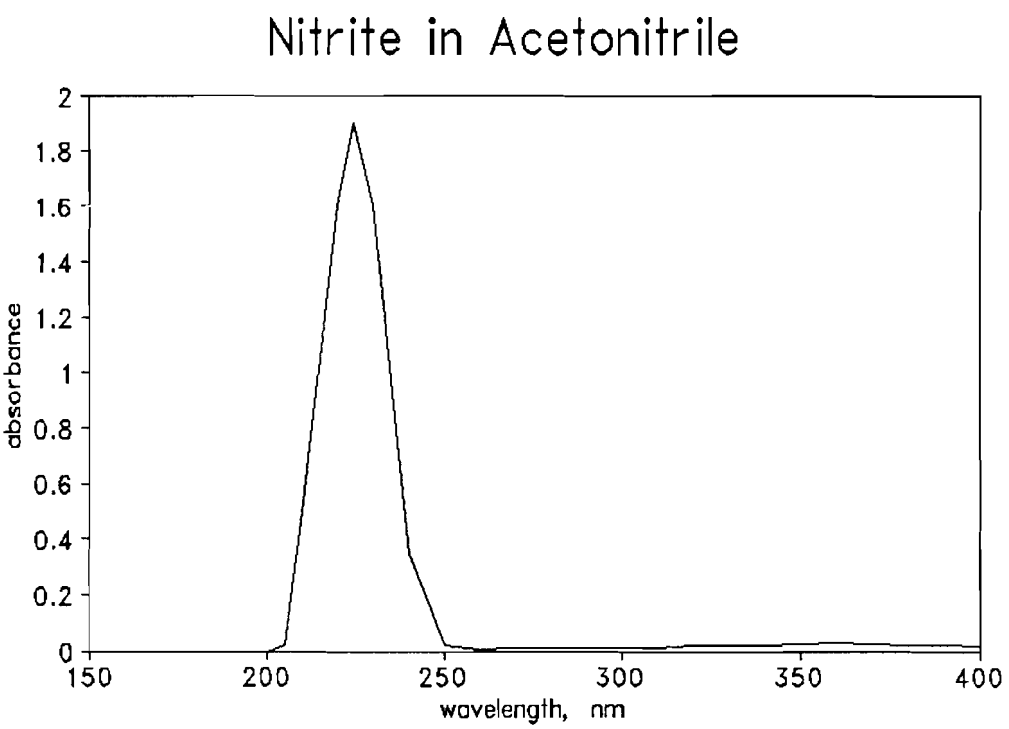
Nitrite in Acetonitrile
absorbance
2
1.8
1.6
1.4
1.2
1
0.8
0.6
0.4
0.2
0
150
200
250
300
350
400
wavelength, nm

Figure 12

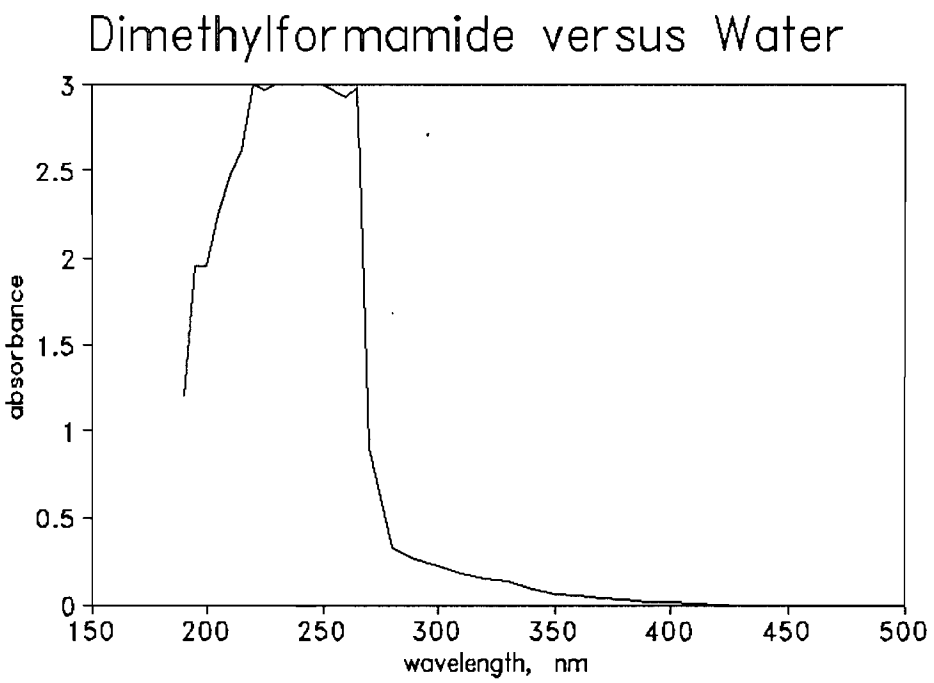
Dimethylformamide versus Water
absorbance
3
2.5
2
1.5
1
0.5
0
150
200
250
300
350
400
450
500
wavelength, nm

Figure 13

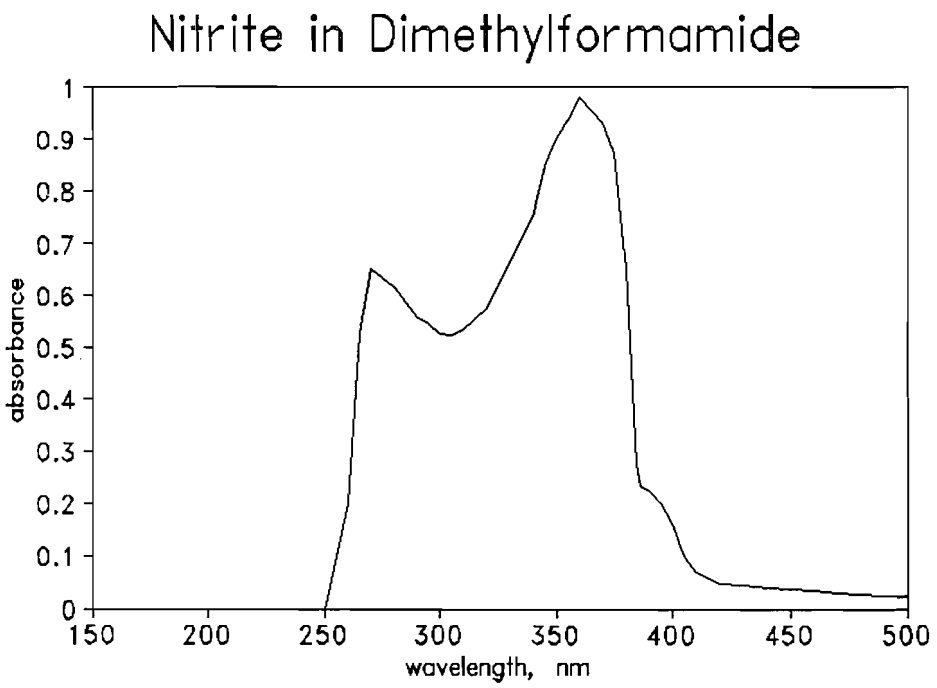
Nitrite in Dimethylformamide
absorbance
1
0.9
0.8
0.7
0.6
0.5
0.4
0.3
0.2
0.1
0
150
200
250
300
350
400
450
500
wavelength, nm

Figure 14

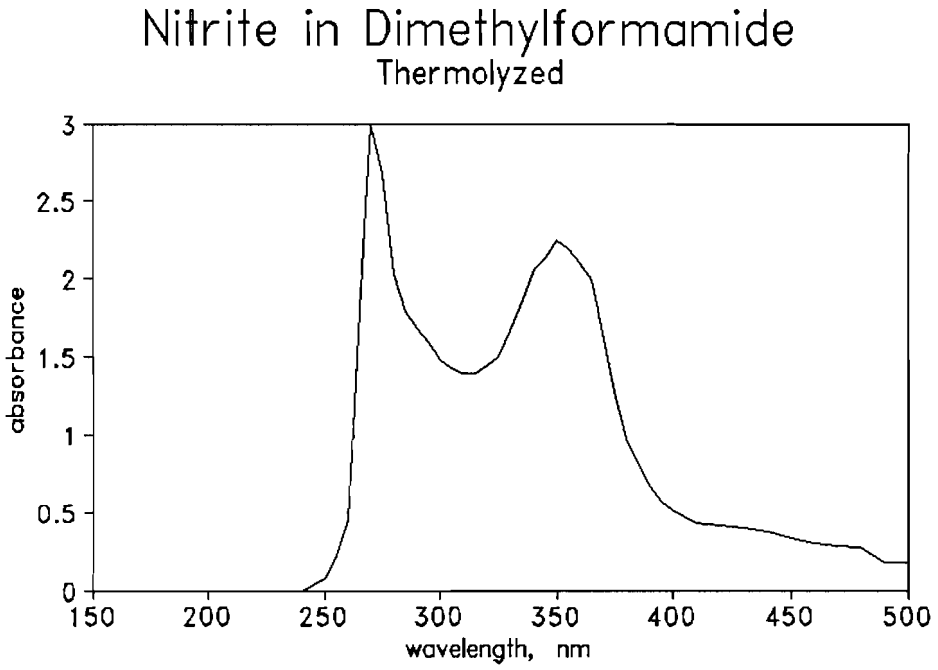
Nitrite in Dimethylformamide
Thermolyzed
absorbance
3
2.5
2
1.5
1
0.5
0
150
200
250
300
350
400
450
500
wavelength, nm

Figure 15

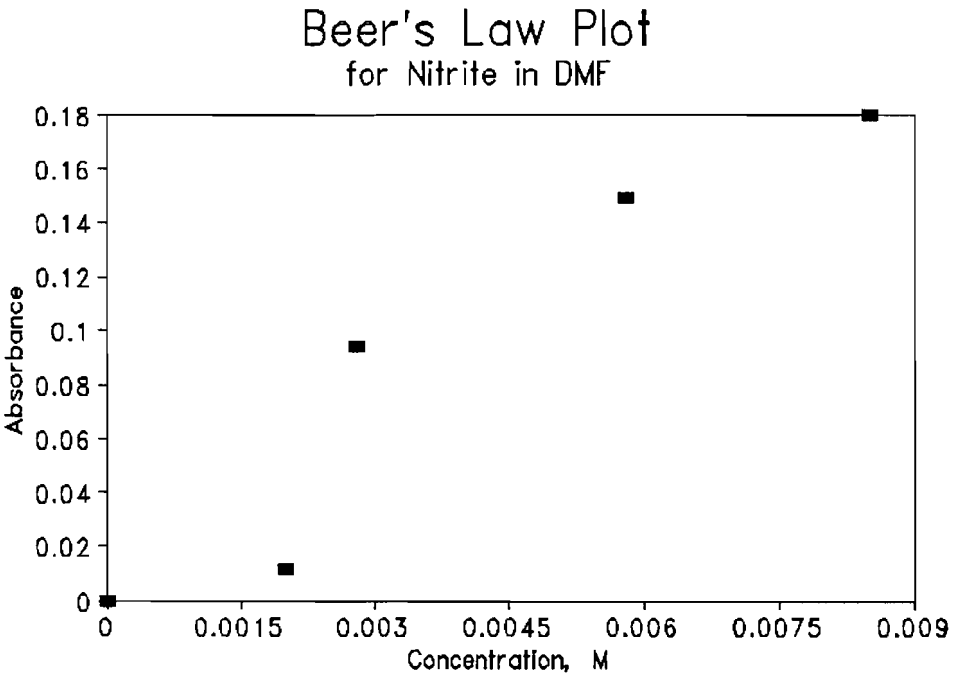
Beer's Law Plot
for Nitrite in DMF
Absorbance
0.18
0.16
0.14
0.12
0.1
0.08
0.06
0.04
0.02
0
0
0.0015
0.003
0.0045
0.006
0.0075
0.009
Concentration, M

Figure 16

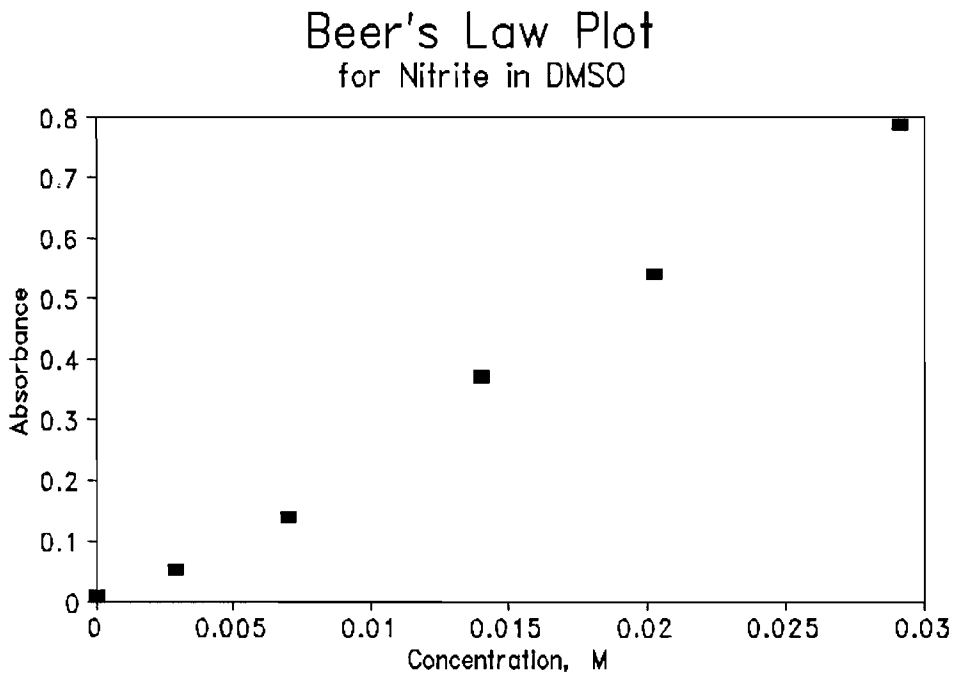
Beer's Law Plot
for Nitrite in DMSO
Absorbance
0.8
0.7
0.6
0.5
0.4
0.3
0.2
0.1
0
0
0.005
0.01
0.015
0.02
0.025
0.03
Concentration, M

Figure 17

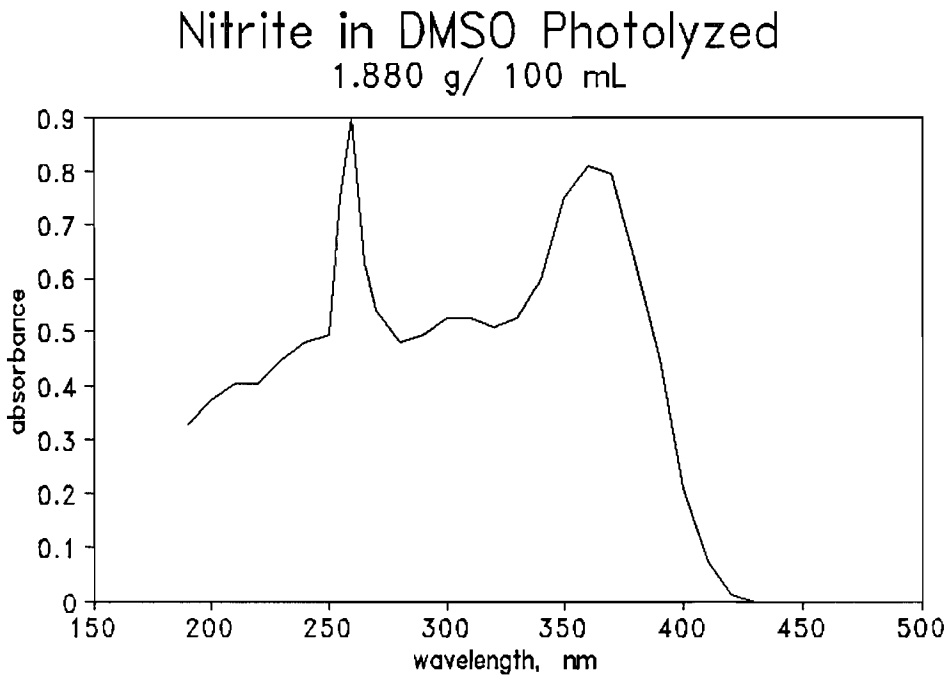
Nitrite in DMSO Photolyzed
1.880 g/ 100 mL
absorbance
0.9
0.8
0.7
0.6
0.5
0.4
0.3
0.2
0.1
0
150
200
250
300
350
400
450
500
wavelength, nm

Figure 18

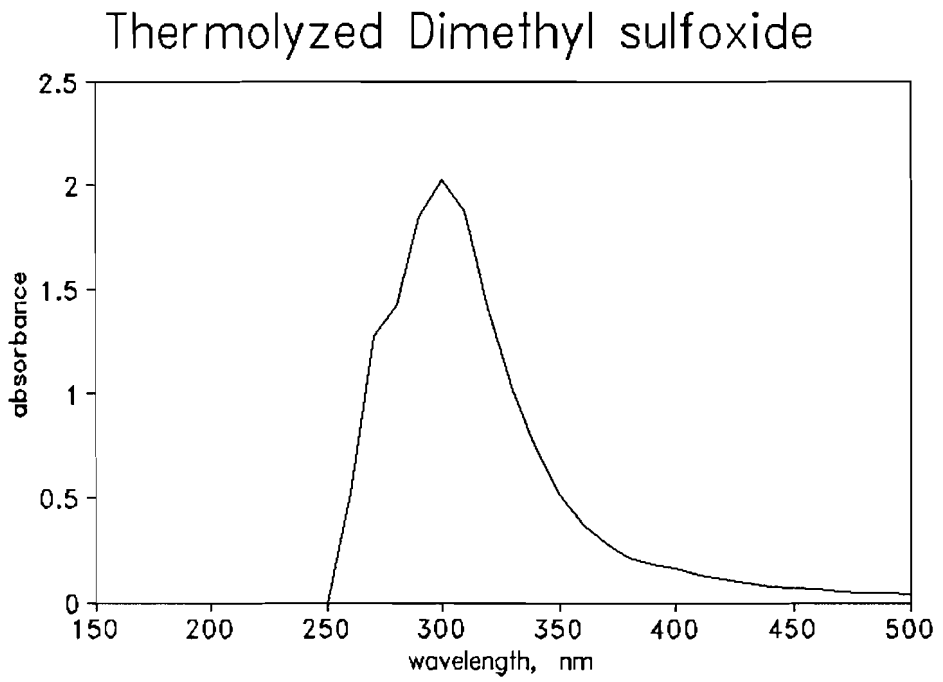
Thermolyzed Dimethyl sulfoxide
absorbance
2.5
2
1.5
1
0.5
0
150
200
250
300
350
400
450
500
wavelength, nm

Figure 19

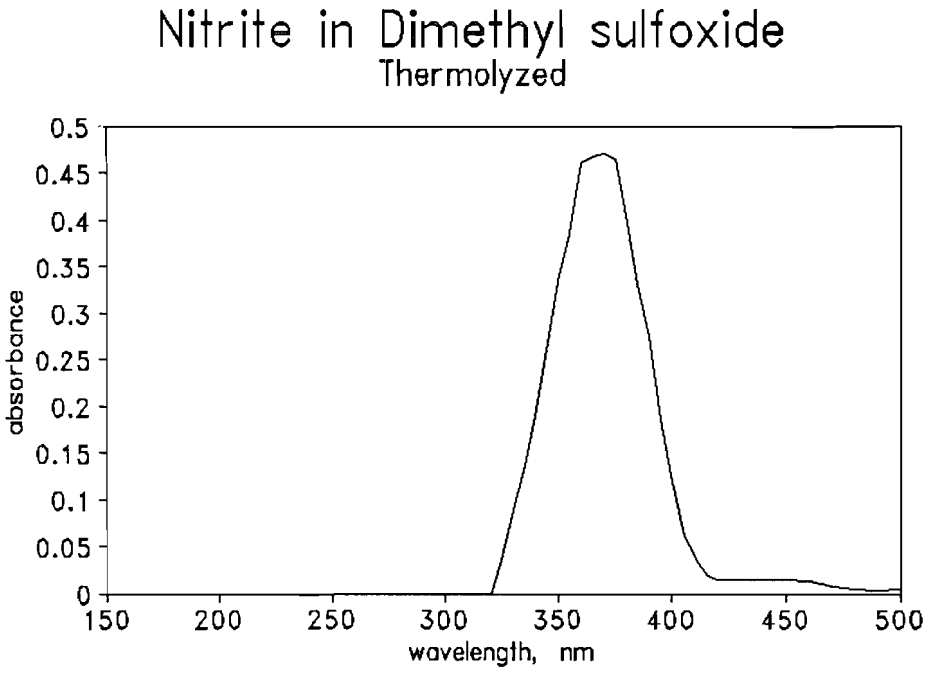
Nitrite in Dimethyl sulfoxide
Thermolyzed
absorbance
0.5
0.45
0.4
0.35
0.3
0.25
0.2
0.15
0.1
0.05
0
150
200
250
300
350
400
450
500
wavelength, nm

Figure 20

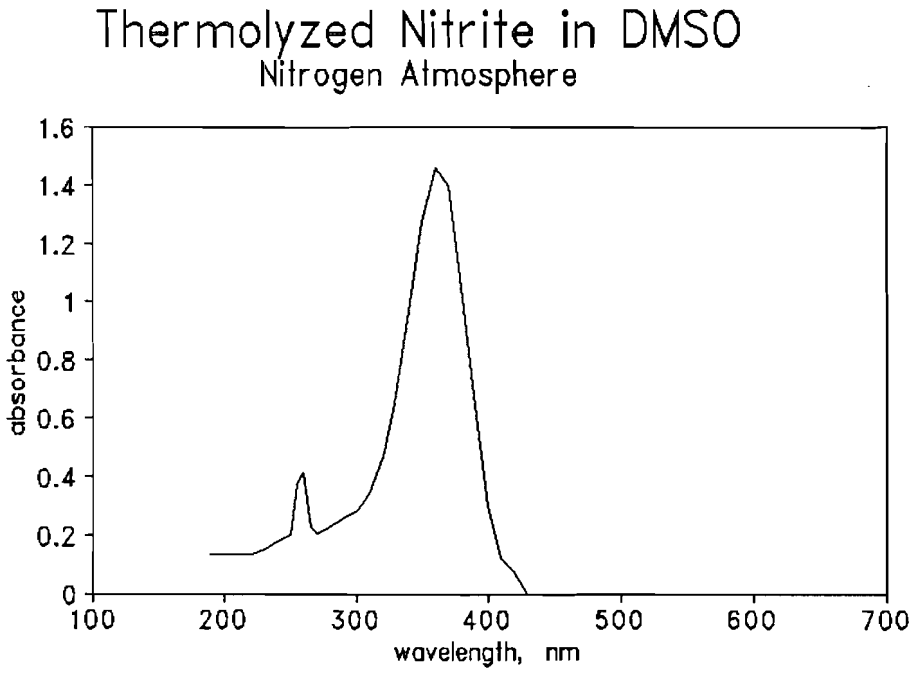
Thermolyzed Nitrite in DMSO
Nitrogen Atmosphere
absorbance
1.6
1.4
1.2
1
0.8
0.6
0.4
0.2
0
100
200
300
400
500
600
700
wavelength, nm

Figure 21

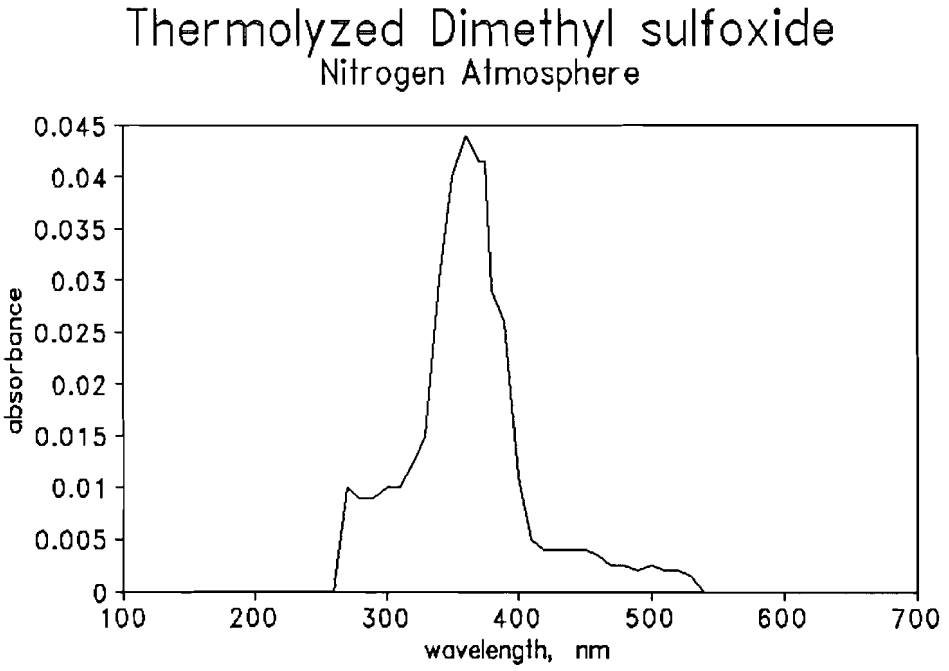
Thermolyzed Dimethyl sulfoxide
Nitrogen Atmosphere
absorbance
0.045
0.04
0.035
0.03
0.025
0.02
0.015
0.01
0.005
0
100
200
300
400
500
600
700
wavelength, nm

Figure 22

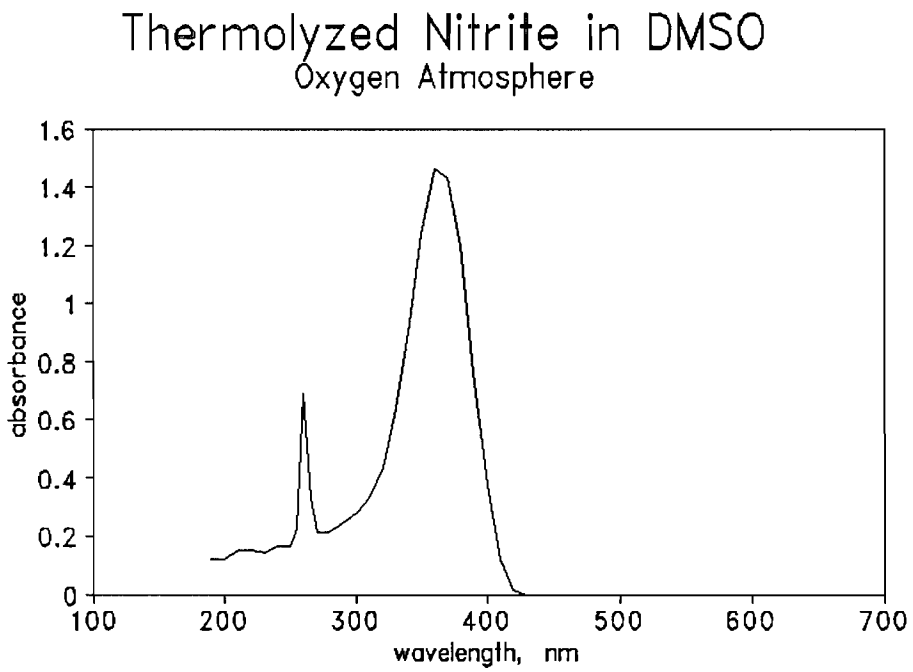
Thermolyzed Nitrite in DMSO
Oxygen Atmosphere
absorbance
1.6
1.4
1.2
1
0.8
0.6
0.4
0.2
0
100
200
300
400
500
600
700
wavelength, nm

Figure 23

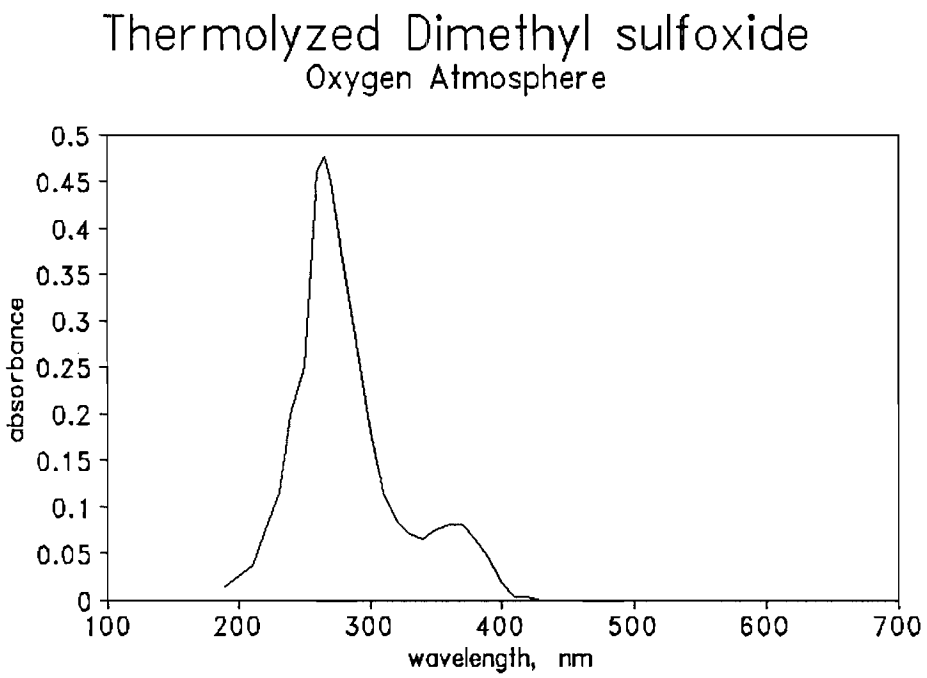
Thermolyzed Dimethyl sulfoxide
Oxygen Atmosphere
absorbance
0.5
0.45
0.4
0.35
0.3
0.25
0.2
0.15
0.1
0.05
0
100
200
300
400
500
600
700
wavelength, nm

Table 2: Table of Beer's Law Data for Nitrite in DMF

Concentration, M	Absorbance @ 368.0 nm
0.0	0.000
2.0e-03	0.012
2.8e-03	0.094
5.8e-03	0.149
8.5e-03	0.180

Table 3: Table of Regression Data for DMF Beer's Law Plot

Regression Output:	
Constant	-9.8e-06
Std Err of Y Est	0.028924
R Squared	0.902477
No. of Observations	5
Degrees of Freedom	3
X Coefficient(s)	22.77743
Std Err of Coef.	4.322946

Table 4: Table of Beer's Law Data for Nitrite in DMSO

Concentration, M	Absorbance @ 364.0 nm
0.0	0.011
2.9e-03	0.052
7.0e-03	0.140
1.4e-02	0.371
2.0e-02	0.540
2.9e-02	0.787

Table 5: Table of Regression Data for DMSO Beer's Law Plot

Regression Output:	
Constant	-0.01916
Std Err of Y Est	0.023224
R Squared	0.995398
No. of Observations	6
Degrees of Freedom	4
X Coefficient(s)	27.50298
Std Err of Coef.	0.935076

DISCUSSION

It is not possible to measure the quantum yield of the photochemical disappearance of nitrite ion in aqueous solution without the contributing complications of nitrous acid. Therefore, to determine the independent photochemistry of nitrite it is necessary to dissolve the nitrite salt in aprotic organic solvents. Several organic solvents were tested for their suitability including dimethylsulfoxide, 1,1-dimethoxyethane, 1,2-dimethoxyethane, p-dioxane, tetrahydrofuran, acetonitrile, and dimethylformamide. These solvents also had to exhibit significant polarity in order to dissolve the ionic sodium nitrite salt. Dimethyl sulfoxide (DMSO) was the first solvent to be used. The entire amount of salt dissolved and the ultraviolet-visible spectrum displayed the peak for dissolved nitrite (λ_{max} = 365 nm) with no sign of the five "finger-like" peaks of HONO in the region of 350-400 nm (Figure 3). DMSO also did not show significant absorbance versus water until 250-190 nm (Figure 2).

1,1-dimethoxyethane did not appear to dissolve any of the sodium nitrite. The UV-visible spectrum for the solvent versus solvent contained large peaks, so 1,1-dimethoxyethane was discarded as a reasonable solvent. It was thought that the solubility of nitrite would be improved with 1,2-dimethoxyethane and it was (Figure 5). The solvent versus water spectrum had significant absorbance in the 260-190 nm region and some as high as 310nm. The spectrum of nitrite indicated the presence of the molecular form (Figure 4). The 1,2-dimethoxyethane was then dried to see if the acid form was due to moisture present in the reagent

solvent. Unfortunately, the acid peaks were still present in the dried solution's spectrum, so it was concluded that the solvent either picked up water very quickly from the air or nitrite was able to remove some of the protons from the solvent molecule.

The next solvent to be tried was p-dioxane. The solvent versus water spectrum had a significant absorbance in the area of 190 to 300 nm (Figure 6). The spectrum of saturated sodium nitrite in p-dioxane exhibited the distinct "fingers" of the molecular form (Figure 7). The p-dioxane was dried by distillation over Na metal in the presence of benzophenone. The blue color of the solution when it was dry disappeared rapidly when the solution was exposed to the atmosphere, so p-dioxane was eliminated as a possible solvent for nitrite photolysis.

Tetrahydrofuran (THF) also did not readily dissolve the entire sample of nitrite. The solvent absorbs in the region 190-280 nm versus water (Figure 8). When the THF solvent versus solvent spectrum was taken, it showed absorbances greater than that of the saturated nitrite in THF (Figure 9). Therefore, tetrahydrofuran is not an appropriate solvent for the nitrite.

Nitrite had an extremely low solubility in acetonitrile. Again, the solvent versus water absorbed more strongly than the nitrite solution (Figures 10 & 11). The only possible evidence of dissolved nitrite is a small absorbance (0.03 Aunits) in the region of 320-400 nm. Thus due to poor solubility, acetonitrile was discarded as a possibility for the nitrite solvent of choice.

Dimethylformamide samples were dried over magnesium sulfate before being used to dissolve the sodium nitrite. The solvent versus water spectrum (Figure 12) shows that DMF absorbs significantly in the region from 190-280 nm and some absorbance occurs in the area of nitrite's λ_{max}. Comparison of the spectra of both "wet" (straight from the bottle) and dry solvents shows them to be quite similar. The solvent versus solvent spectrum (A24) has an interesting absorbance in the region 250-260 nm, however this was corrected in A25. Nitrite seems to have a broad absorbance in DMF from 260-400 nm; it is a large peak at 360 nm with a wide shoulder at 280 nm (Figure 13). Another spectrum of the same solution of saturated nitrite in DMF was taken at a later time to see if the absorbance pattern changed with time. Unfortunately, the solution did not seem to be thermally stable because the spectrum did change; the shoulder at 280 nm became more pronounced and a slight shoulder appeared at 390-400 nm. The absorbance values for saturated nitrite in wet DMF (A29) were significantly lower than those of the corresponding "dry" solution. A Beer's law plot was prepared (Figure 15); it had a least squares correlation value of 0.90 (Table 3). A thermolysis was performed with both solvent and nitrite in DMF to test the thermal stability of the solutions. Spectrum A28 is the nitrite solution before thermolysis and A35 is the same solution after thermolysis. Thermolysis resulted in significant spectral changes (Figure 14). The peak at 270 nm grew to be larger than the peak at 350 nm but all of the absorbance values increased as evidenced in the necessary change of the scale maximum from 1 absorbance unit to 3 Aunits.

Similar effects were seen with "wet" solvent but a change of scale maximum was not required. The effect of thermolysis on the spectrum of dimethylformamide versus water is a change of shape in the 240 nm peak; it falls and rises differently at the beginning and end of the peak (A37 & A38). Finally, sodium nitrate was dissolved in DMF as comparison for nitrite to see the effects of thermolysis. Saturated nitrate in DMF had a λ_{max} of 310 nm (A39). Thermolysis of the nitrate solution resulted in a significant growth at 270 nm, very near the region of growth in the nitrite spectra (A40).

From all of the above information, dimethyl sulfoxide was chosen as the best solvent to study the photochemical and thermal reactions of nitrite ion. Spectra A41 through A45 are for the Beer's law plot of nitrite in DMSO. The least squares regression correlation is 0.995 (Table 4). Before photolysis, UV-visible spectra were taken of the four concentrations of nitrite in DMSO from 0.125 to 1.00 M (A48-A51). The solutions were photolyzed for 60 minutes with 365 nm light. There did not to appear to be any volume change with photolysis, so any concentration change was not due to solvent evaporation. There was, however, a significant change in temperature from 28°C to 60°C due to the heat produced by the photolysis lamps. Spectra A52 to A56 are from DMSO samples that were photolyzed for varying times. DMSO does not absorb at 365 nm so no photolysis reaction could occur. Thus, these spectra show the effect of the lamp heating on the solvent. DMSO must undergo some type of thermal reaction as evidenced by the growth with time of the peak at 260 nm. Spectra A57 to A64

show the changes in the nitrite-DMSO solution upon photolysis. There is a peak growing in at 300 nm in between the two peaks of the solutions before photolysis. This peak is more obvious in the lower concentrations; it seems to be overwhelmed by the peak at 350 nm.

Since there was significant heating of the photolysis solutions, it was necessary to investigate the possibility that the results were due to a thermal process rather than the light. Spectra A65 and A66 are of thermolyzed DMSO versus non-thermolyzed DMSO; there is a large absorbance in the region of 260-400 nm. The spectra of nitrite in DMSO did not appear to change significantly upon thermolysis, but a small peak at 440 nm was seen when the maximum scale was changed to 1 Aunit (A67-A68). The thermolyzed solutions of nitrite in DMSO were bubbled with nitrogen gas to determine if any of the thermolysis products were dissolved gases. The spectra remained unaltered after purging with N_2 (A69-A70). The effect of different gases on the thermal reaction of both DMSO and nitrite in DMSO was studied. Solutions were bubbled with either nitrogen or oxygen gas for several minutes and then they were capped. The thermolysis was performed under conditions similar to those that occur in photolysis; the solutions were heated for 60 minutes at the peak temperature of photolysis, 60°C. The thermolyzed DMSO in the nitrogen environment (A71 and A72) seemed to show an absorbance at 365 nm, where nitrite absorbs. It seems probable that that particular peak is due to contamination. The thermolyzed nitrite in DMSO under nitrogen appeared unchanged except for the shoulder

developing at 420 nm (A73 and A74). The thermolzyed DMSO in an oxygen environment showed a peak at 365 nm, where nitrite's λ_{max} is, perhaps due to contamination (A75). The thermolyzed nitrite in DMSO under oxygen conditions displayed no obvious sign of thermolysis; there were only the same two peaks seen in the unthermolyzed solution.

The effects of thermolysis and photolysis on the nitrite in DMSO system are still not fully understood. It is not clearly indicated whether or not the products in the photolysis spectrum are due to the influence of light or perhaps partially due to the heating from the light source. The thermolysis study was rather inconclusive since there is some question as to the reliability of the results. Therefore, more careful work needs to be done to prevent possible contaminants. Another feasible method to study the effect of photolysis alone is to cool the sample as it is being photolyzed with an antifreeze bath to counteract the effect of source heating. One could also use a lower intensity source that would produce significantly less heat. Work still needs to be done in the area of product separation and identification for both heat and light induced phenomena.

FUTURE RESEARCH

Future research could concentrate on the continued study of the thermal reaction of NO_2^- in dimethylsulfoxide. Further work also needs to be done on the photochemical reaction of nitrite in DMSO. Specifically, the effect of controlled amounts of water on the photolysis of nitrite and the effect of controlled amounts of water in the presence of hydroxyl radical scavengers on nitrite photolysis. Also, the identification of the photolysis products from both the molecular and ionic forms needs to be addressed.

REFERENCES

[1] Jenkin, M.E., Cox, R.A., *Chem. Phys. Lett.*, **1987**, *137*(6), pp. 548-52.

[2] Seinfeld, J.H., *Atmospheric Chemistry and Physics of Air Pollution*; Wiley: New York, **1986**, pp. 118-134, as cited in reference 11.

[3] Finlayson-Pitts, B.J., Pitts, J.N., Jr., *Atmospheric Chemistry: Fundamentals and Experimental Techniques*; Wiley: New York, **1986**, as cited in reference 11.

[4] Cox, R.A., Atkins, D.H., *U.K. At. Energy Res. Establ. Rep.*, **1973**, AERE-R7615, as cited in reference 8.

[5] Ray, P.C., Dey, M.L., Ghosh, J.C., *J. Chem. Soc.*, **1917**, *111*, p. 413.

[6] Montemartini, D., *Acc. Lincei. Roma* [IV], **1890**, *6, II,* p. 263, as cited in reference 8.

[7] Usubillaga, A.N., Ph.D. Thesis, University of Illinois, Urbana, Illinois, 1962.

[8] Rettich, T.R., Ph.D. Thesis, Case Western Reserve University, Cleveland, Ohio, 1978.

[9] Abel, E., Schmid, H., *A. Phys. Chem.*, **1928,** *132,* p.55.

[10] Thie, J., *J. Phys. Chem.*, **1947**,*51,* p. 540.

[11] Park, J., Lee, Y., *J. Phys. Chem.*, **1988**, *92*, pp. 6294-302.

[12] Cox, R.A., Derwent, J., *J. Photochem.*, **1976/77,** *6,* p.23.

[13] Nash, T., *Tellus,* **1974,** *26,* p. 1, as cited in reference 8.

[14] Murty, K.S., Dhar, N.R., *J. Indian Chem. Soc.,* **1930,** *7,* p. 985.

[15] Holmes, M., *J. Chem. Soc.,* **1926,** p. 1898, as cited in reference 16.

[16] Treinin, A., Hayon, E., *J. Am. Chem. Soc.,* **1970**, *92*(20), pp. 5821-9.

[17] Zafiriou, O.C., McFarland, M., *J. Geophys. Res.,* **1981**, *86*(C4), pp. 3173-82.

[18] Zafiriou, O.C., Bonneau, R., *Photochem. Photobio.,* **1987**, *45*(6), pp. 723-7.

[19] McMurray, J., Organic Chemistry, second edition, Brooks/Cole: Pacific Grove, CA, 1988.

[20] Abel, E., *Montash.,* **1952,** *83*(422), as cited in *Chem. Abstr.*, **1952,** *46,* 10182g.

[21] Hunt, J.P., Taube, H., *J. Am. Chem. Soc.,* **1952**, *74*, pp. 5999-6001.

[22] Mansour, M., *Bull. Environ. Contam. Toxicol.*, **1985**, *34*, pp. 89-95.

[23] Haber, F., Weiss, J., *Proc. Roy. Soc.,* **1952,** p. 928.

[24] Exstrom, C., Research Honors Paper, Illinois Wesleyan University, Bloomington, Illinois, 1990.

[25] Davis, D.D., Bollinger, W., Fischer, S., *J. Phys. Chem.,* **1975**, *79*(3), pp. 293-4.

[26] Sloane, T.M., *Chem. Phys. Lett.*, **1978**, *54*(2), pp. 269-72.

[27] Perry, R.A., Atkinson, R., Pitts, J.N., Jr., *J. Phys. Chem.,* **1975,** *79,* p. 1763, as cited in reference 28.

[28] Tully, F.P., Ravishankara, A.R., Thompson, R.L., Nicovich, J.M., Shah, R.C., Kreutter, N.M., Wine, P.H., *J. Phys. Chem.*, **1981**, *85*(15), pp. 2262-9.

[29] Jacob, N., Balakrishnan, I., Reddy, M.P., *J. Phys. Chem.,* **1977**, *81*(1), pp. 17-22.

[30] Eberhardt, M.K., *J. Am. Chem. Soc.,* **1981**, pp. 3876-8.

[31] Eberhardt, M., Colina, R., *J. Org. Chem.,* **1988,** *53*(5), p. 1071-4.

[32] Norman, R.O.C., Dixon, W.T., Buley, A.C., *J. Chem. Soc.,* **1964,** p. 3625, as cited in reference 31.

[33] Challis, B.C., Lawson, A.J., *J. Chem. Soc. (B),* **1971**, pp. 770-3.
[34] Challis, B.C., Higgins, R.J., Lawson, A.J., *Chem. Comm.,* **1970**, pp. 1223-4.
[35] Morrison, D.A., Turney, T.A., *J. Chem. Soc.,* **1960**, p. 4827.
[36] Johnson, J.A., Research Honors Paper, Illinois Wesleyan University, Bloomington, Illinois, 1992.
[37] Hurd, K., Research Paper, Illinois Wesleyan University, Bloomington, Illinois, 1992.
[38] Gibson, M., Research Paper, Illinois Wesleyan University, Bloomington, Illinois, 1993.

Appendix of Spectra
Kathryn E. Shanks
Honors Research Paper
May, 1993

Appendix of Spectra

S#1 9-18-92

400 – 190 nm
120 nm/min
chart 20 nm/cm
slit = ~~0.25~~ 1.0 nm
0 – 1.00 Aunits

3.56×10^{-2} M $NaNO_2$ in water

1.0
.8
.6
.4
.2
0

80
60
40
20
0

200 220 240 260 280 300 320 340 360 380 400

H_2O vs. H_2O

PART NO. B0093925

S#2 9-23-92

500-190nm
~0mm/min
out 20nm/cm
slit = 0.25nm
~0.100 to 1.00 Aunits

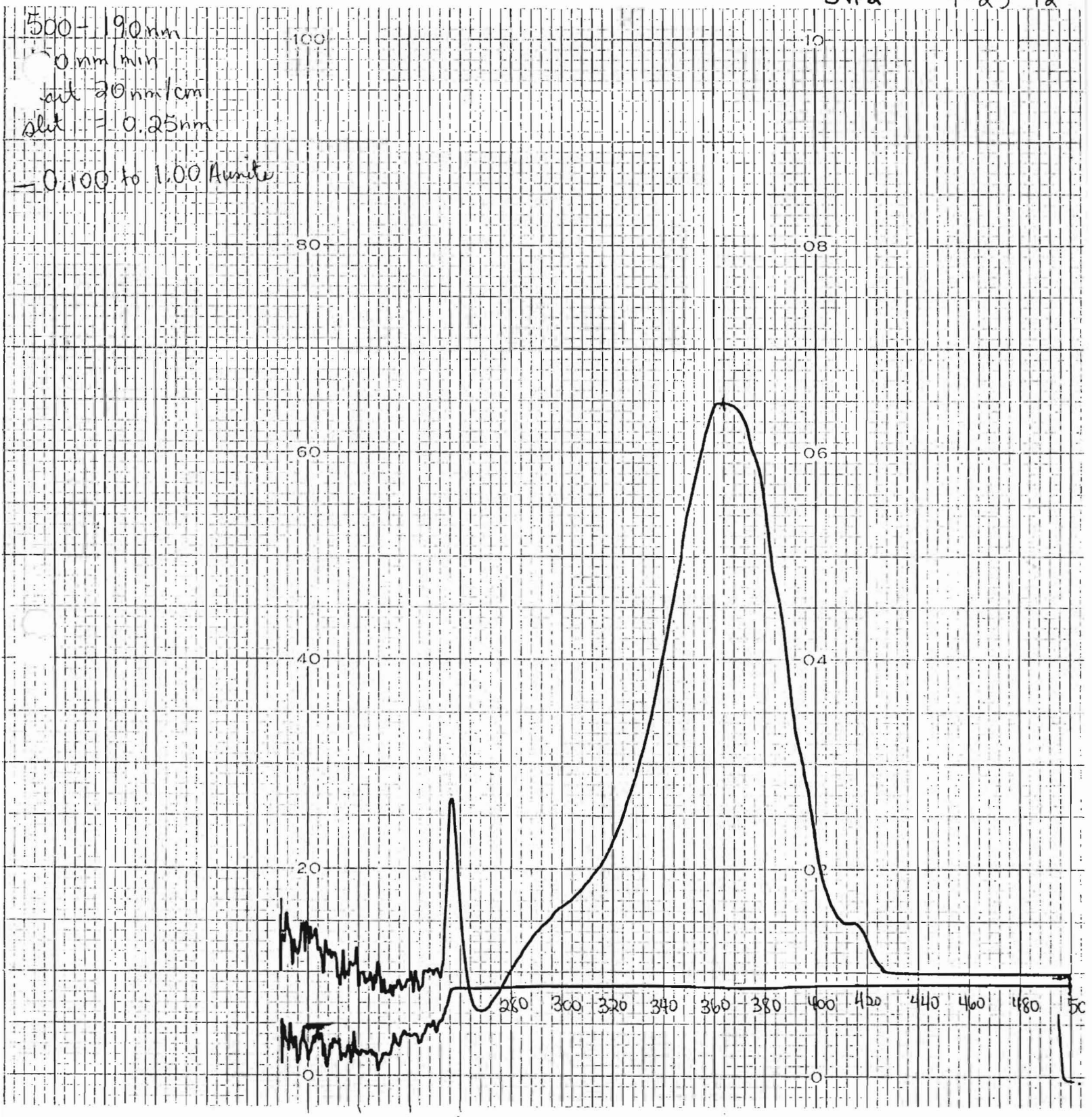

3.41×10^{-2} M $NaNO_2$
in DMSO $\lambda_{max} \approx 365$

3925 PERKIN ELMER PART NO. B0093925

S# 66

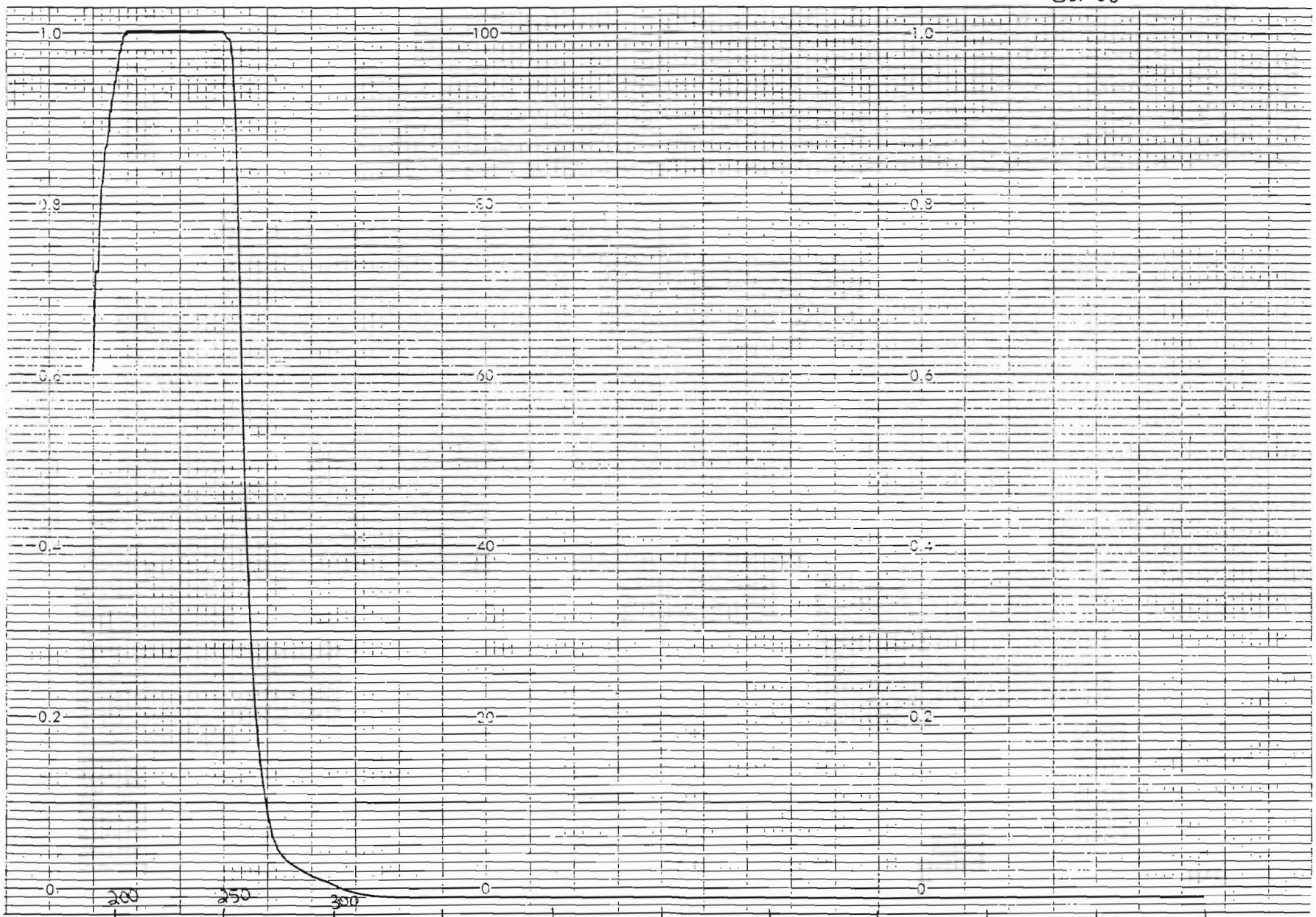
1.0
0.8
0.6
0.4
0.2
0
100
80
60
40
20
0
200
250
300
350
400
450
500
550
600
650
700
700– 190nm
60nm/min
20 nm/cm
slit = 1.0 nm
0-3 Abs
DMSO vs. water
3-5-93

A 3

S#67

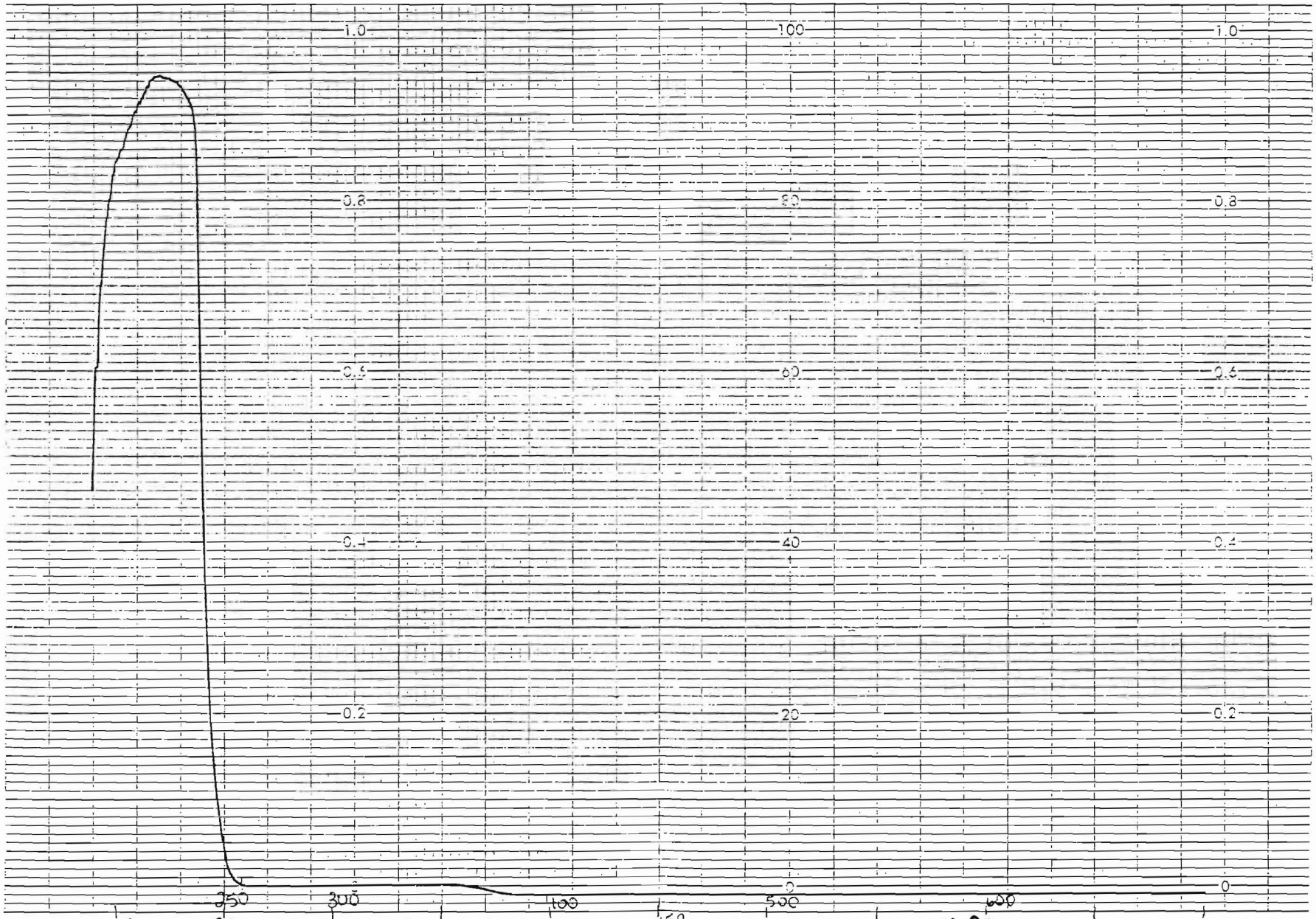

700 – 190 nm
60 nm/min
20 nm/cm
slit = 1.0 nm

0- 3 Acetate

1 mL DMSO / 10 mL w/ H2O

3-5-93

A 4

S#72

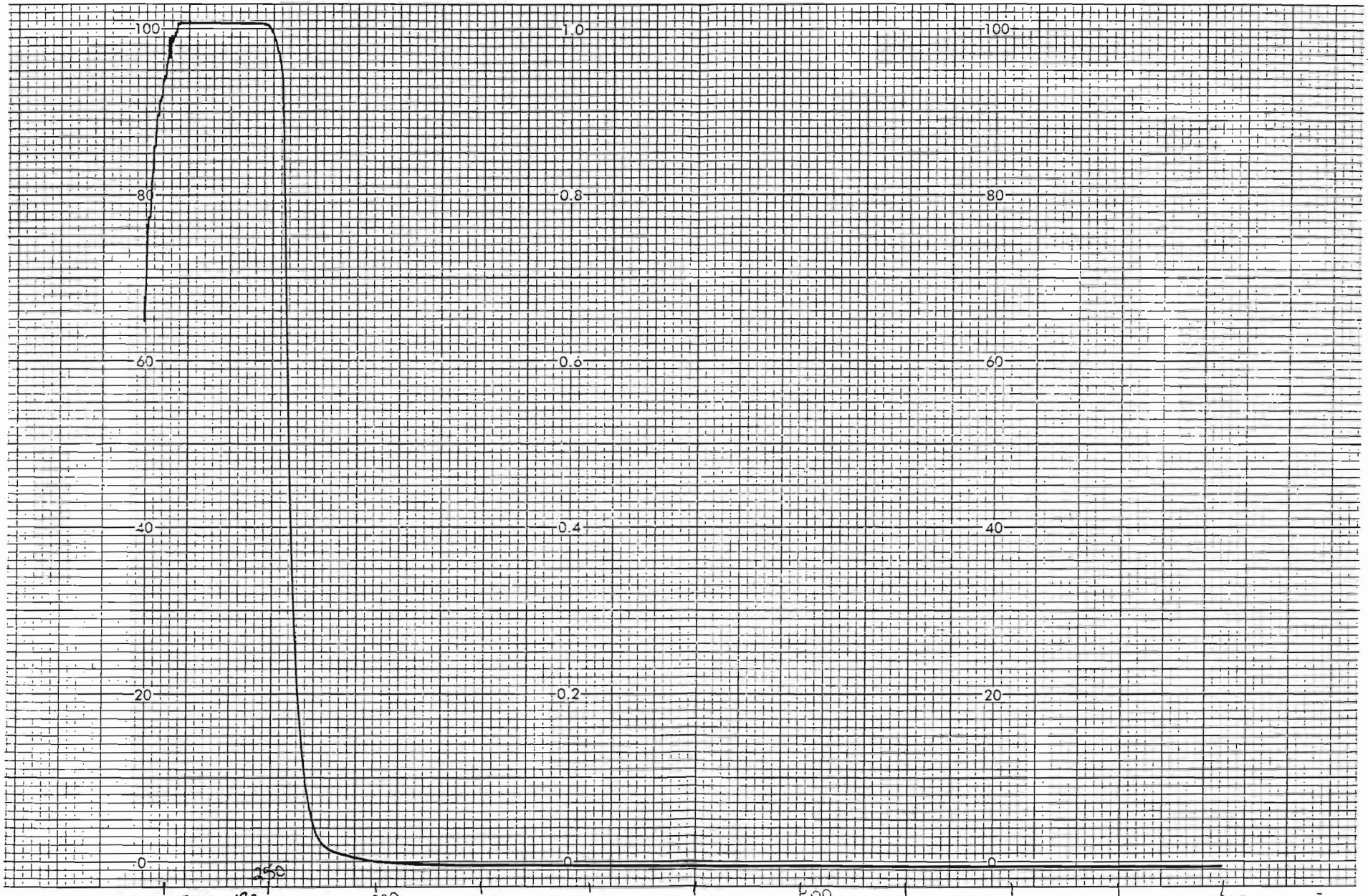
100
80
60
40
20
0
1.0
0.8
0.6
0.4
0.2
0
100
80
60
40
20
0
200
250
300
350
400
450
500
550
600
650
700
700 - 190 nm
60 nm/min
20 nm/cm
slit = 1.0 nm
0-3 Aunits
DMSO vs. H2O
3-23-93

A 5

SA71

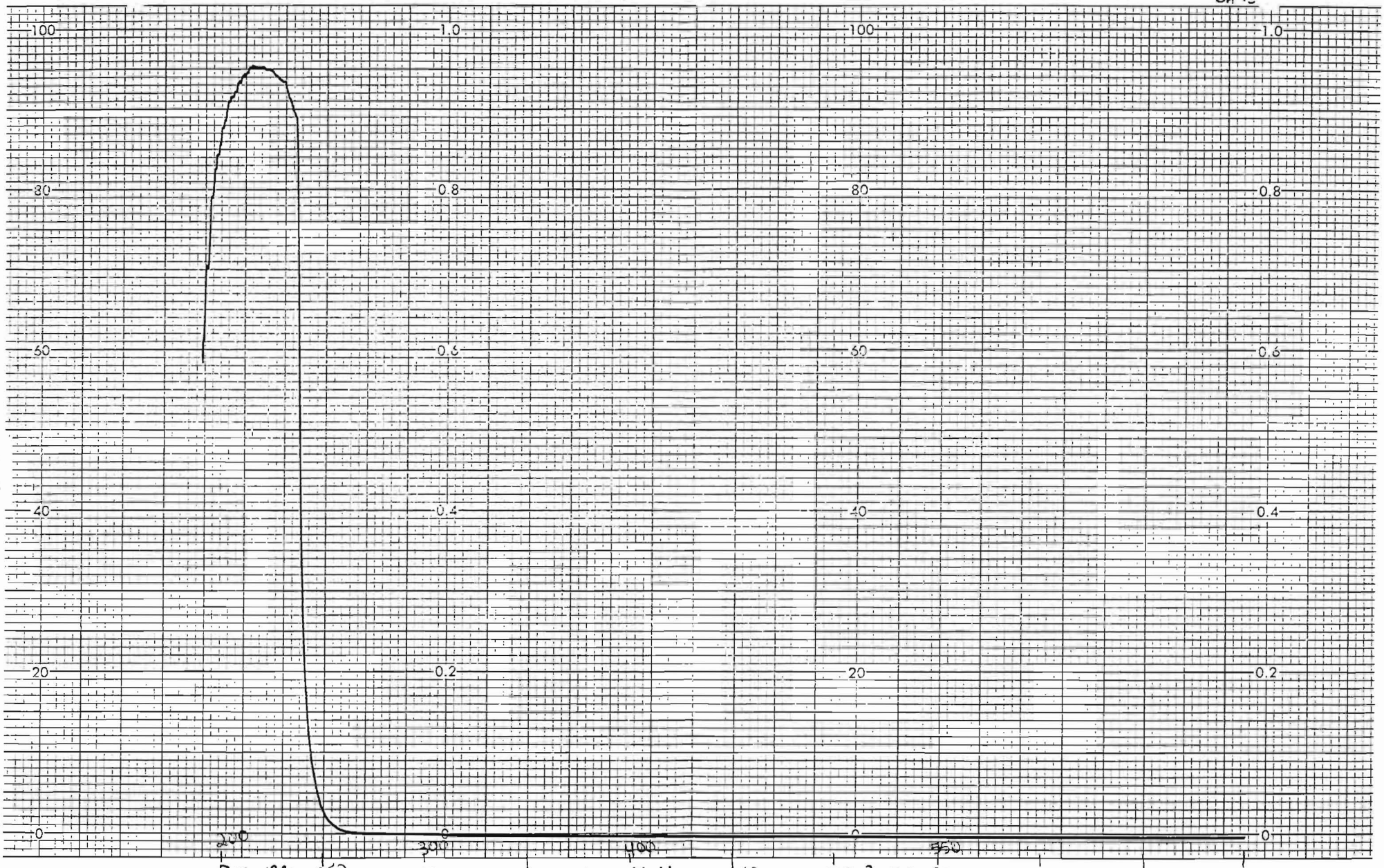

A 6

S#9

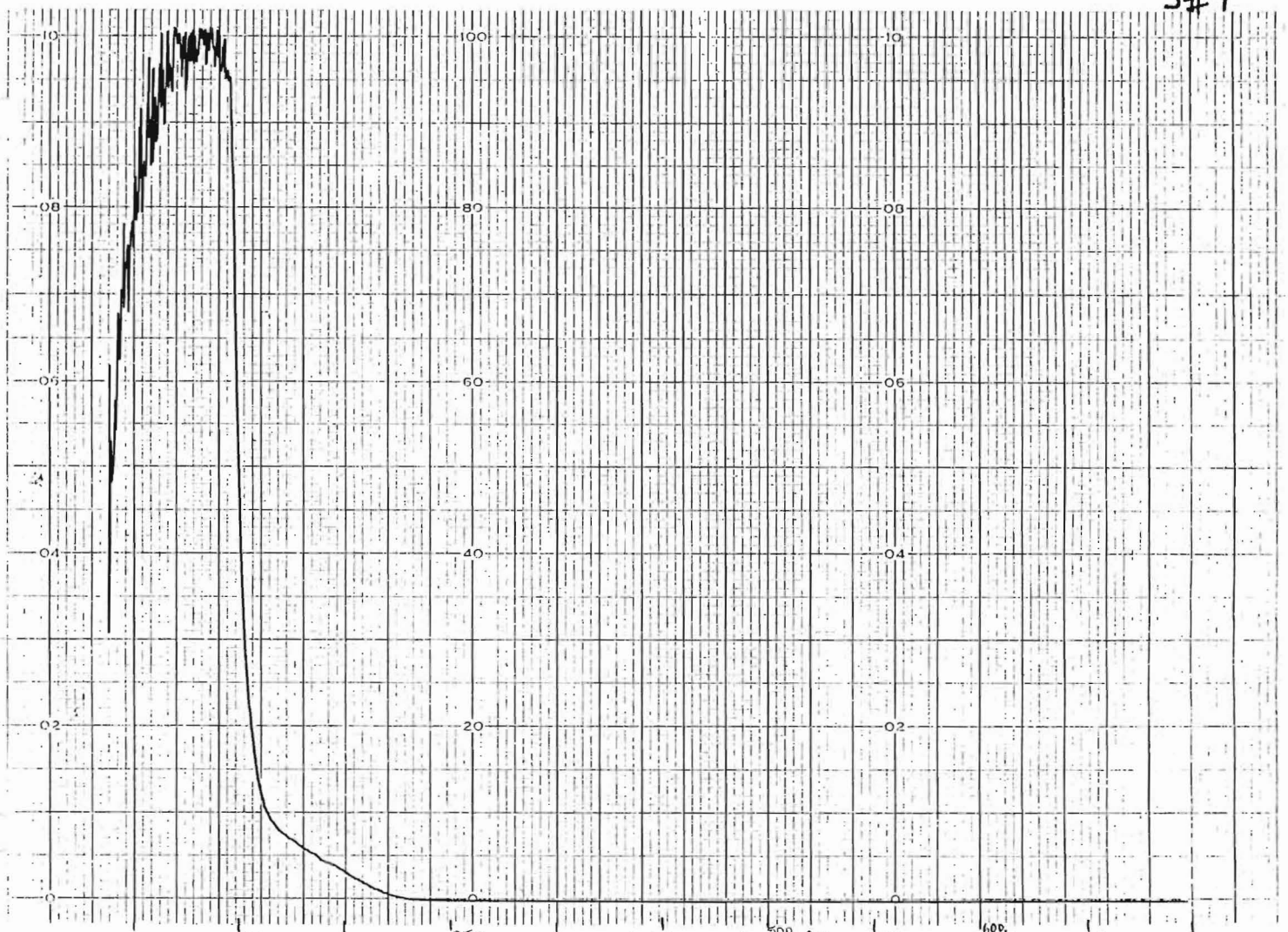

PART NO. B0093925 PERKIN ELMER PART NO. B0093925

S#8

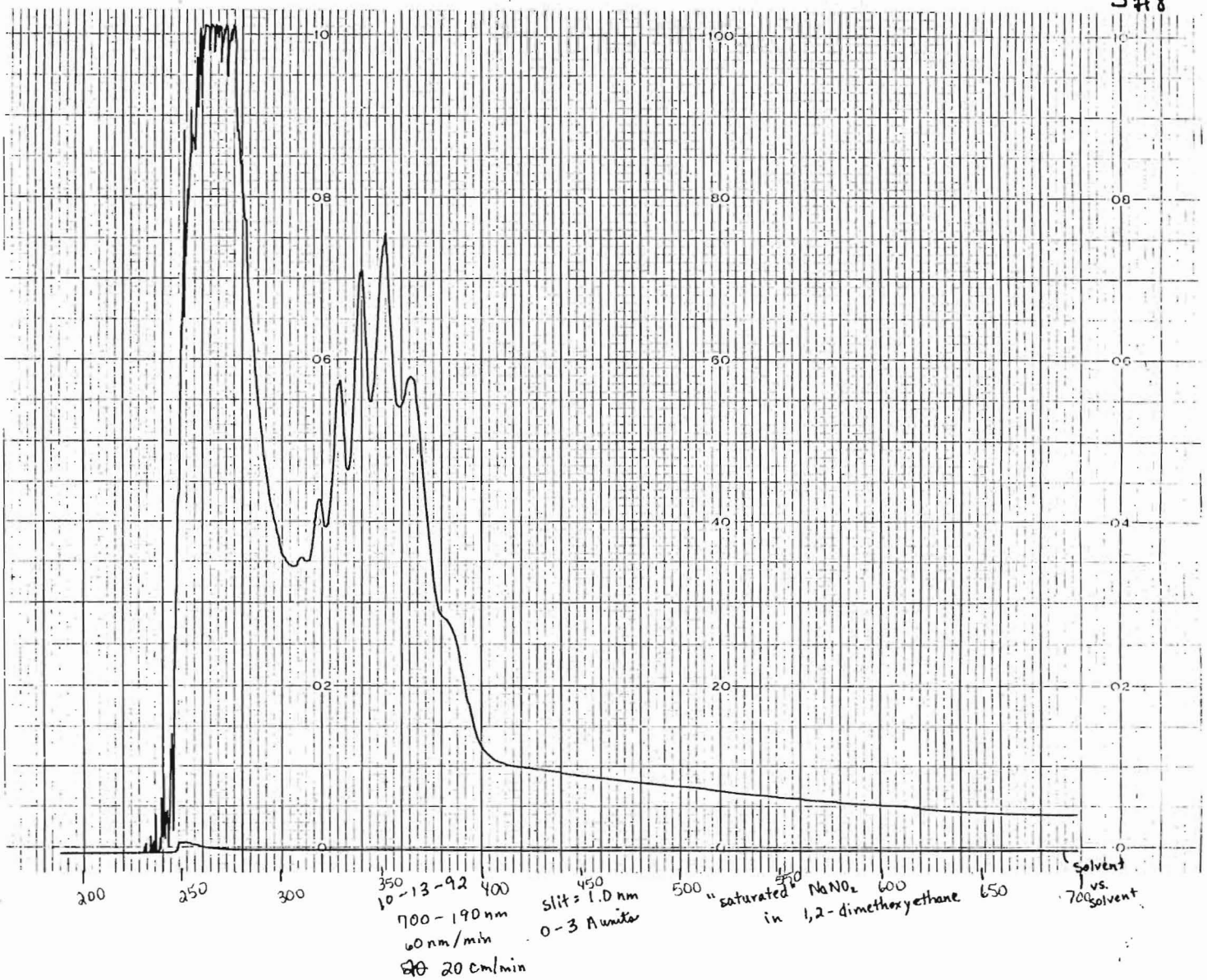

PERKIN ELMER PART NO. 80093025 PERKIN ELMER PART

S#19

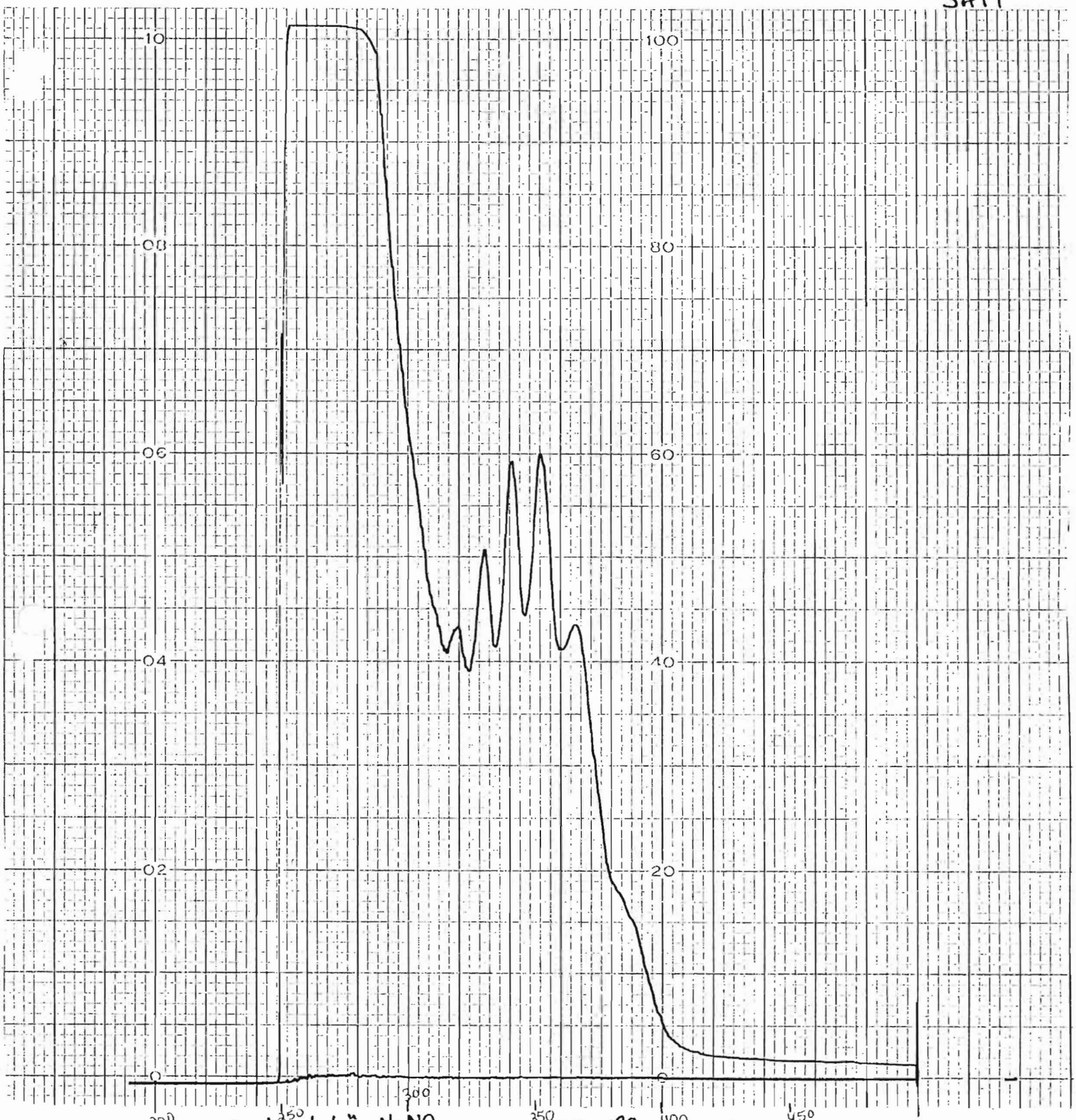

"saturated" $NaNO_2$ in "dry" 1,2-DME

500 - 190 nm

60 nm/min

20 cm/min

slit = 1.0nm

~~0 - 3 t~~

0 - 1 Aunits

11-6-92

PART NO. B0093925 PERKIN ELMER

S# 20

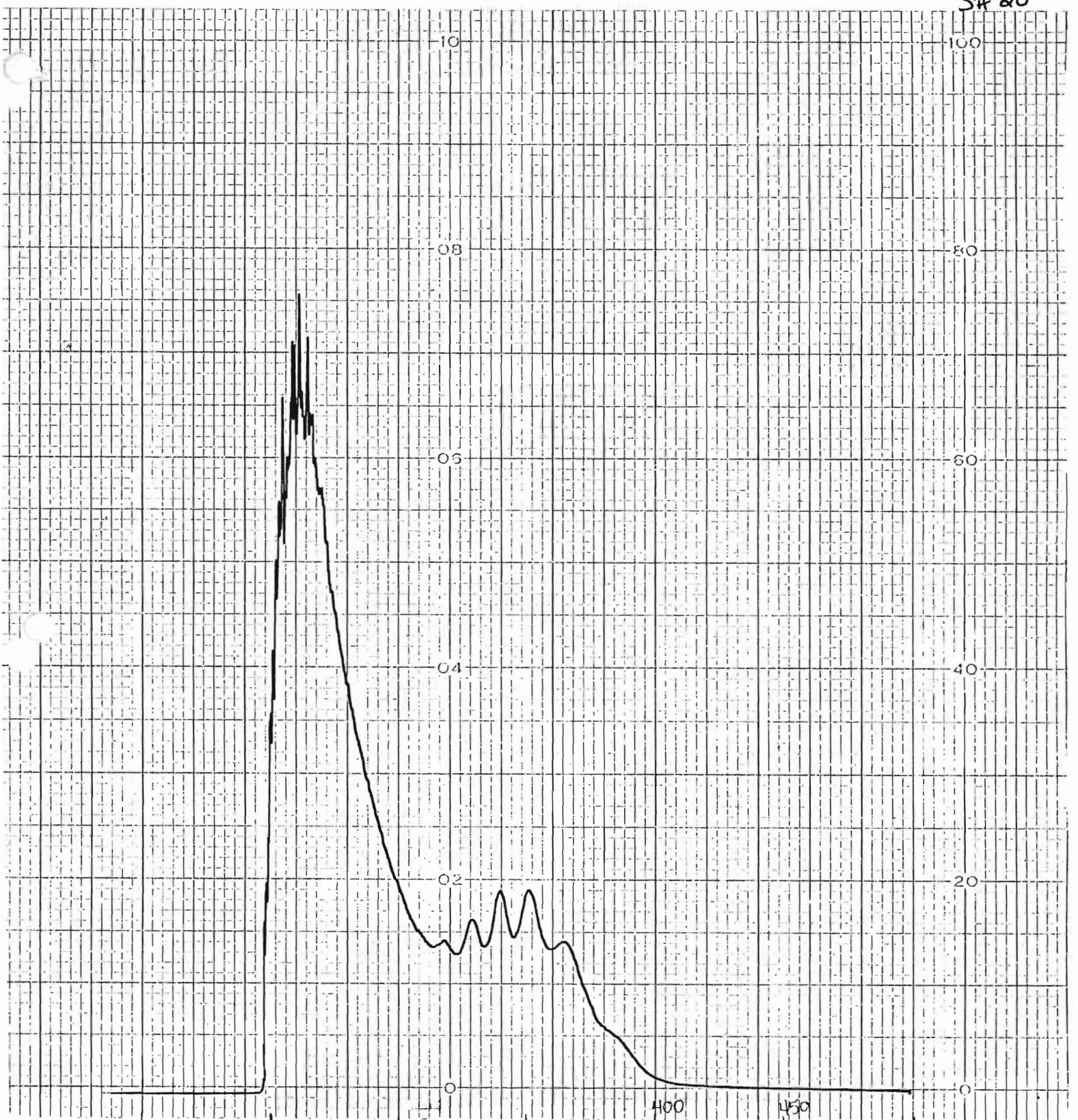

"saturated" $NaNO_2$ in "dry" 1,2-DME

500 – 190 nm
60 nm/min
20 cm/min
Slit = 1.0 nm

0 – 3 Aunits

11-6-92

S#3

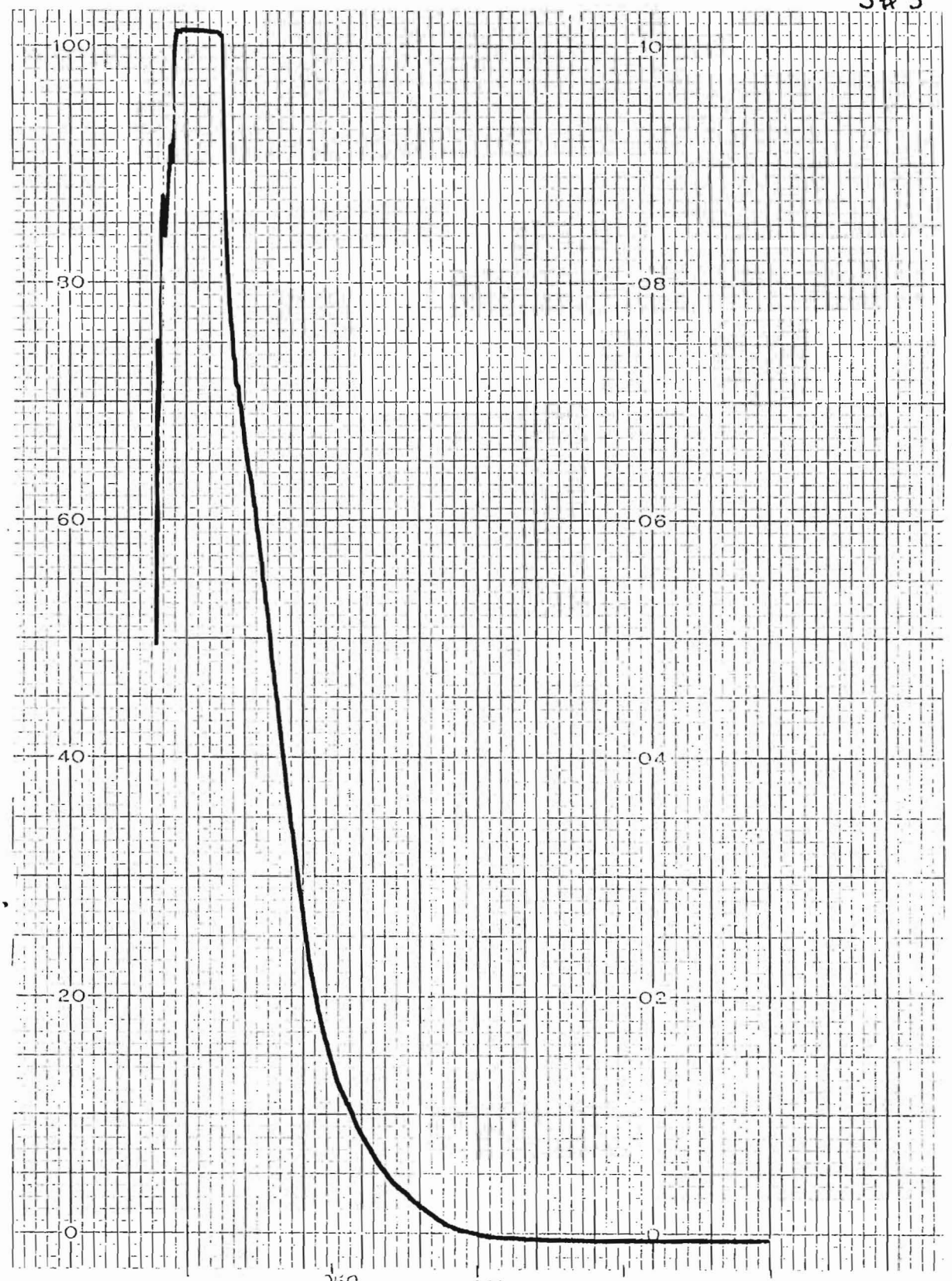

p-Dioxane vs. H_2O

400 - 190 nm
0 - 2 Aunits
60 nm/min
20 cm/min

slit = 1.0 nm

9-30-92

PERKIN ELMER

PART NO. B0003921

S#4

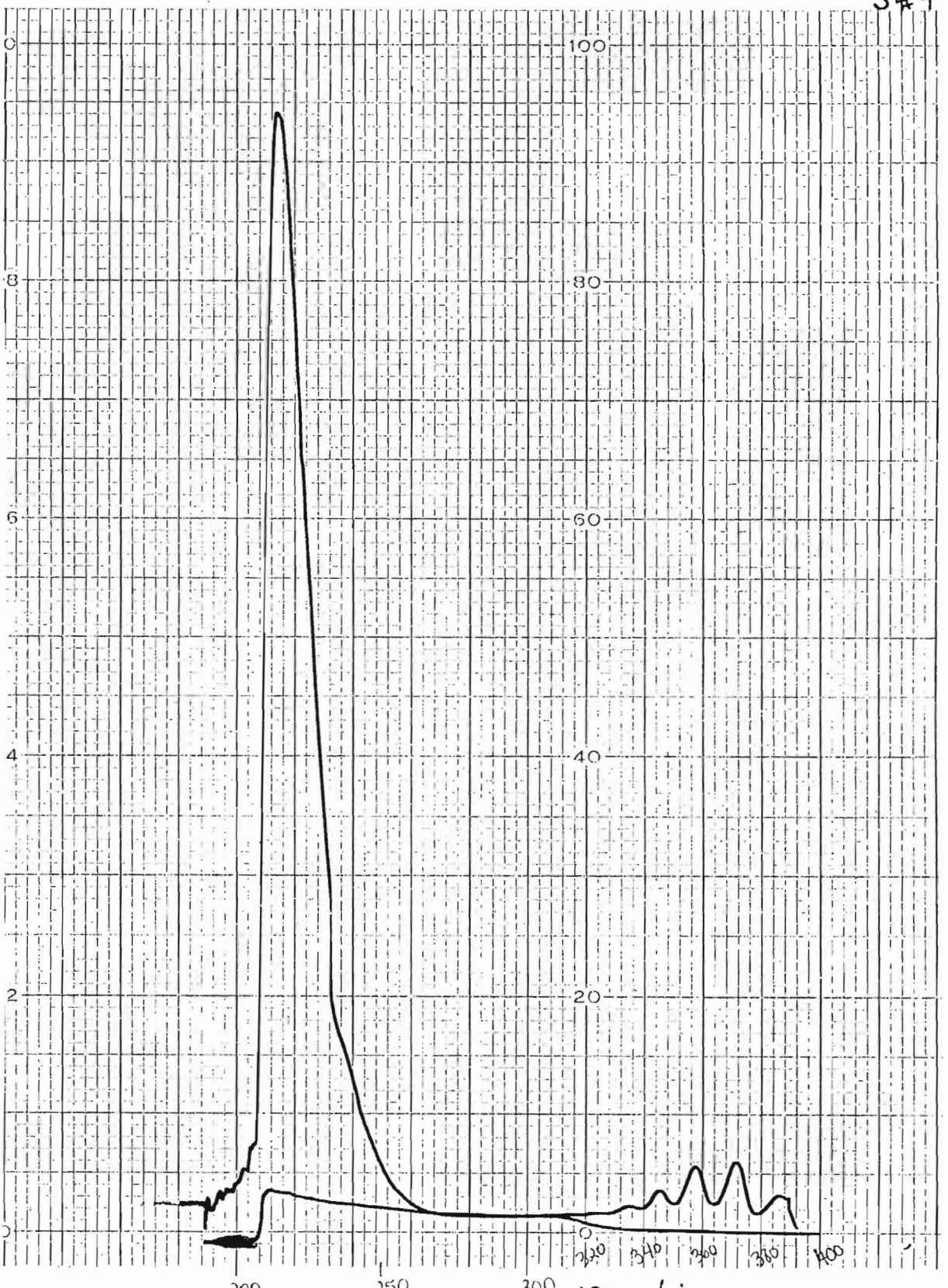

"saturated" $NaNO_2$ in P-Dioxane

120 nm/min
20 nm/cm
slit 0.25 nm
0 - 1.0 A units
400 - 190 nm

9-30-92

PERKIN ELMER

PART NO. B0093925

S# 5

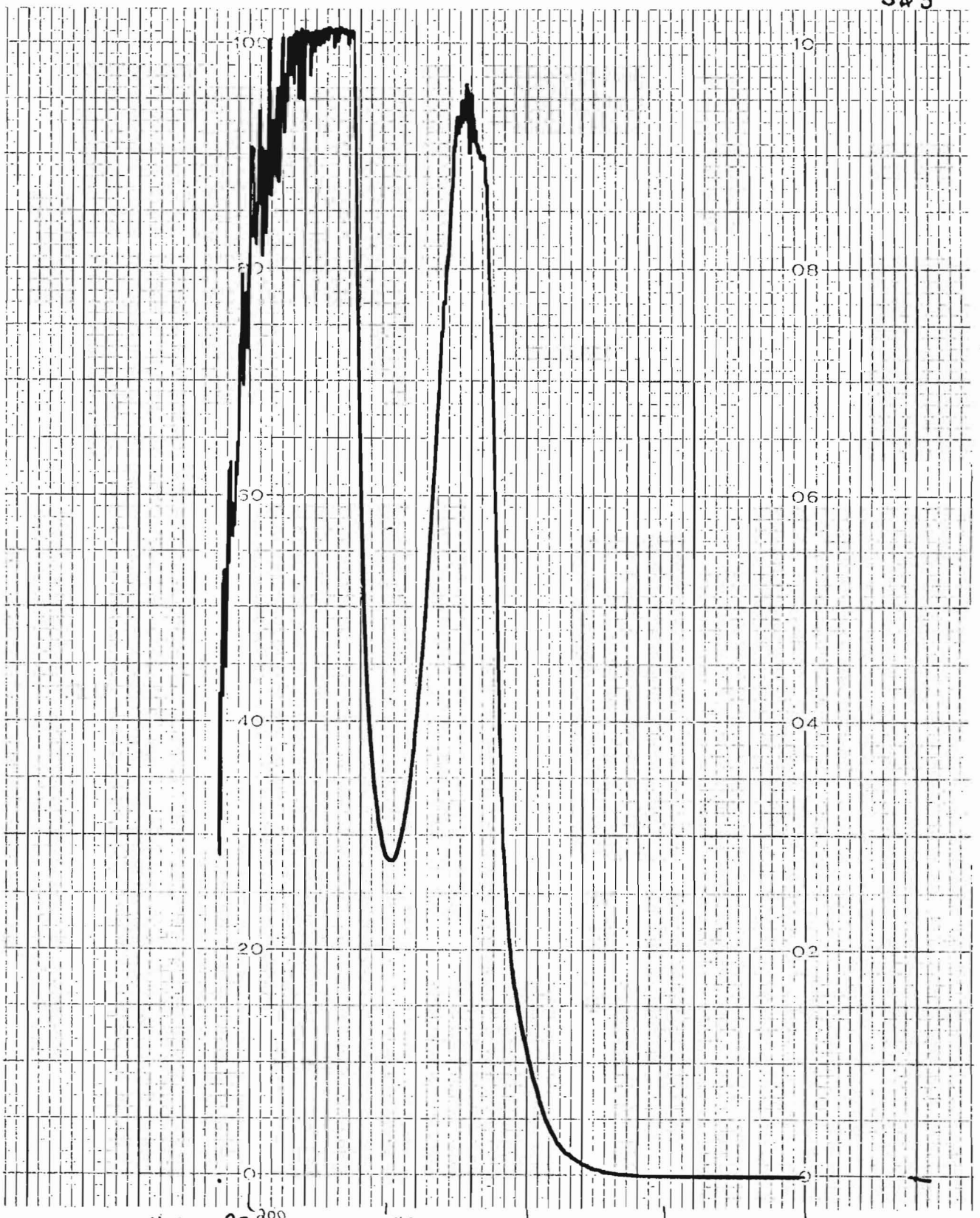

400 – 190 nm
60 nm/min
20 cm/min
slit = 1.0 nm
0 – 3 A units

THF vs. H_2O

9-30-92

S#6

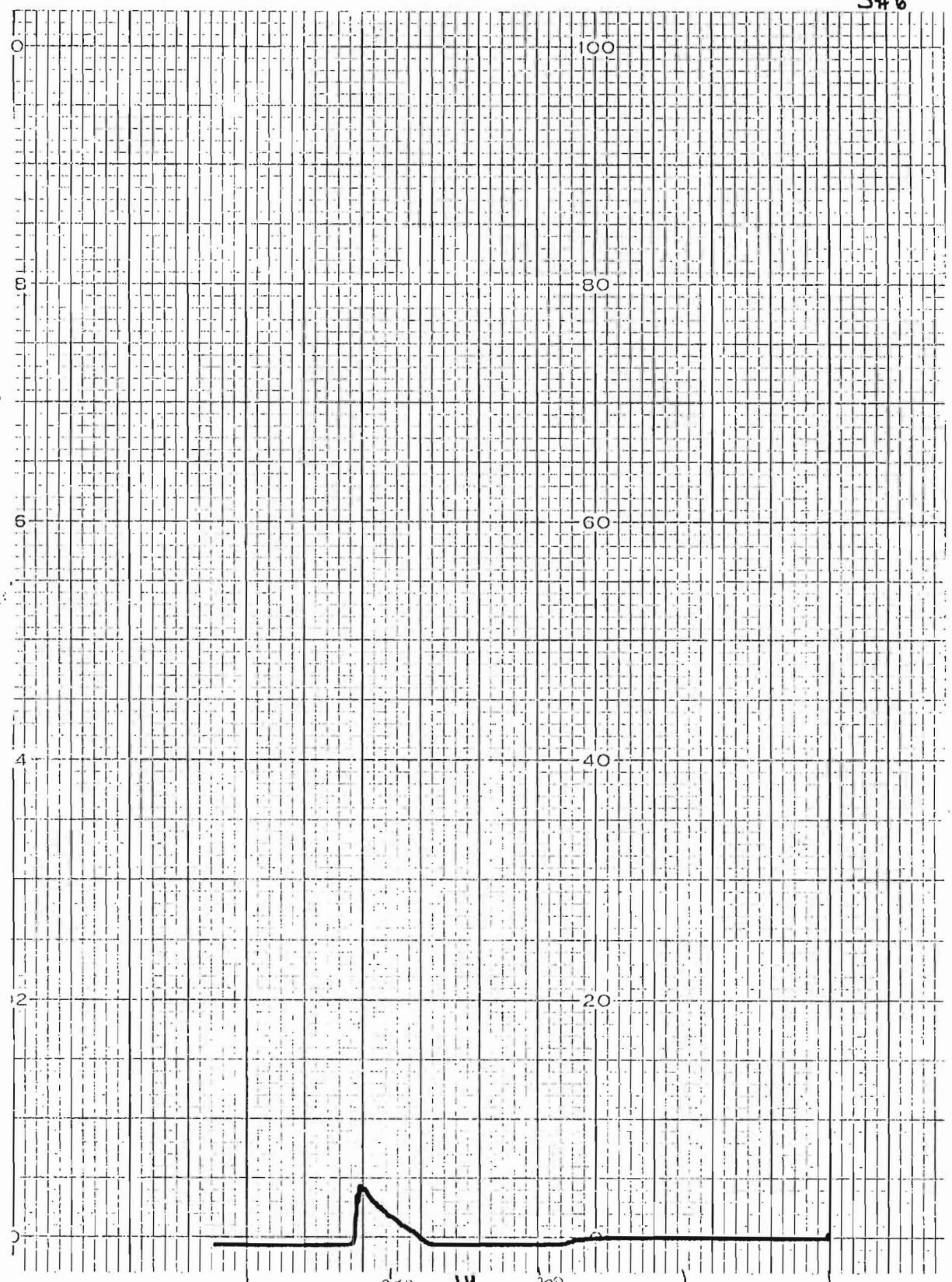

$NaNO_2$ "saturated"
THF

400 – 190nm
60nm/min
20 cm/min
0-2 Aunits
slit: 1.0nm

9-30-92

S#7

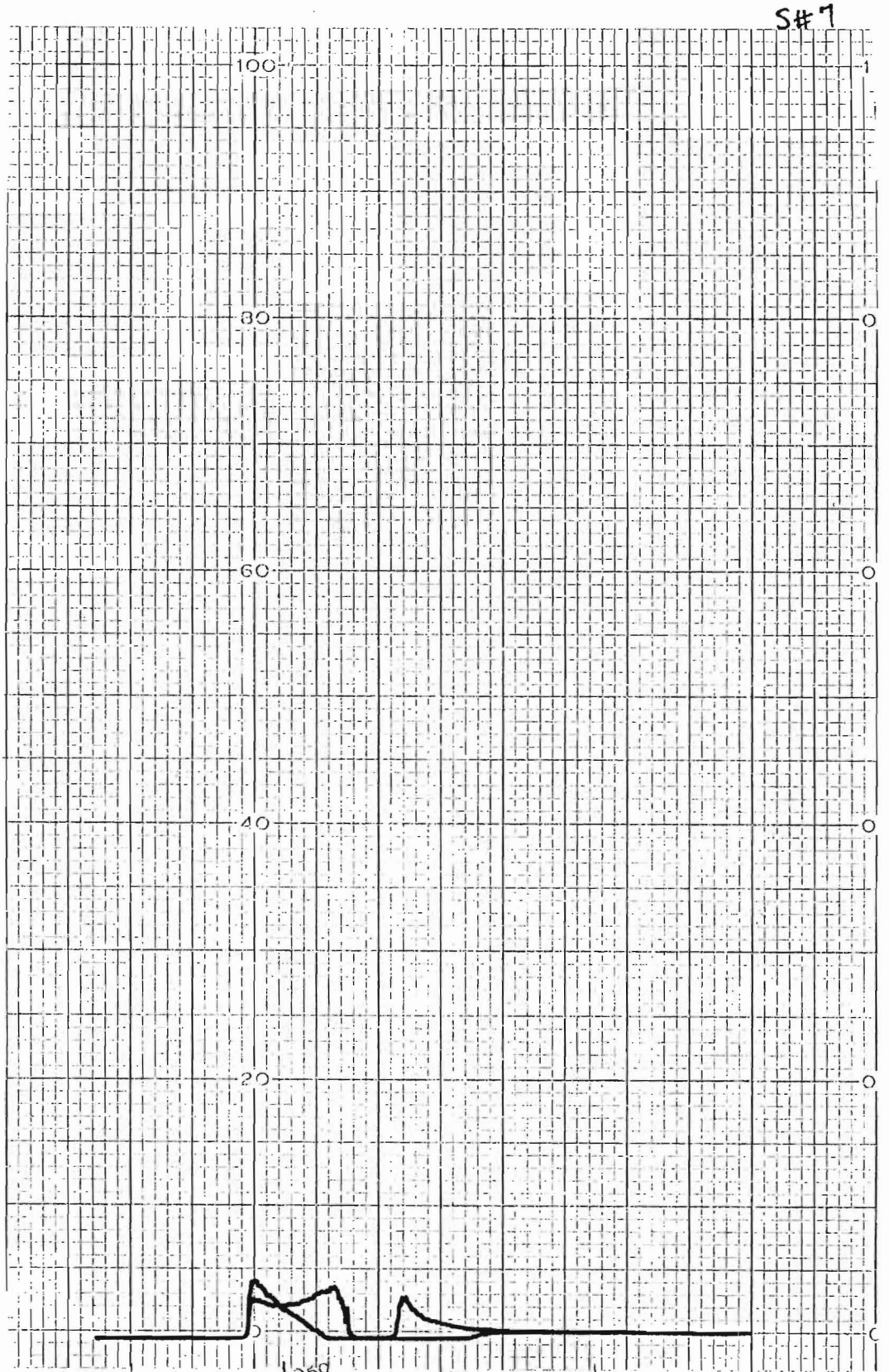

THF vs. THF "saturated"

$NaNO_2$ THF

400 – 190 nm

60 nm/min

20 cm/min

0 – 2 Aunits

Slit = 1.0 nm

9-30-92

PERKIN ELMER

S#11

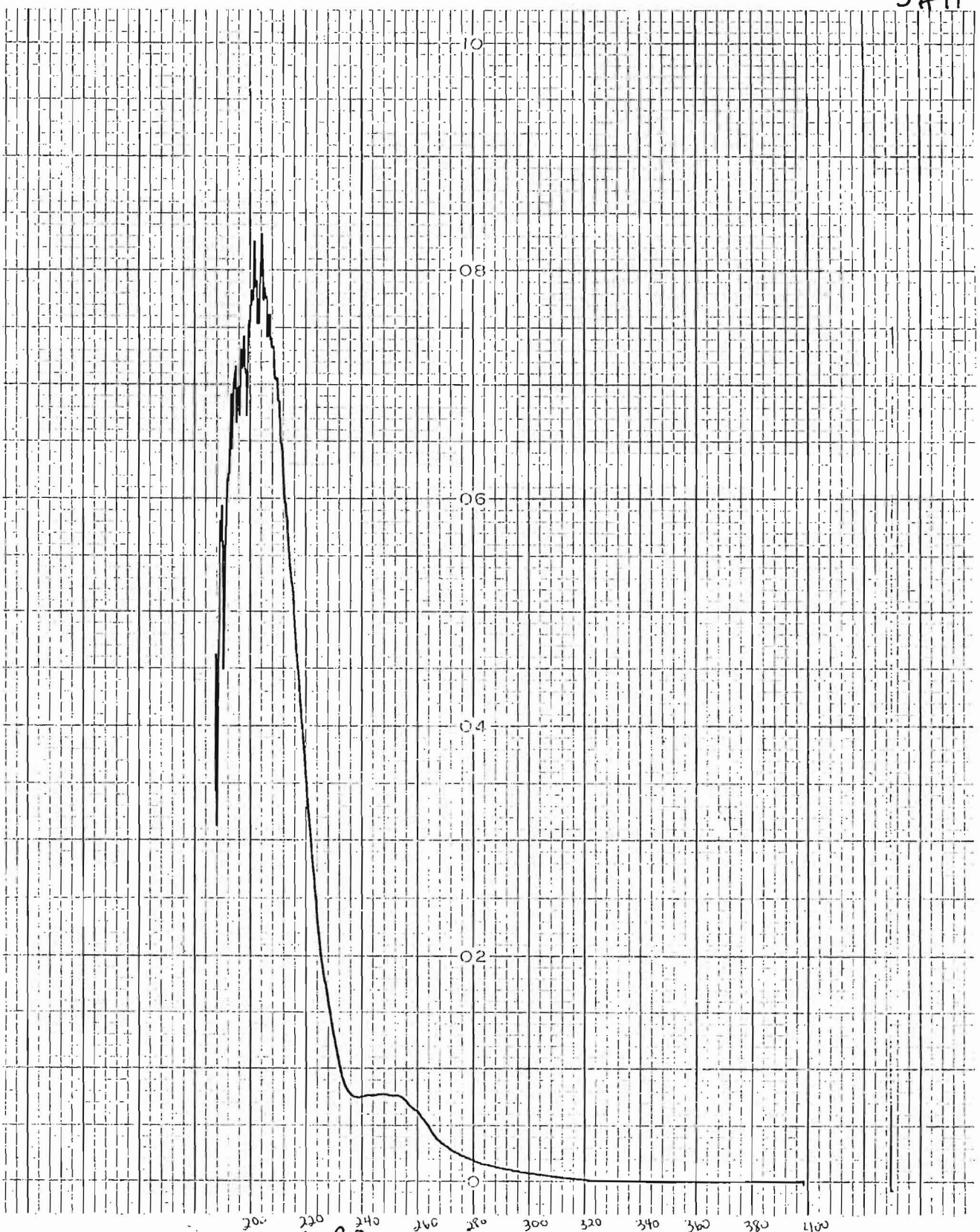

10-14-92

400 - 190 nm
60 nm/min
20 cm/min
0-3 A units
Slit = 1.0 nm

acetonitrile
vs
H_2O

PERKIN ELMER

PART NO. B0093925

S#10

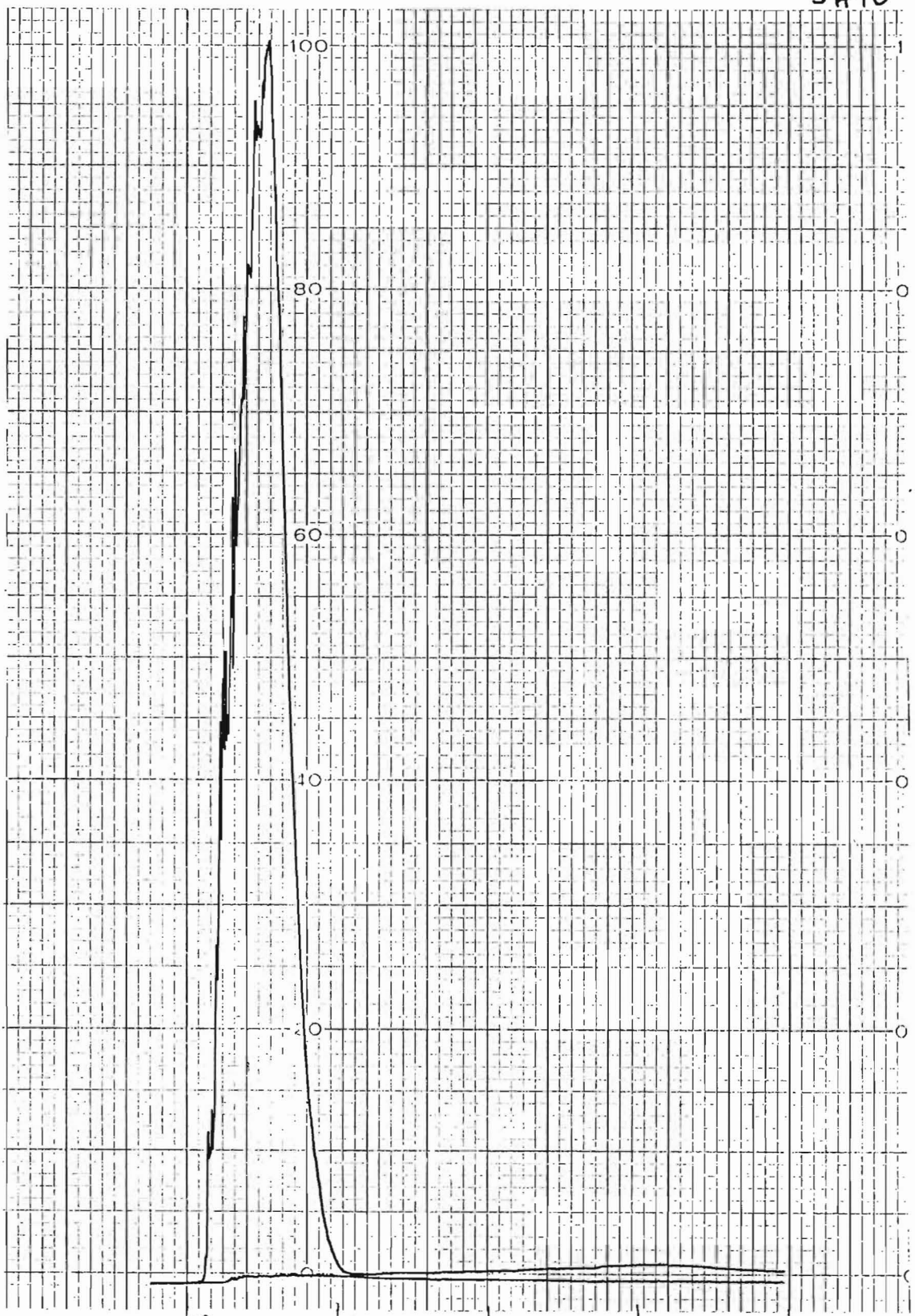

10-14-92
400 - 190 nm
60 nm/min
20 cm/min
0-2 A units
slit = 1.0 nm

"Saturated"
$NaNO_2$
in
acetonitrile

PERKIN-ELMER

S# 15

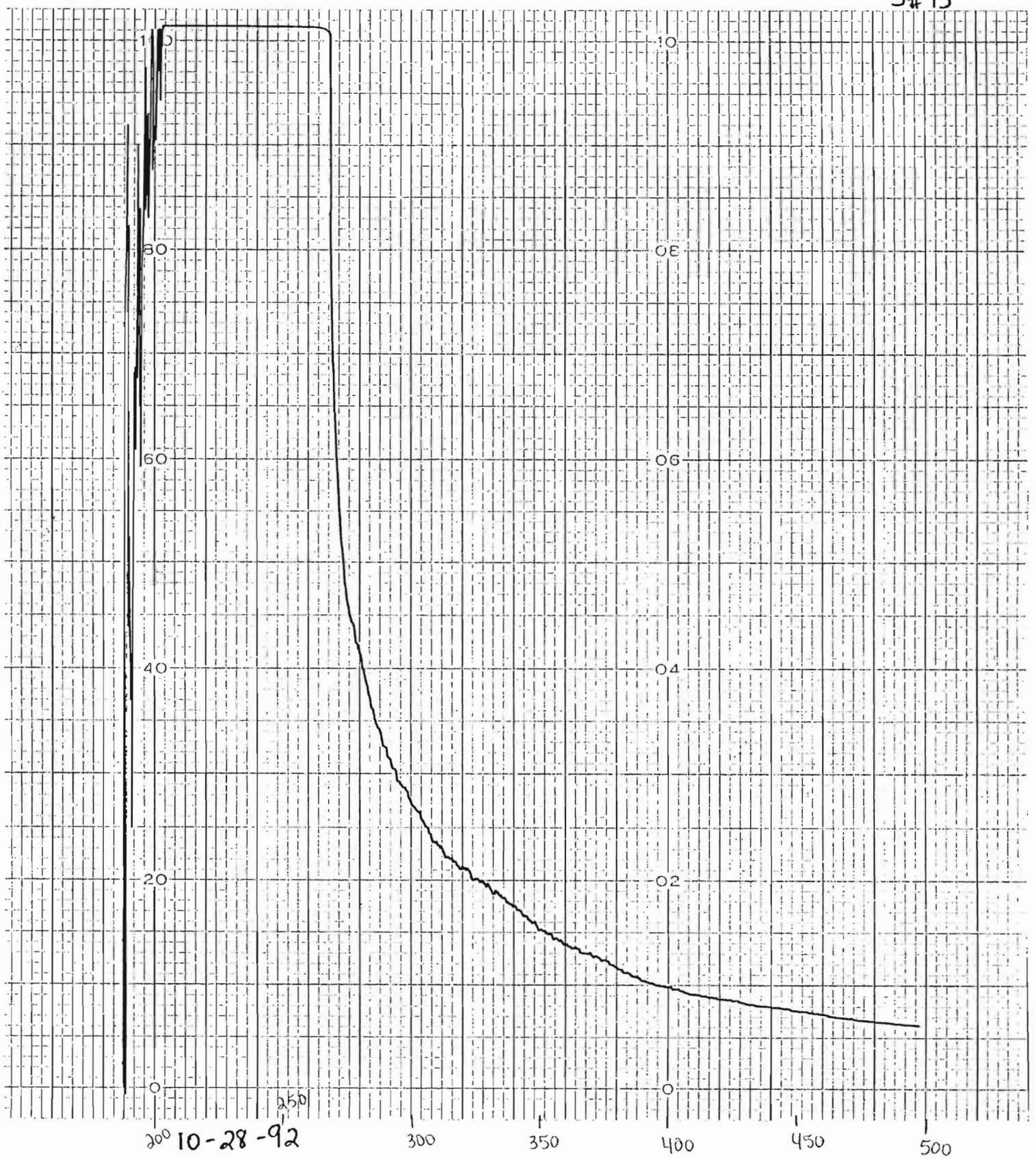

DMF vs. H_2O

20 cm/min

slit = 1.0 nm

500 - 190 nm

60 nm/min

0 - 1 A unit

PERKIN ELMER

PART NO. B0093025

S# 37 A

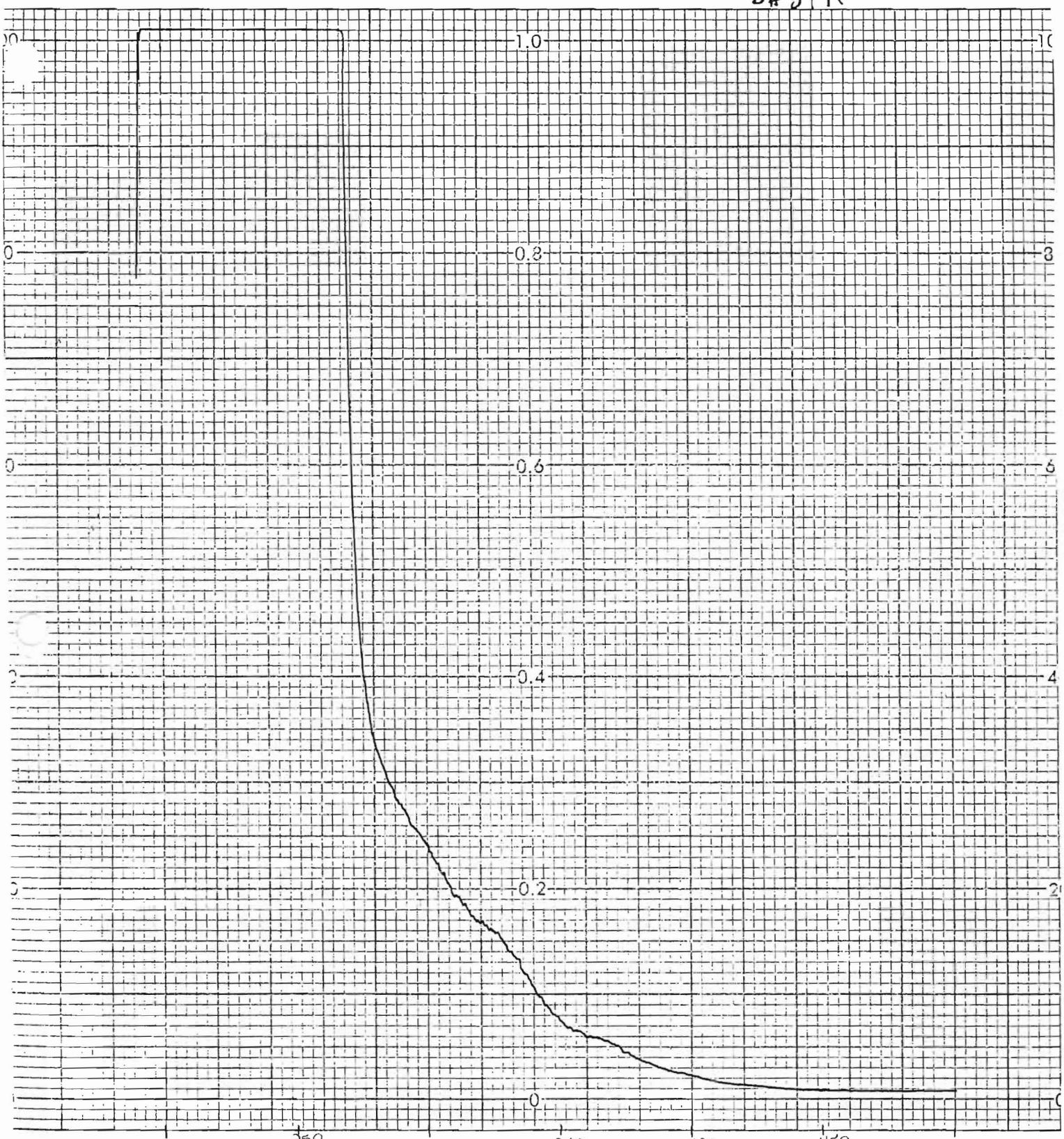

500 – 190 nm
60 nm/min
20 cm/min
slit = 1.0 nm

0 – 1 A unit

11-20-92

dry DMF
vs. H_2O

S# 38

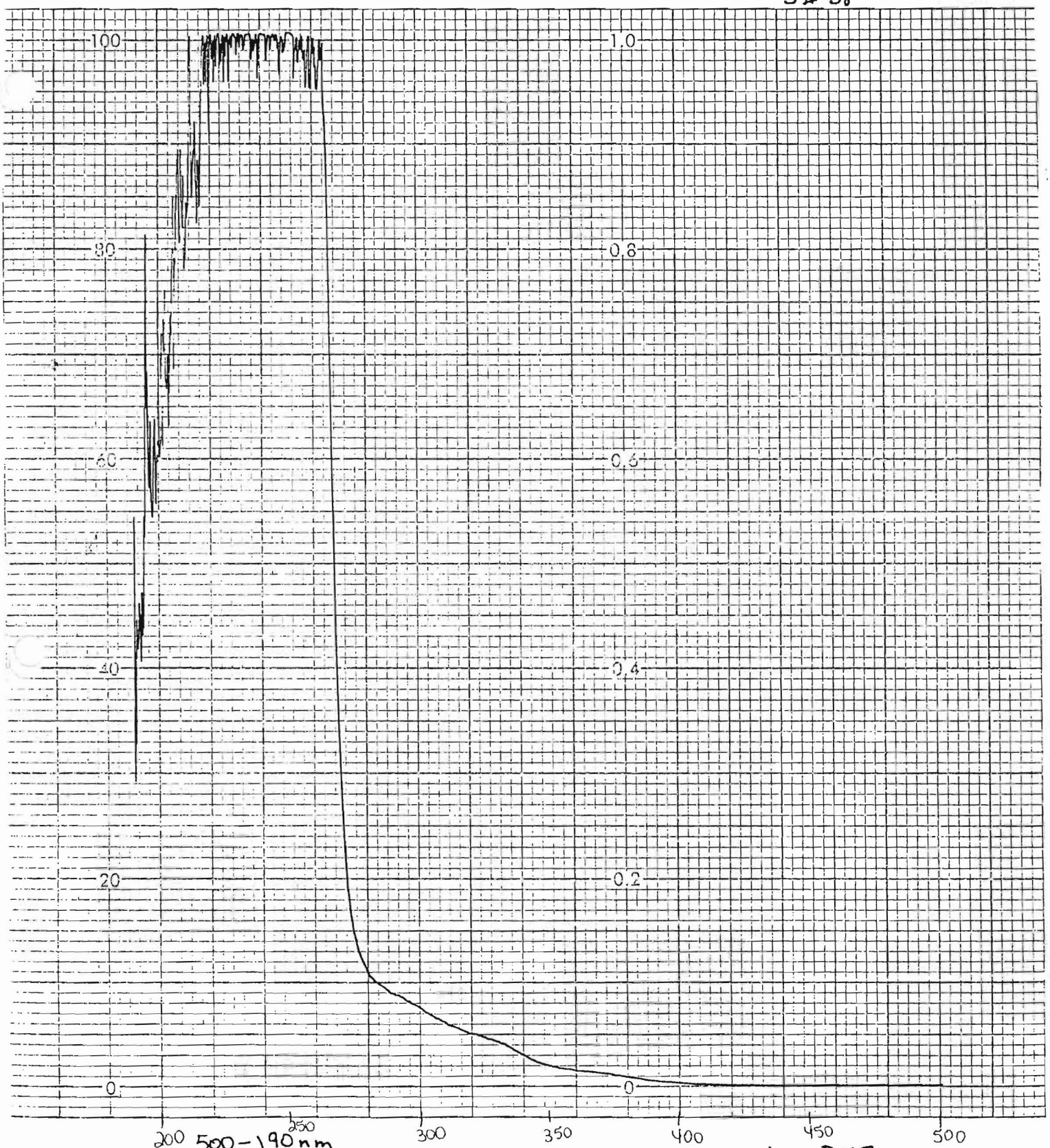

500-190 nm
60 nm/min
20 cm/min
slit = 1.0nm

0 - 3 Aunit

11-20-92

dry DMF
vs. H_2O

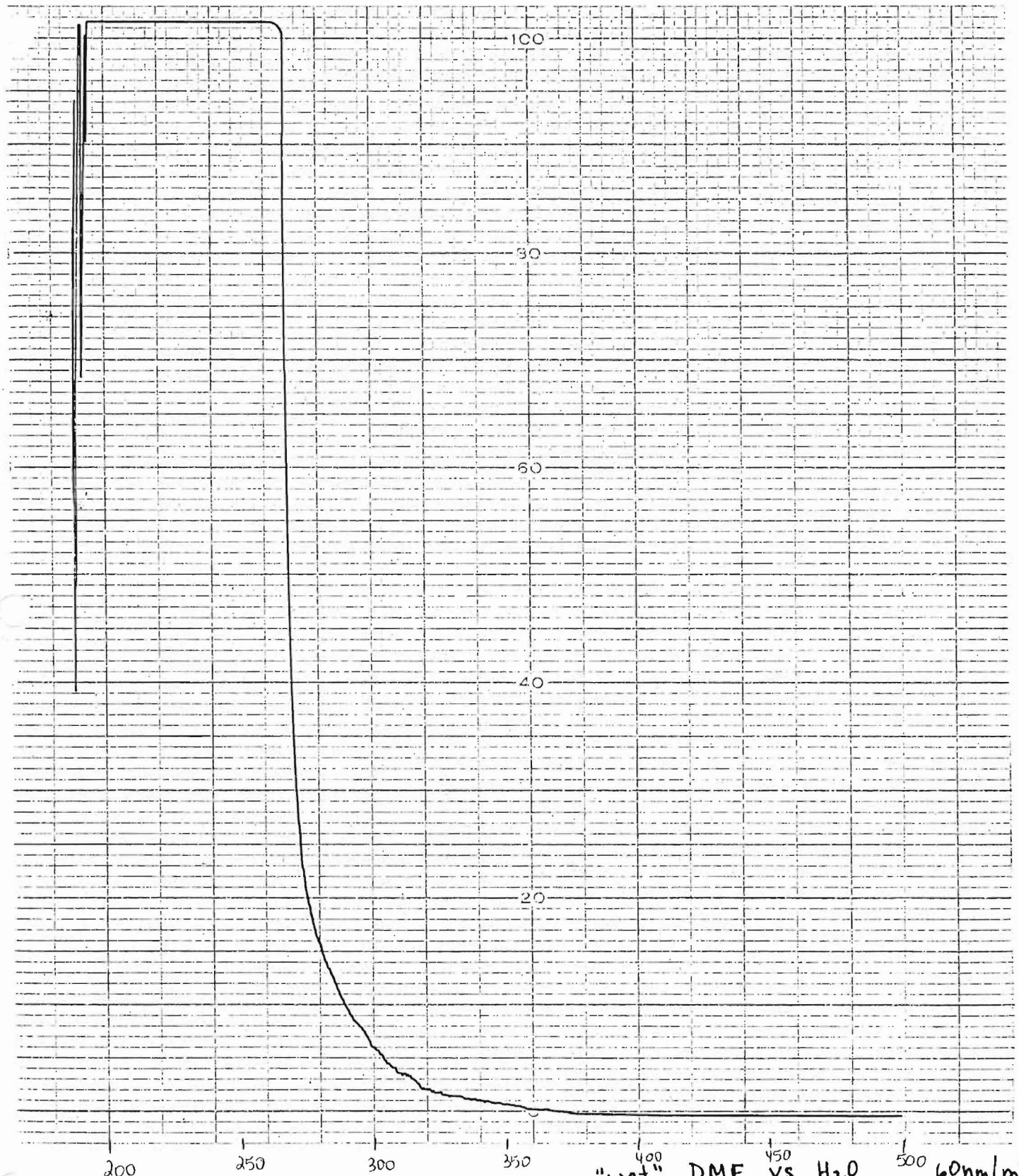

S#21

"wet" DMF vs H_2O

500 - 190nm

0 - 3 Aunit

60nm/min
20 nm/cm
slit = 1.0nm

S#39

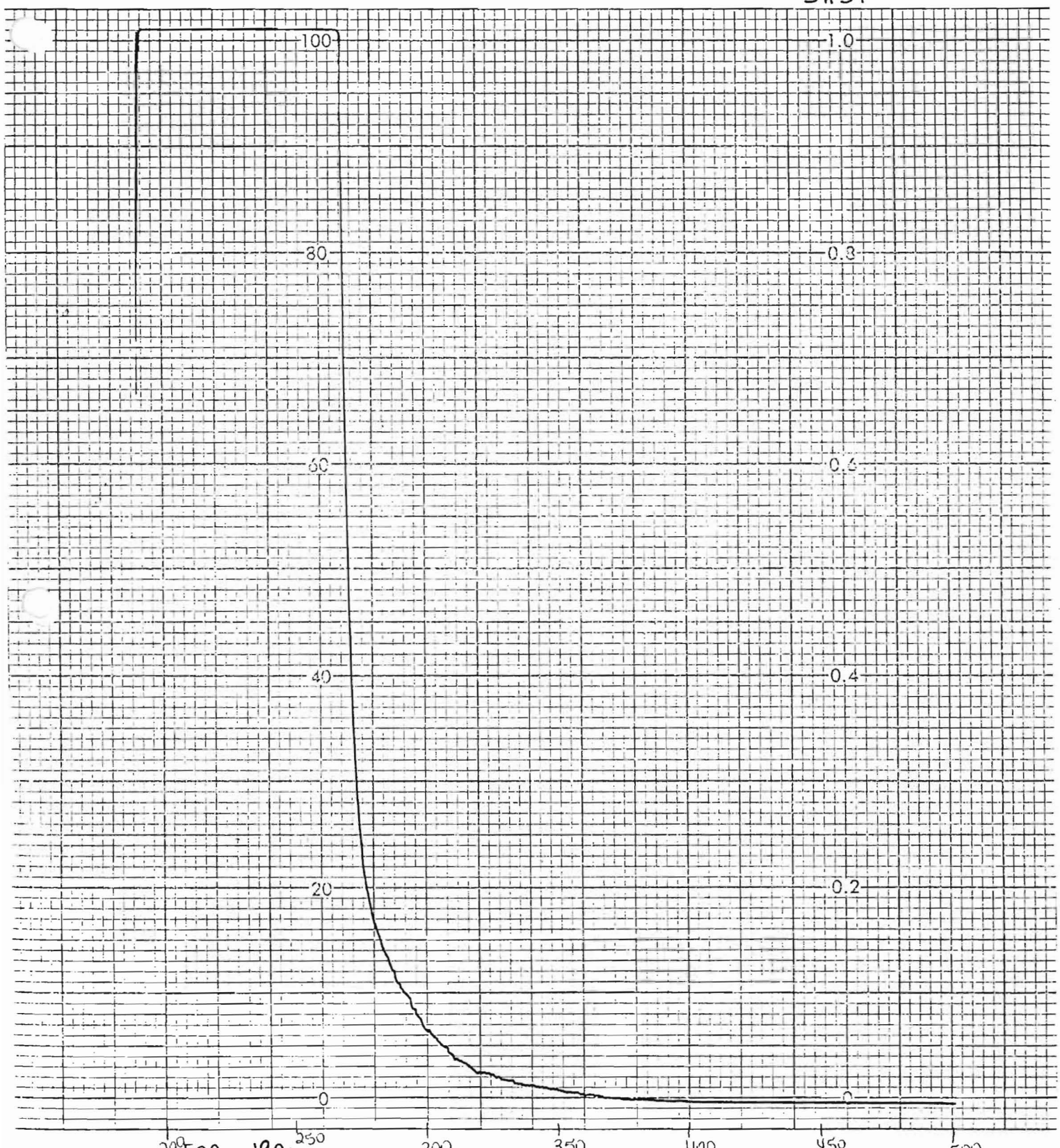

500 - 190 nm
60 nm/min
20 cm/min
slit = 1.0 nm

0 - 1 Aunit

11-20-92

wet DMF
vs. H_2O

S#40

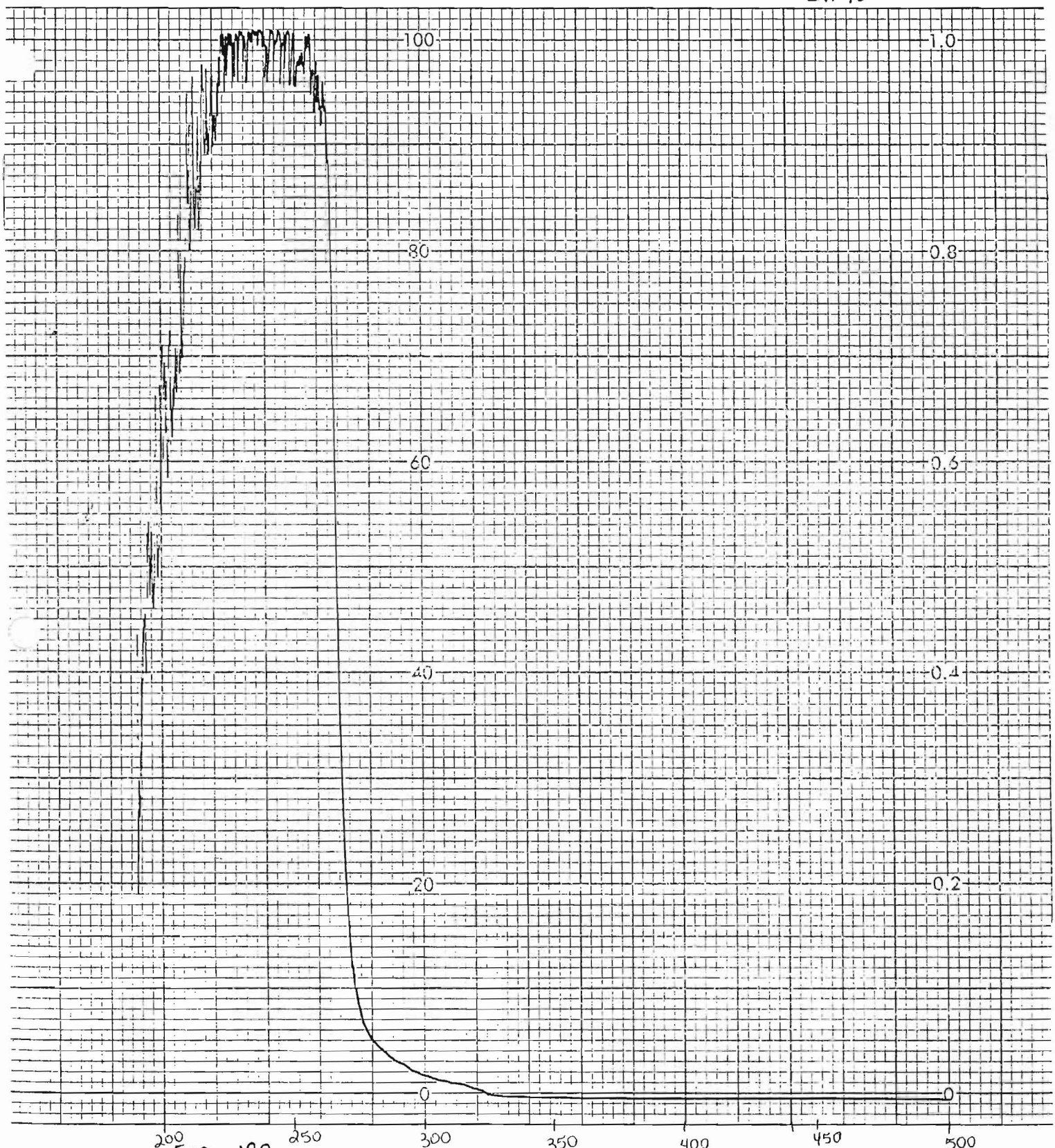

500 - 190nm
60 nm/min
20 cm/min
Slit = 1.0nm

0 - 3 Aunit

11-20-92

wet DMF
vs. H_2O

S# 14

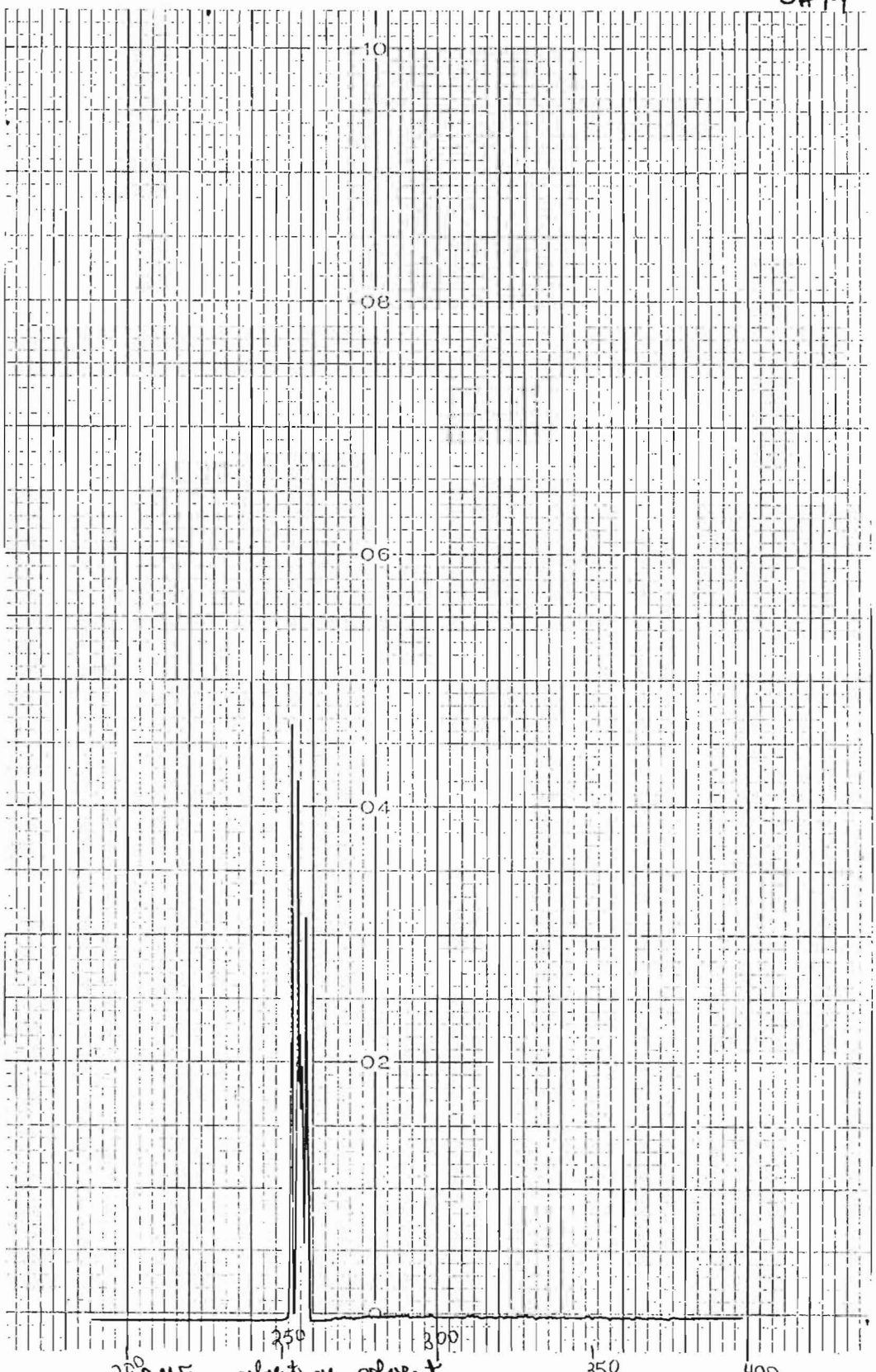

DMF solvent vs. solvent

10-28-92

400 - 190 nm
120 nm/min
20 cm/min
slit = 1.0 nm

0 - 1 Aunit

S#28

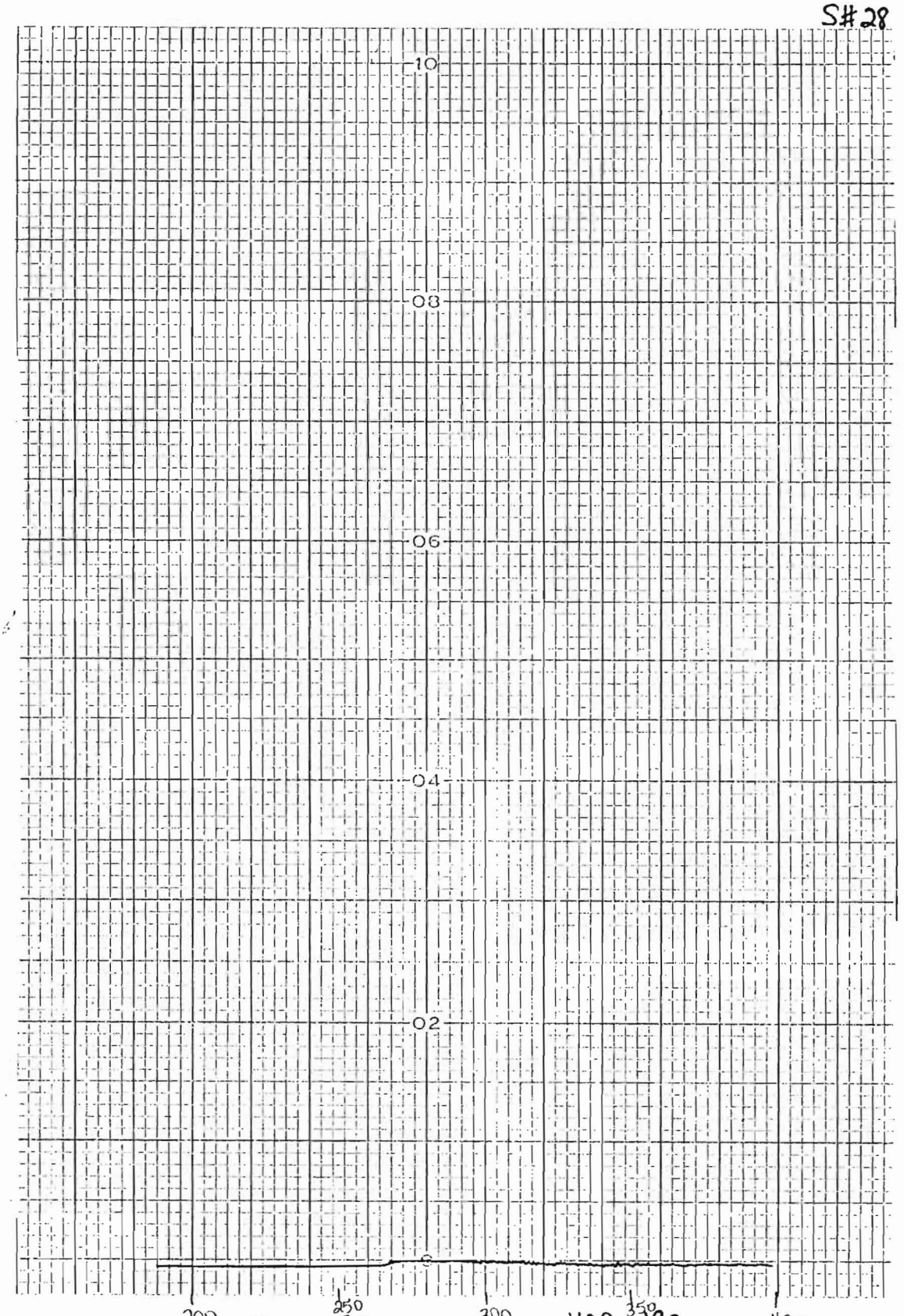

11-11-92

DMF vs. DMF

400 - 190 nm
60 nm/min
20 cm/min
slit = 1.0nm
0 - 1 Aunit

MER

PART NO. B0093925

S#12

"saturated" $NaNO_2$ in DMF

400 - 190 nm
60 nm/min
20 cm/min
slit = 1.0 nm

0 - 1 Aunit

10-28-92

S#13

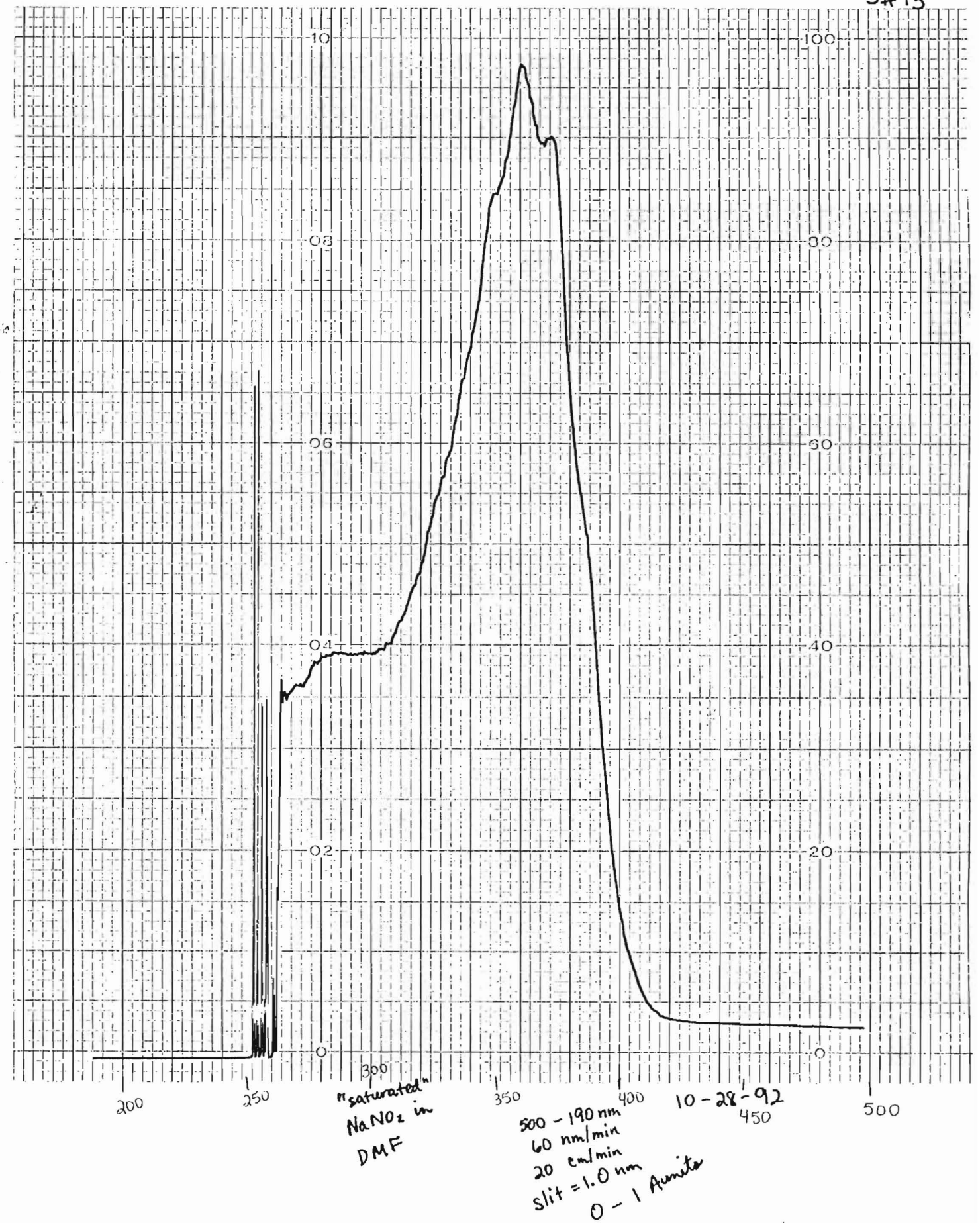
1.0
0.8
0.6
0.4
0.2
0
100
80
60
40
20
0
200
250
300
350
400
450
500
"saturated" NaNO2 in DMF
500 - 190 nm
60 nm/min
20 cm/min
slit = 1.0 nm
0 - 1 Aunits
10-28-92

S#16

"saturated" $NaNO_2$ in DMF

500 - 190 nm
60 nm/min
20 cm/min
Slit 1.0 nm
0 - 1 Aunit

11 - 4 - 92

S#30

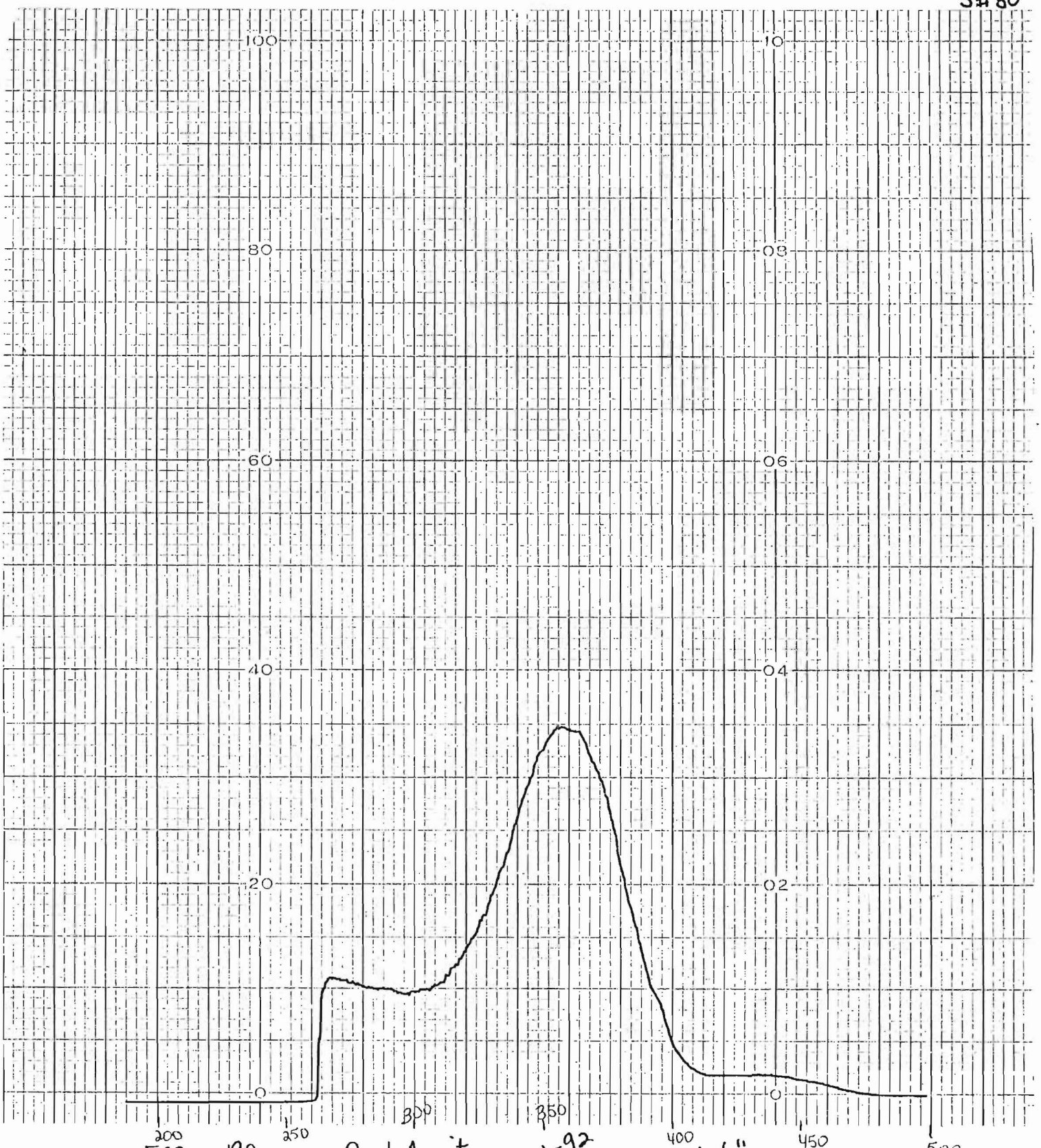

500 - 190 nm
60 nm/min
20 cm/min
slit = 1.0 nm

0 - 1 Aunit

11-11-92

"saturated" $NaNO_2$ in "wet" DMF

PERKIN ELMER

PART NO. B009392

S# 27

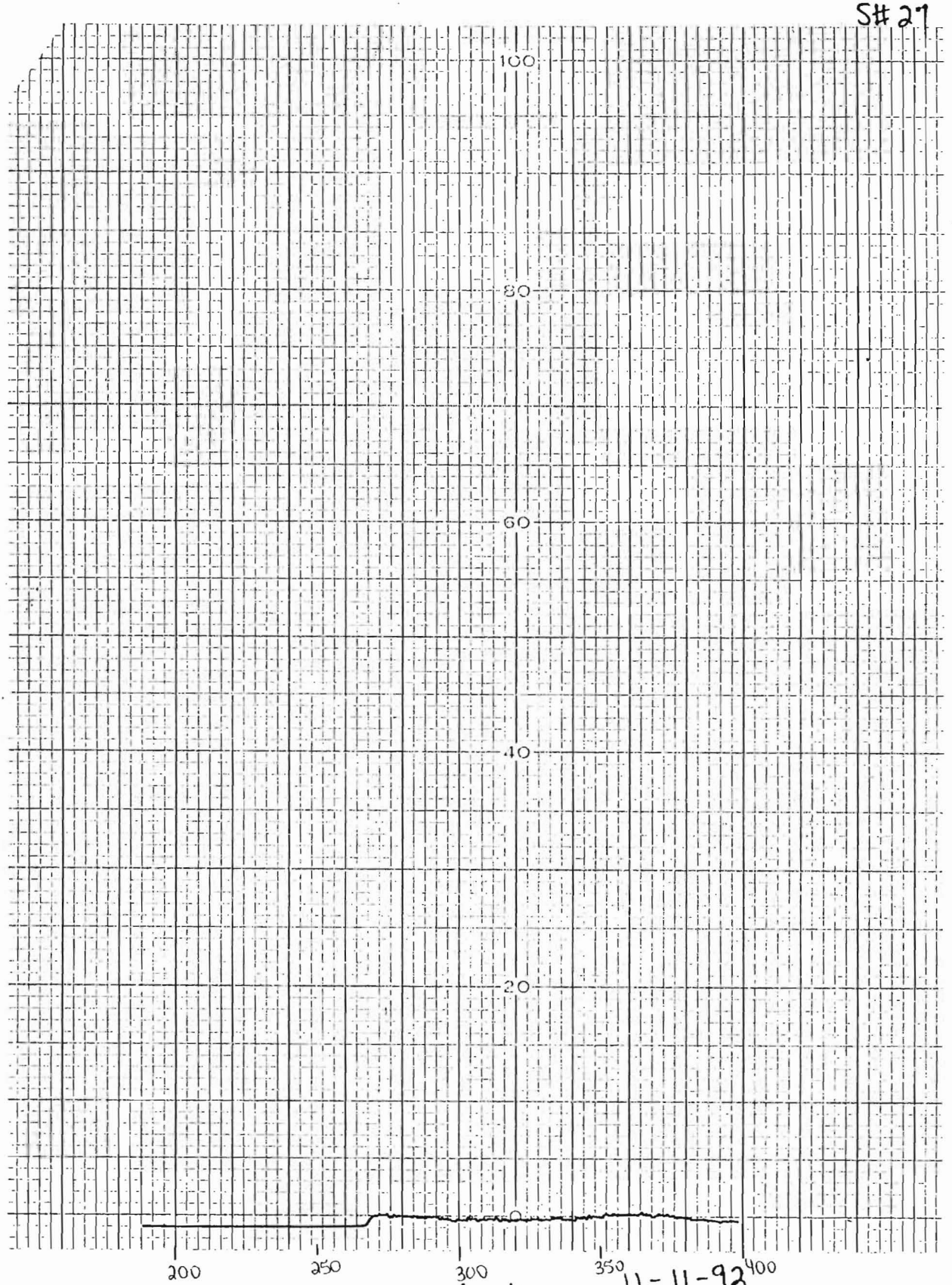

11-11-92

400-190 nm
60 nm/min
20 cm/min
slit = 1.0 nm

0-1 Aunit

2.0×10^{-3} M $NaNO_2$ in DMF

S# 26

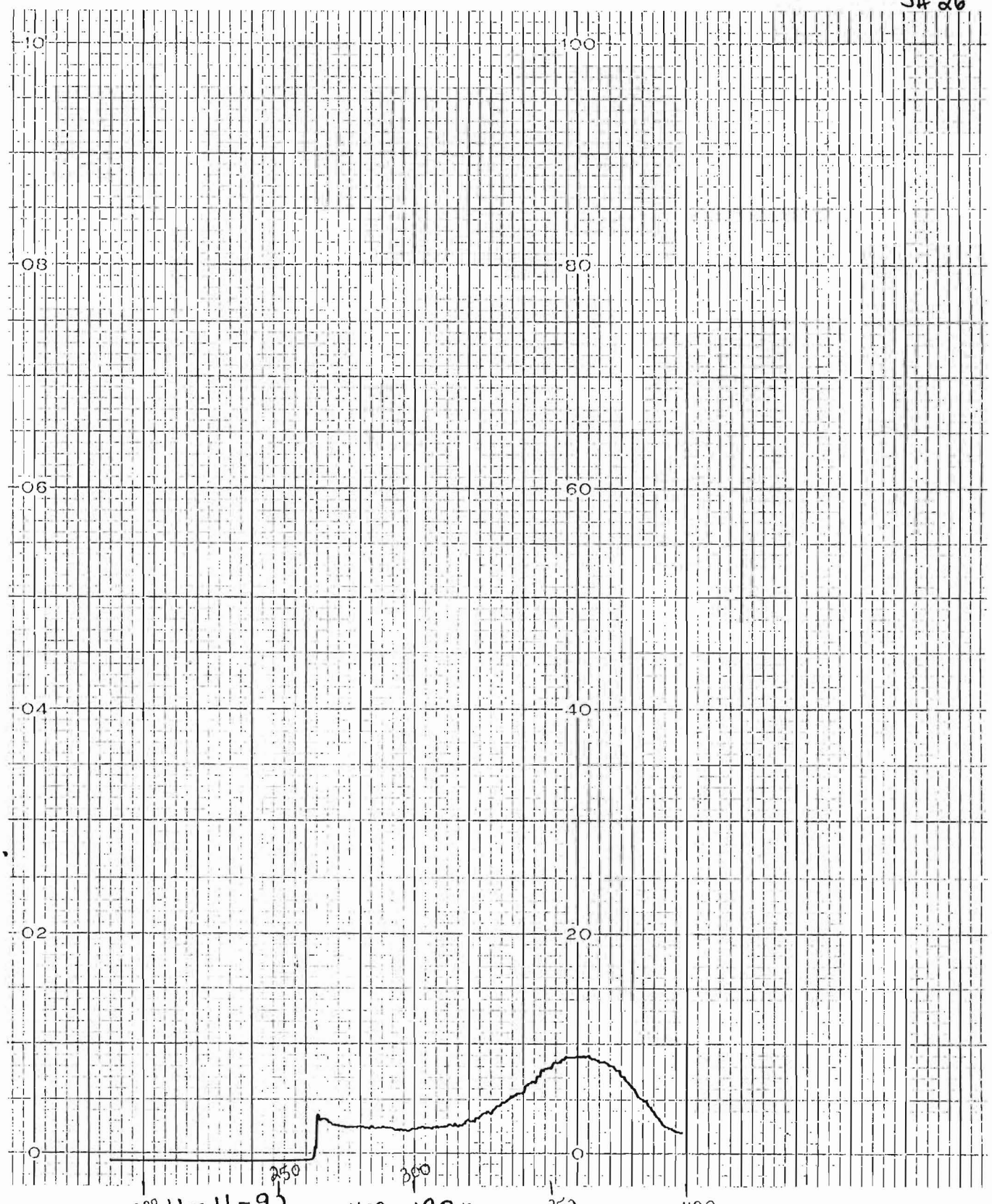

11-11-92

400 - 190 nm
60 nm/min
20 cm/min
slit = 1.0 nm
0 - 1 A unit

2.8×10^{-3} M $NaNO_2$ in DMF

S# 25

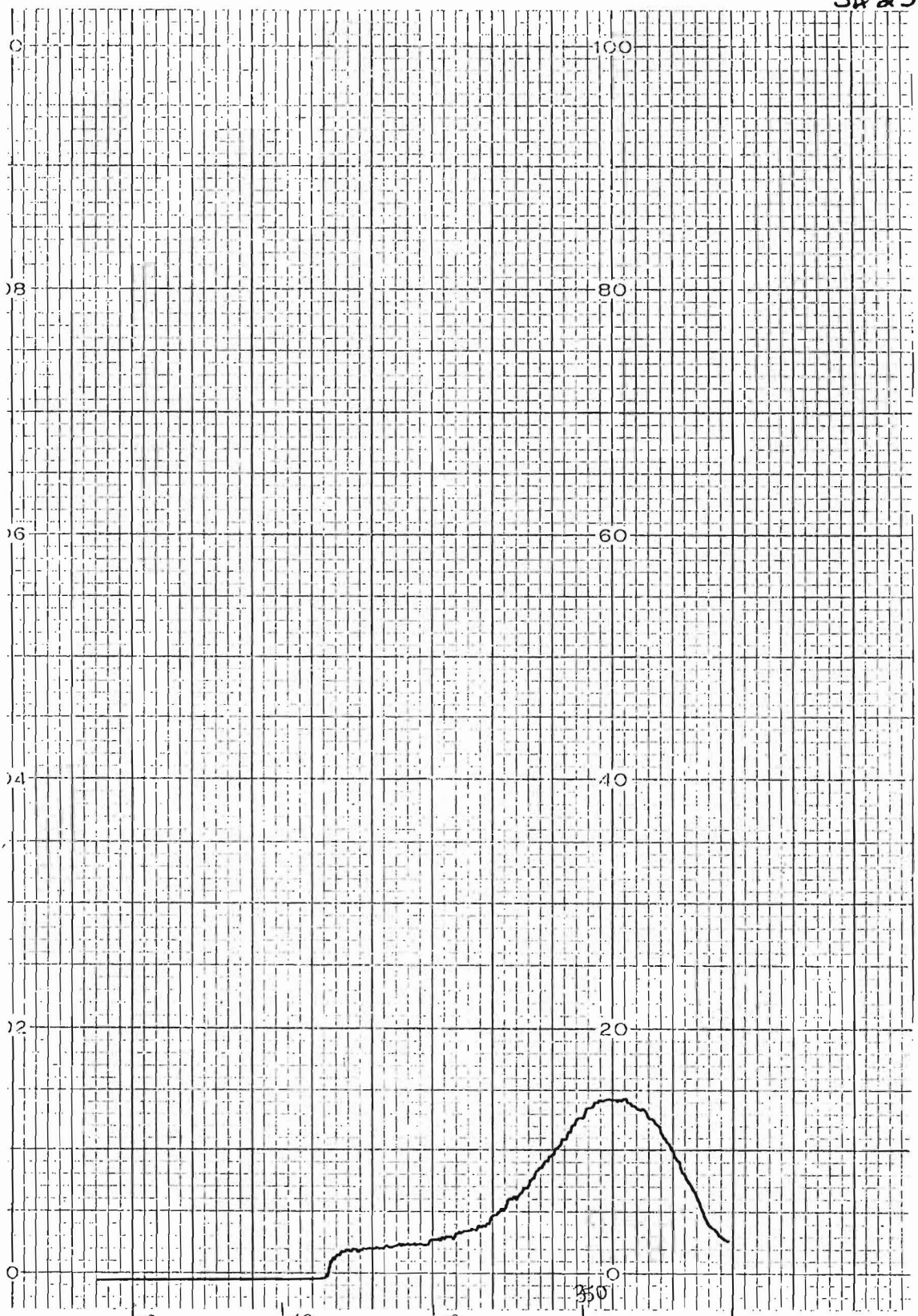

400 - 190 nm
60 nm/min
20 cm/min
Slit = 1.0 nm

0-1 Aunit

11-11-92

5.8×10^{-3} M $NaNO_2$
in DMF

S#24

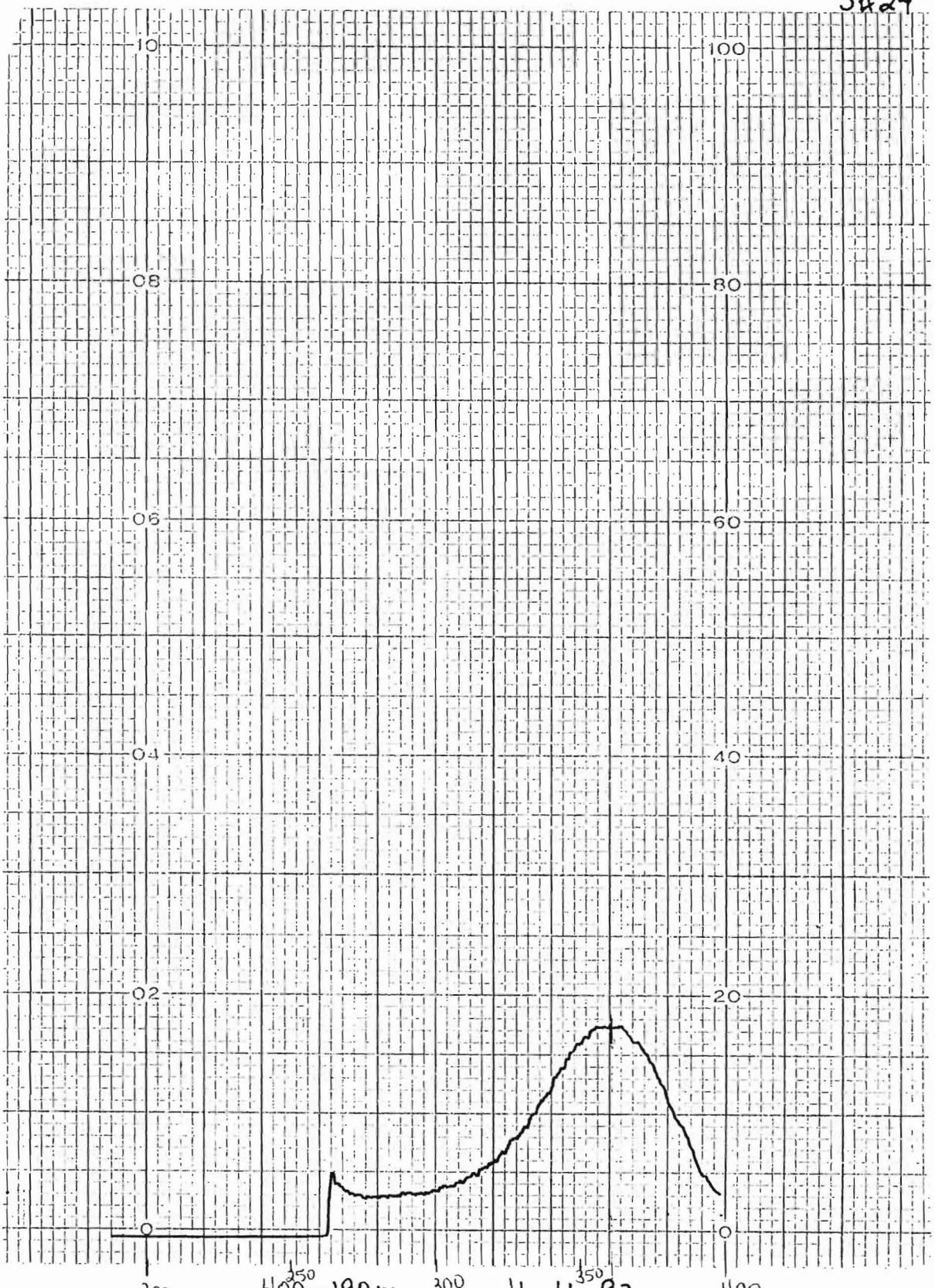

400 - 190 nm
60 nm/min
20 cm/min
slit = 1.0nm
0 - 1 Aunit

11-11-92

8.5×10^{-3} M $NaNO_2$ in DMF

PART NO. B0093925

PERKIN ELMI

S#17

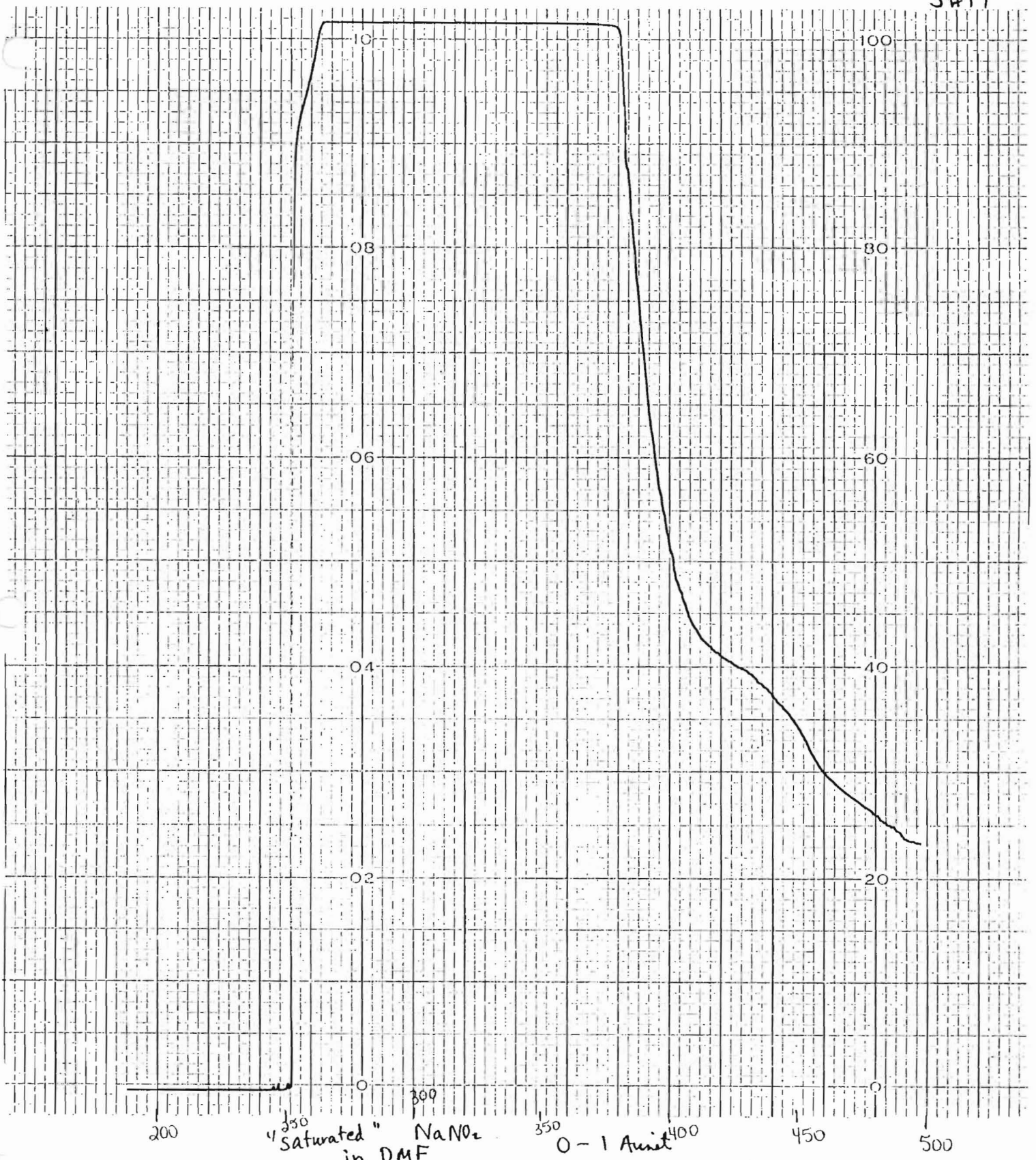

"Saturated" $NaNO_2$ in DMF thermolyzed

0 – 1 Aunit
500 – 190 nm
20 cm/min
60 nm/min
Slit = 1.0nm

S# 18

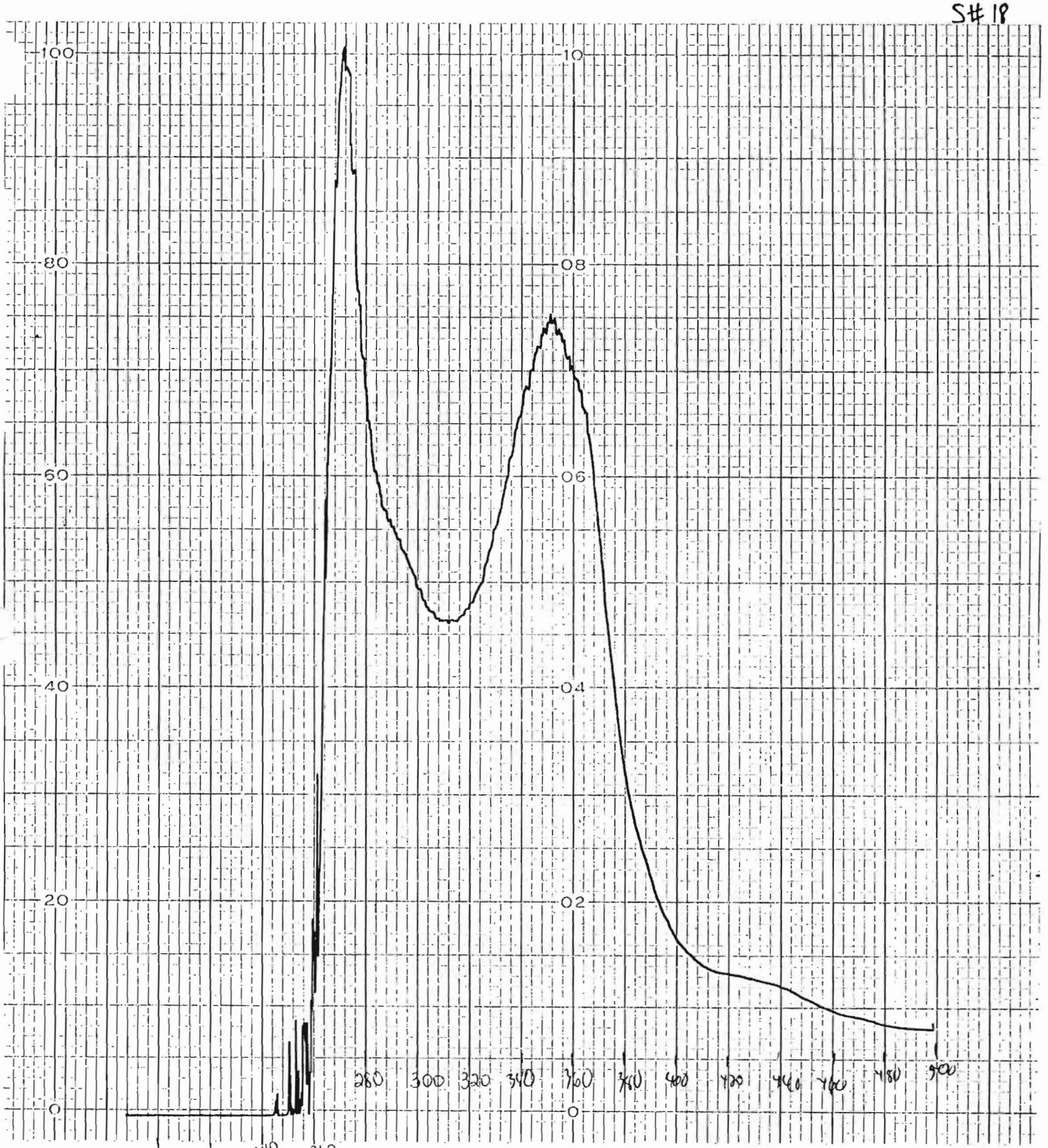

"saturated" $NaNO_2$ in DMF thermolyzed

0 – 3 A units
500 – 190 nm
20 cm/min
60 nm/min

slit = 1.0 nm

PERKIN ELMER

PART NO. B0093925

S# 31

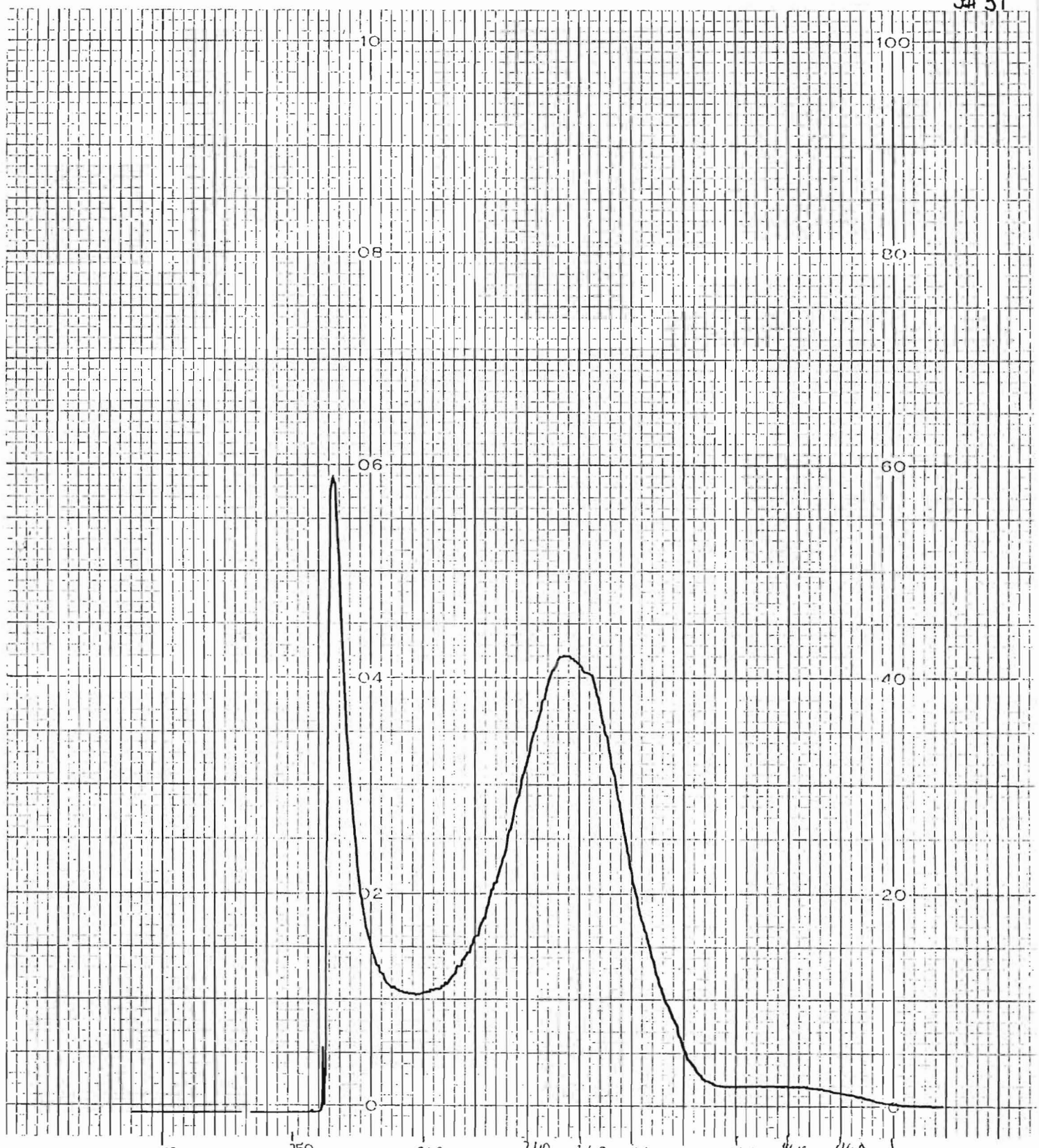

500 - 190 nm
60 nm/min
20 cm/min
slit = 1.0nm
0 - 1 Aunit

"Saturated" $NaNO_2$ in "wet" DMF thermolyzed

11-11-92

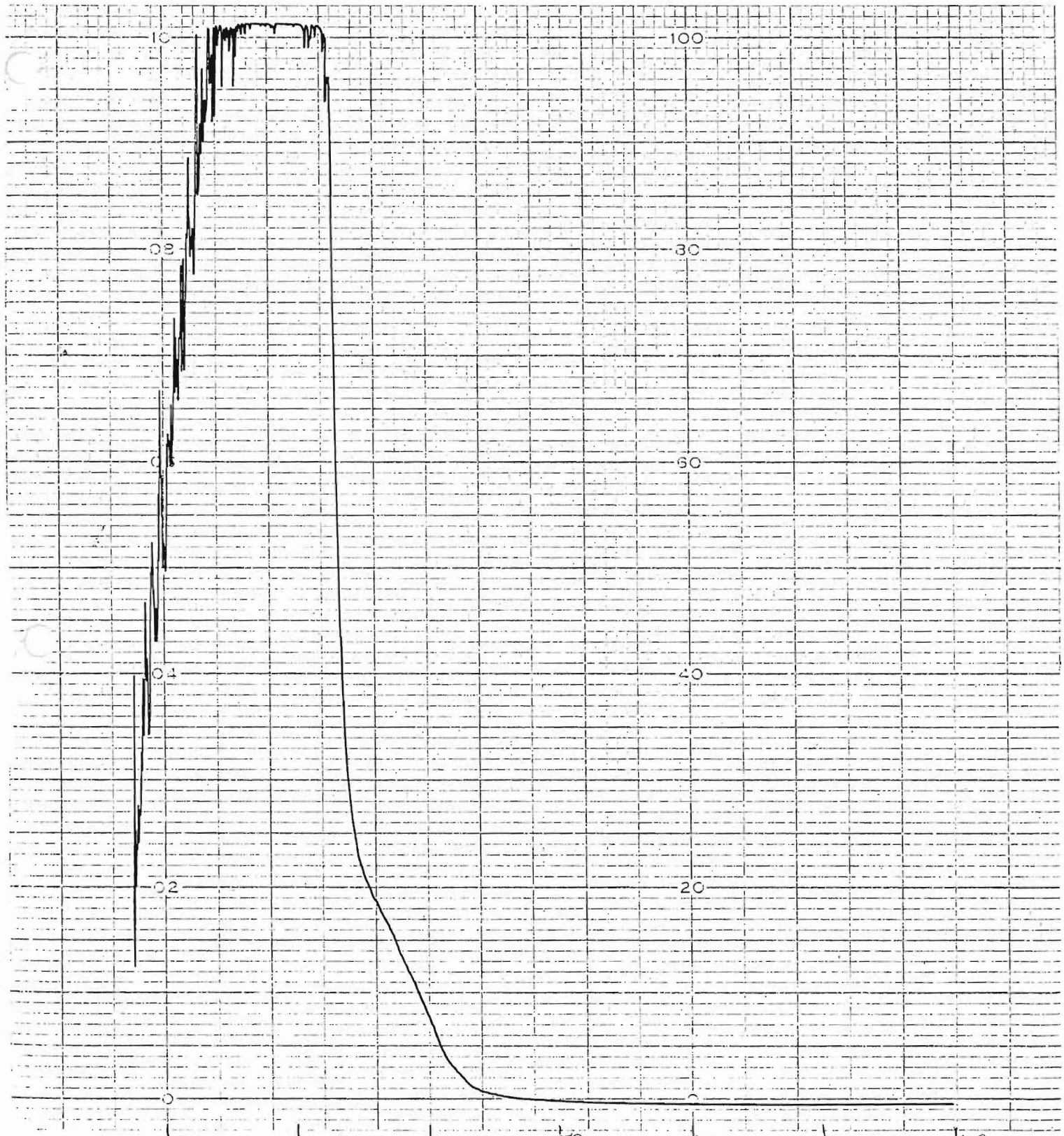

S#23

thermolysis of "wet" DMF

0-1 Aunit
500 - 190nm

60 nm/min
20 nm/cm
slit = 1.0nm

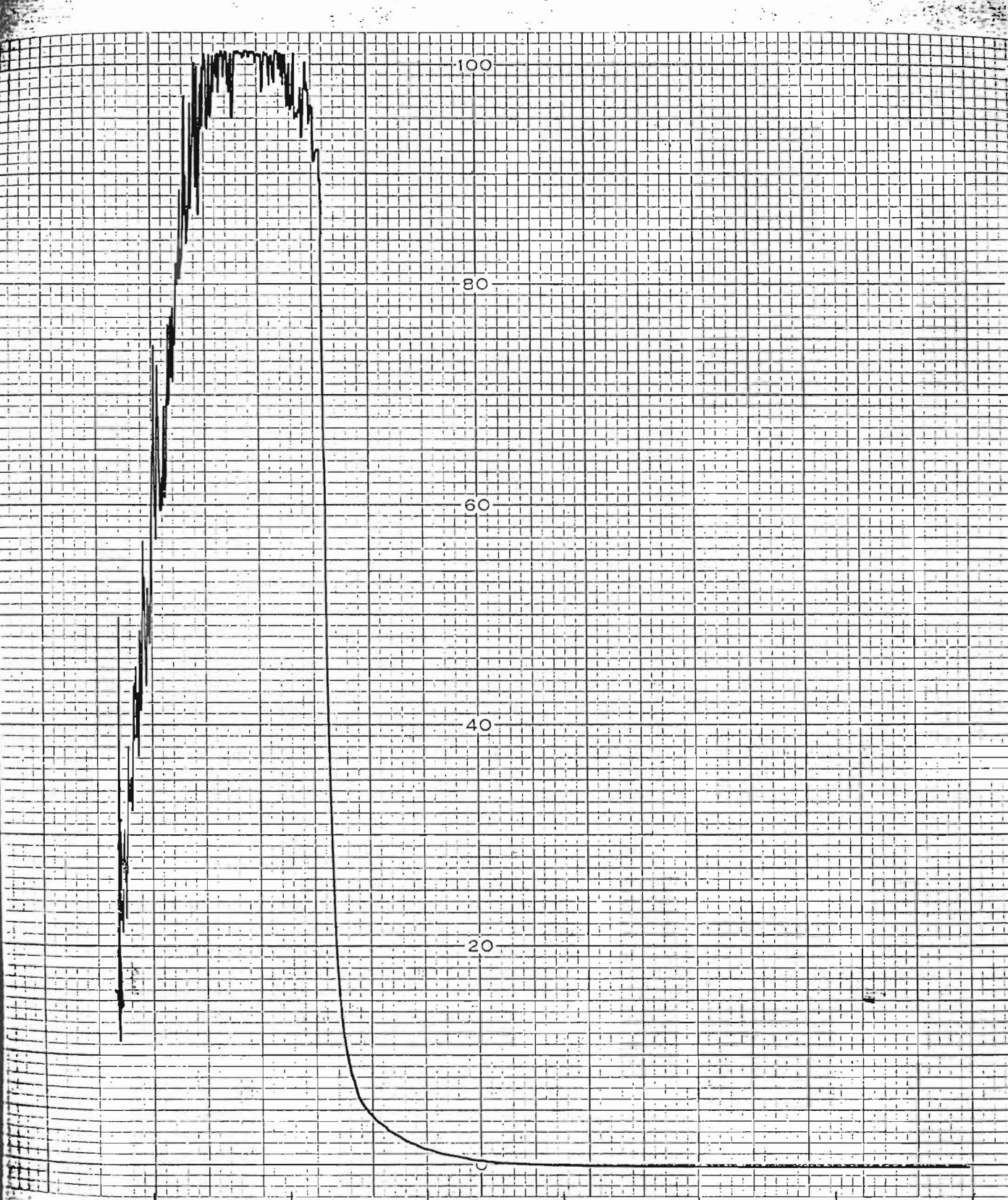

S# 22

thermolysis of "wet" DMF

0-3 Aunit
500-190nm

60 nm/min
20 nm/cm
slit = 1.0mm

PART NO. B0093925

PERKIN-ELMER

S#29

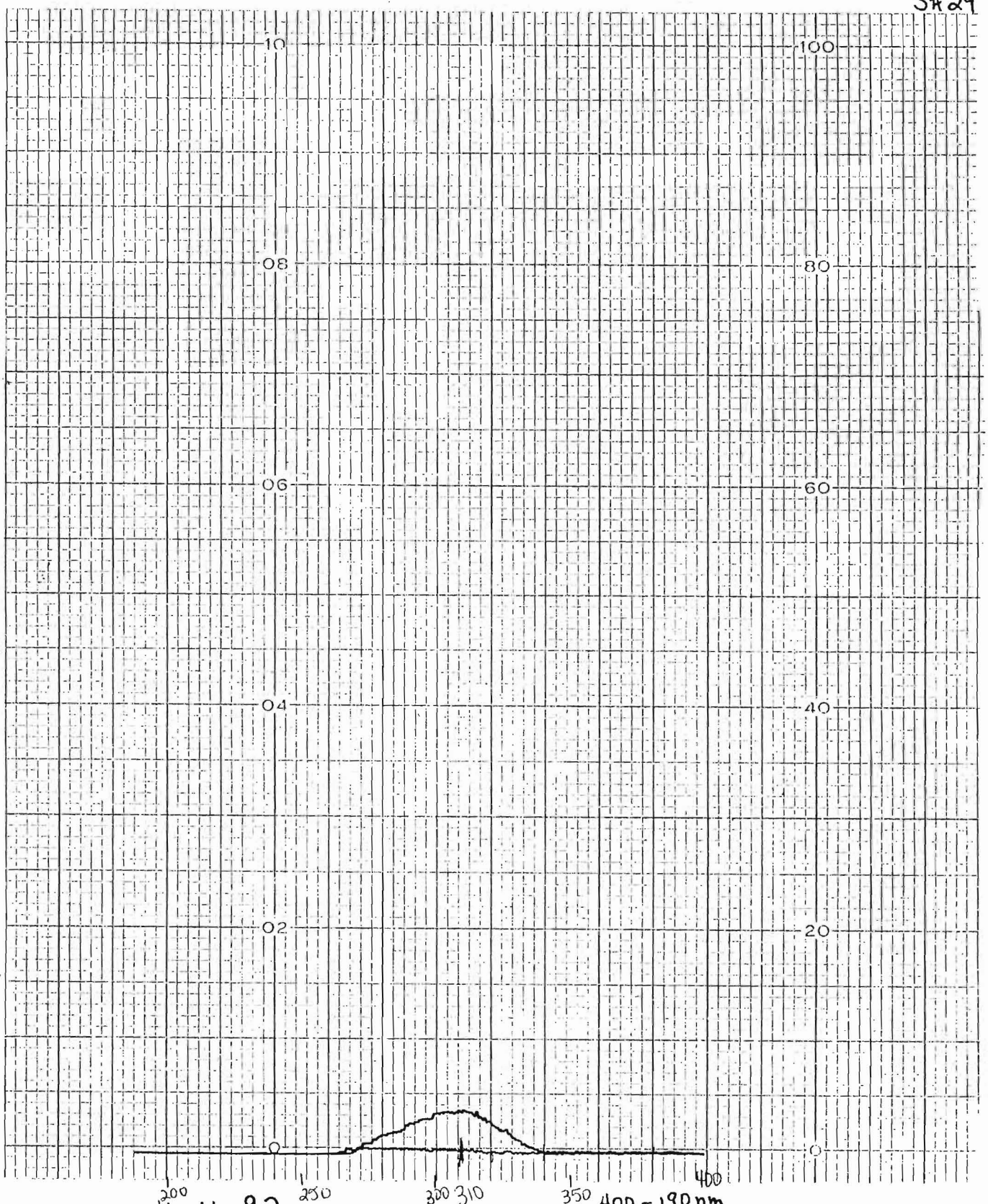

11-11-92

0: "saturated" $NaNO_3$ in DMF

400 - 190 nm
60 nm/min
20 cm/min
slit = 1.00 nm
0 - 1 Aunit

S# 32

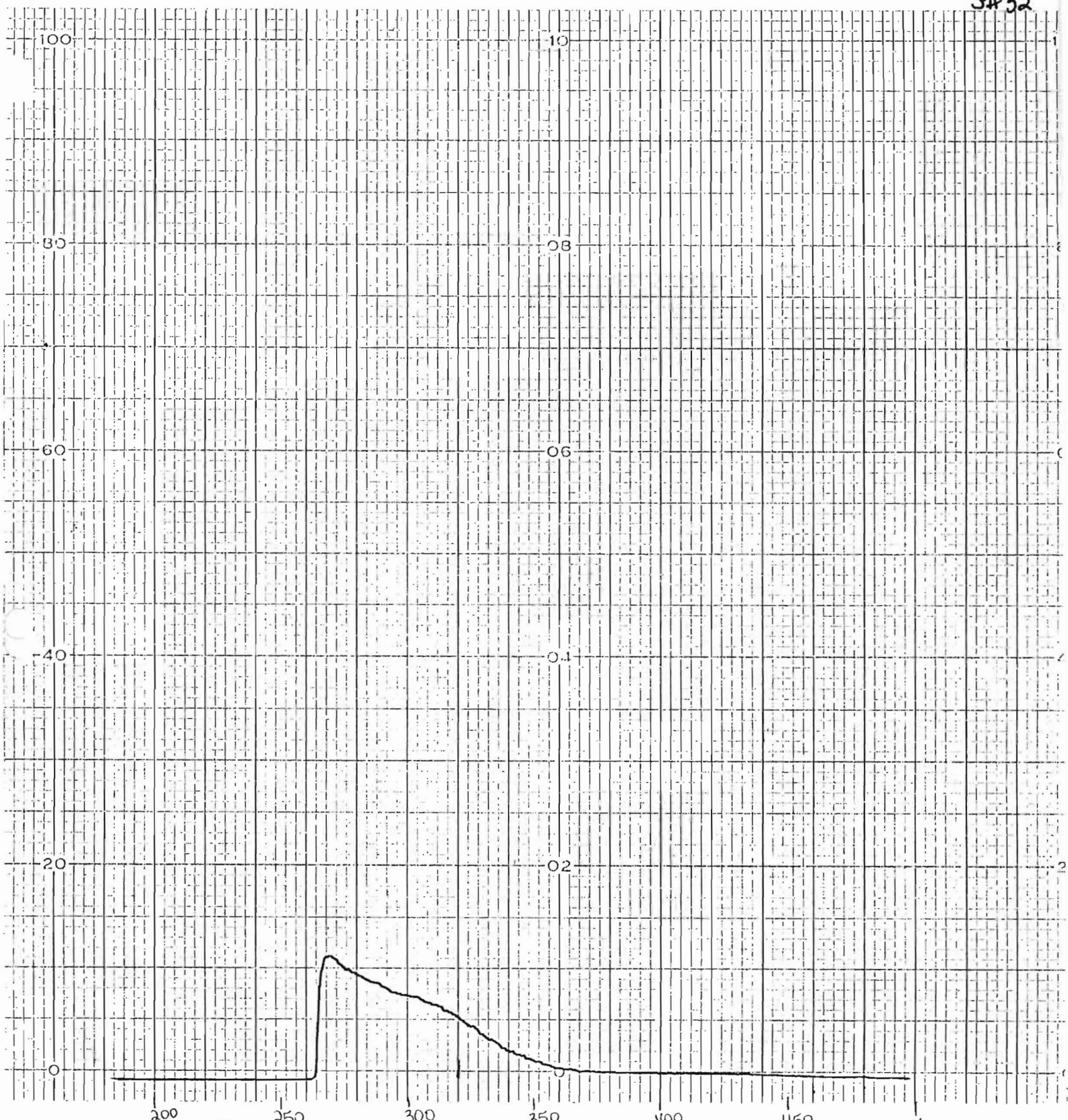

500 - 190 nm
60 nm/min
20 cm/min
Slit = 1.0 nm

0 - 1 A unit

11-11-92

"Saturated" $NaNO_3$ in "wet" DMF - thermolyzed

PERKIN ELMER

PART NO. B0093925

S# 37

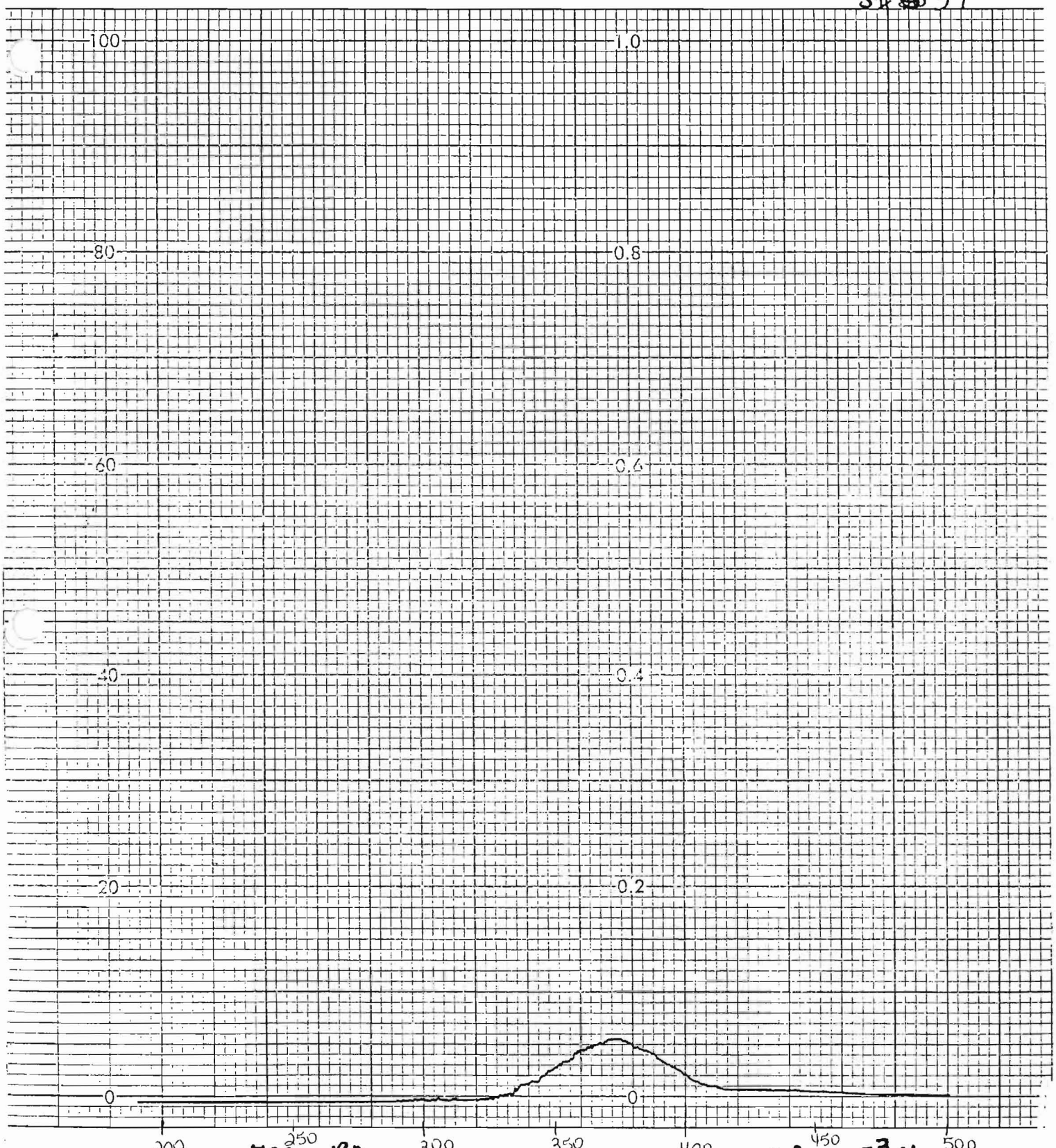

500 – 190nm
60nm/min
20 cm/min
Slit = 1.0 nm

0 – 1 Aunit

2.9×10^{-3} M
$NaNO_2$ in
DMSO

S#36

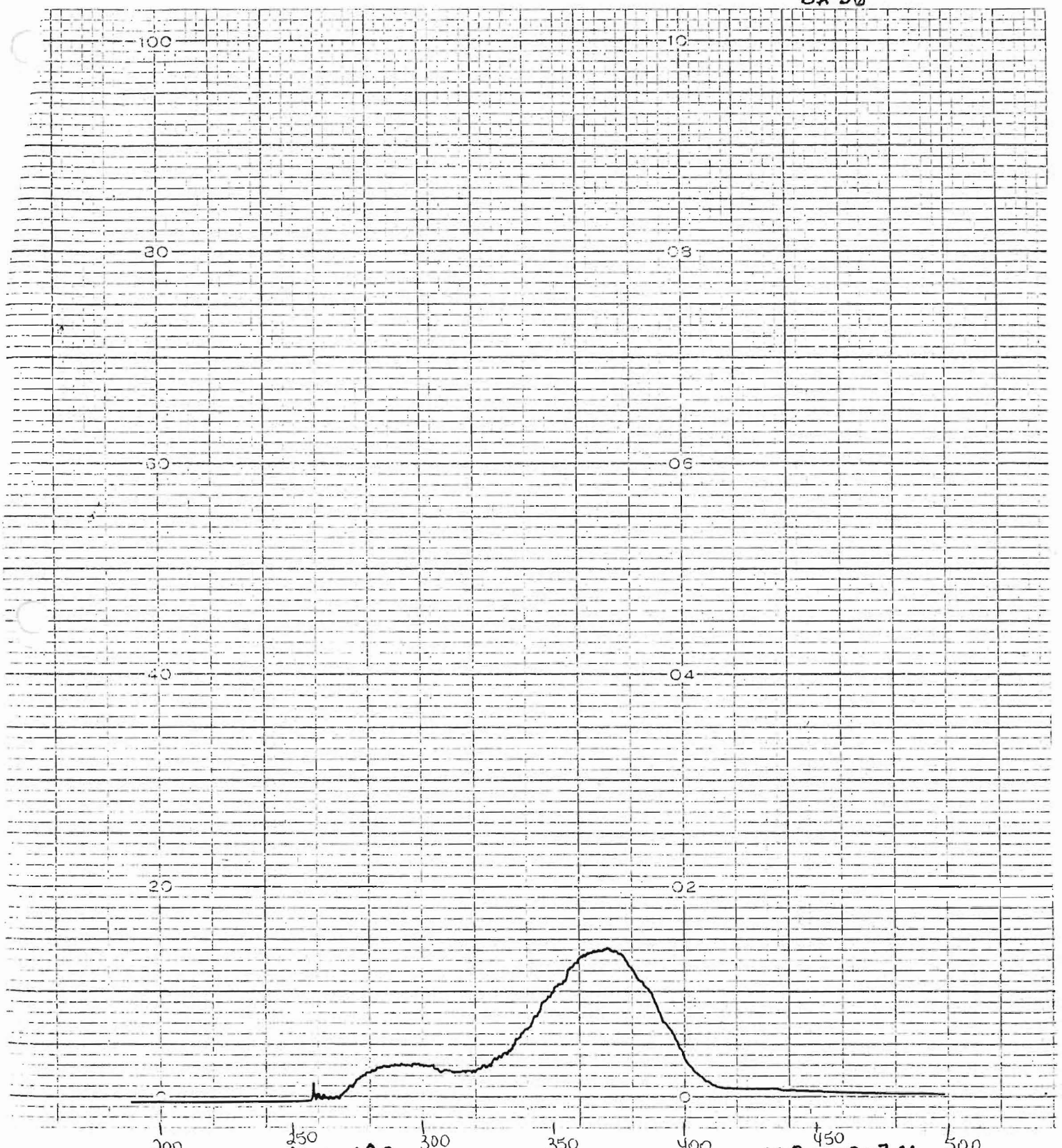

500 - 190nm
60 nm/min
20 cm/min
slit = 1.0nm

0 - 1 A unit

7.0×10^{-3} M
$NaNO_2$ in
DMSO

S# 35

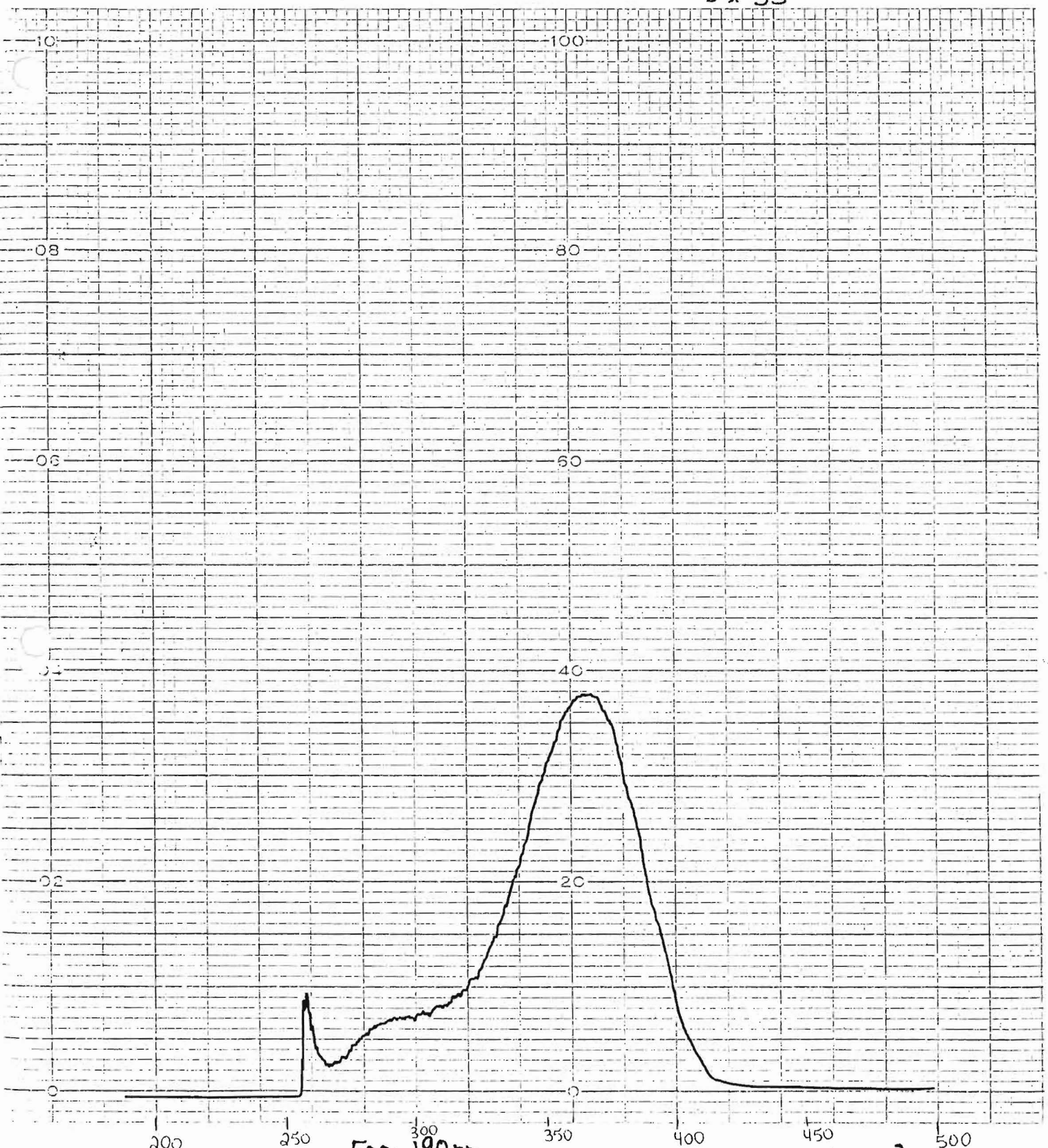

500-190 nm
60 nm/min
20 cm/min
slit=1.0nm

0-1 Aunit

1.4×10^{-2} M
$NaNO_2$ in
DMSO

PART NO. 30033925

PERKIN ELMER

S#34

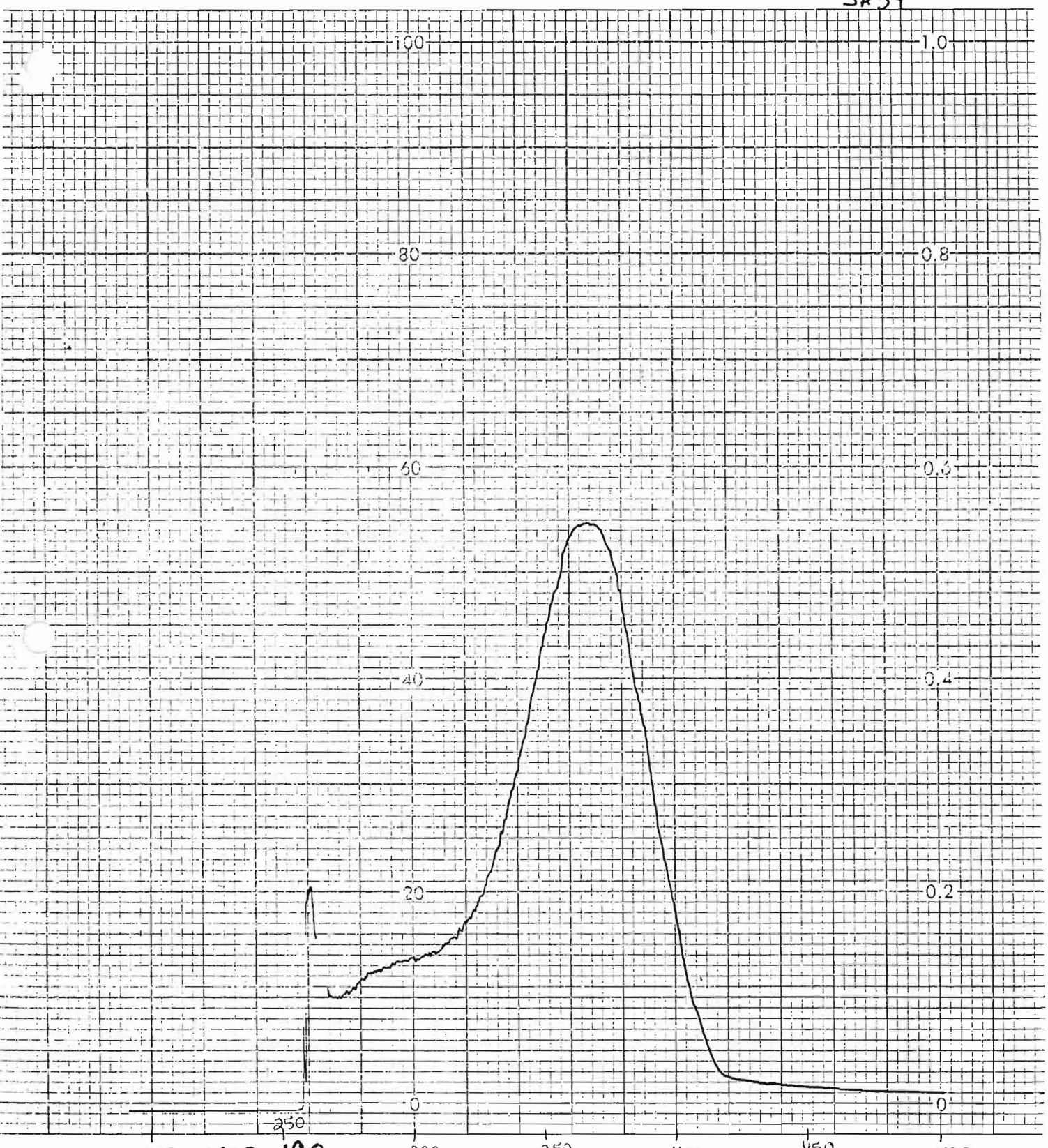

500-190nm
60 nm/min
20 cm/min
slit = 1.0nm

0-1 Aunit

2.03×10^{-2} M
$NaNO_2$ in
DMSO

S#33

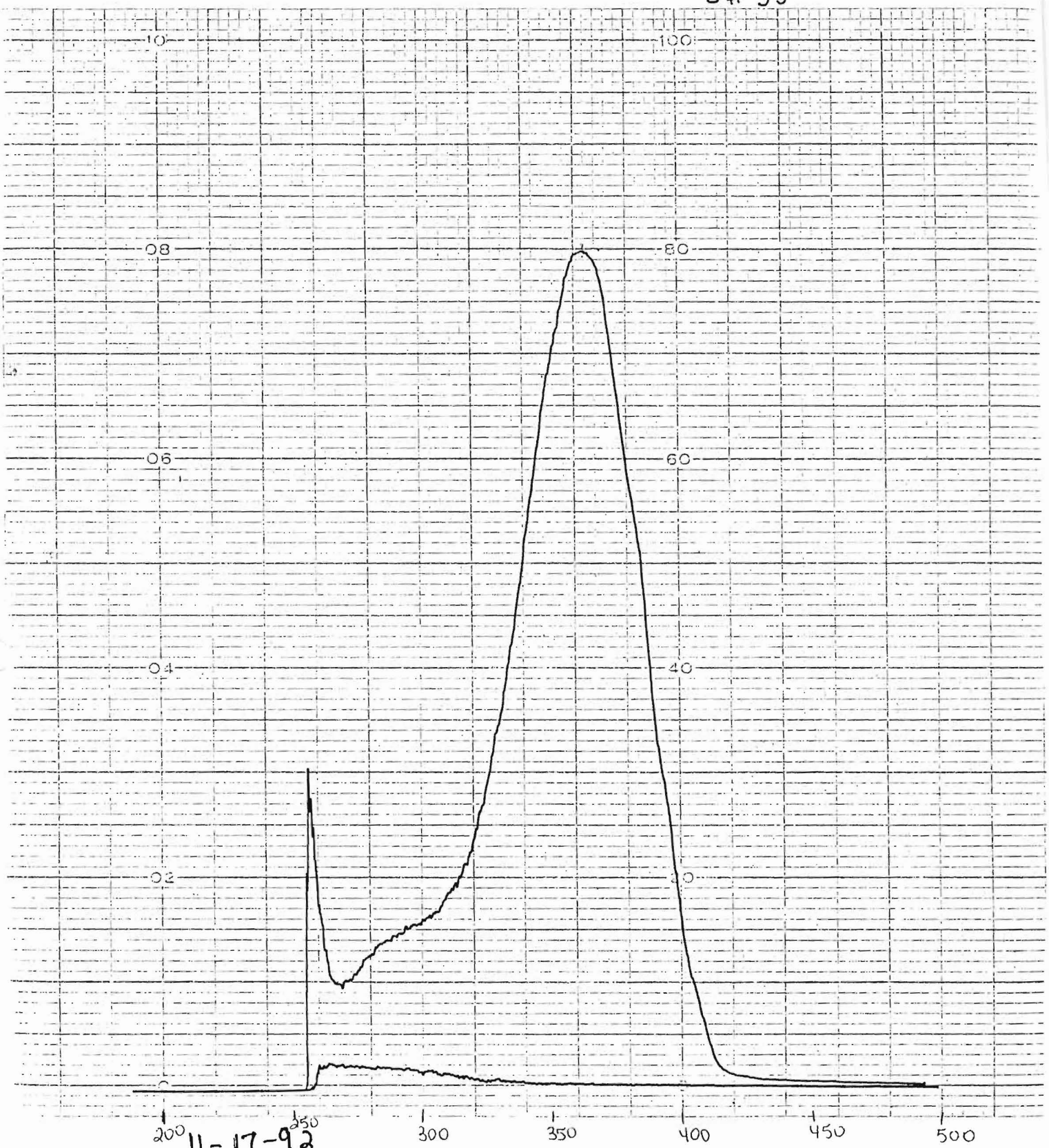

11-17-92

500 – 190 Nm
60nm/min
20 cm/min

Slit = 1.0 nm
0 – 1 Aunit

0.0201 g $NaNO_2$ in DMSO

PART NO. 3C093925

PERKIN-ELMER

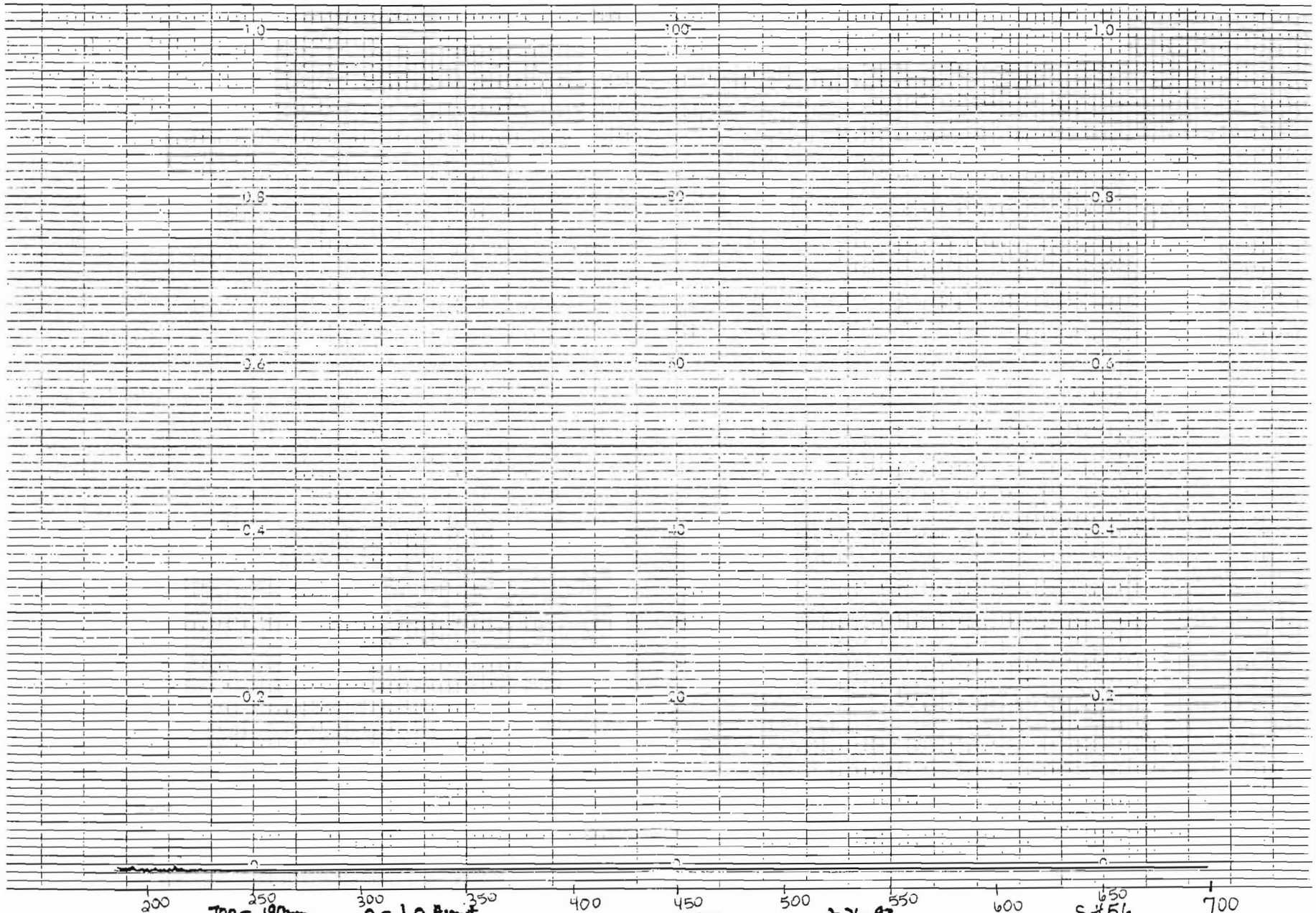
1.0
0.8
0.6
0.4
0.2
0
100
80
60
40
20
0
200
250
300
350
400
450
500
550
600
650
700
700 – 190nm
60 nm/min
20 cm/min
slit = 1.0mm
θ – 1.0 Auto
DMSO vs. DMSO
2-26-93
S#56

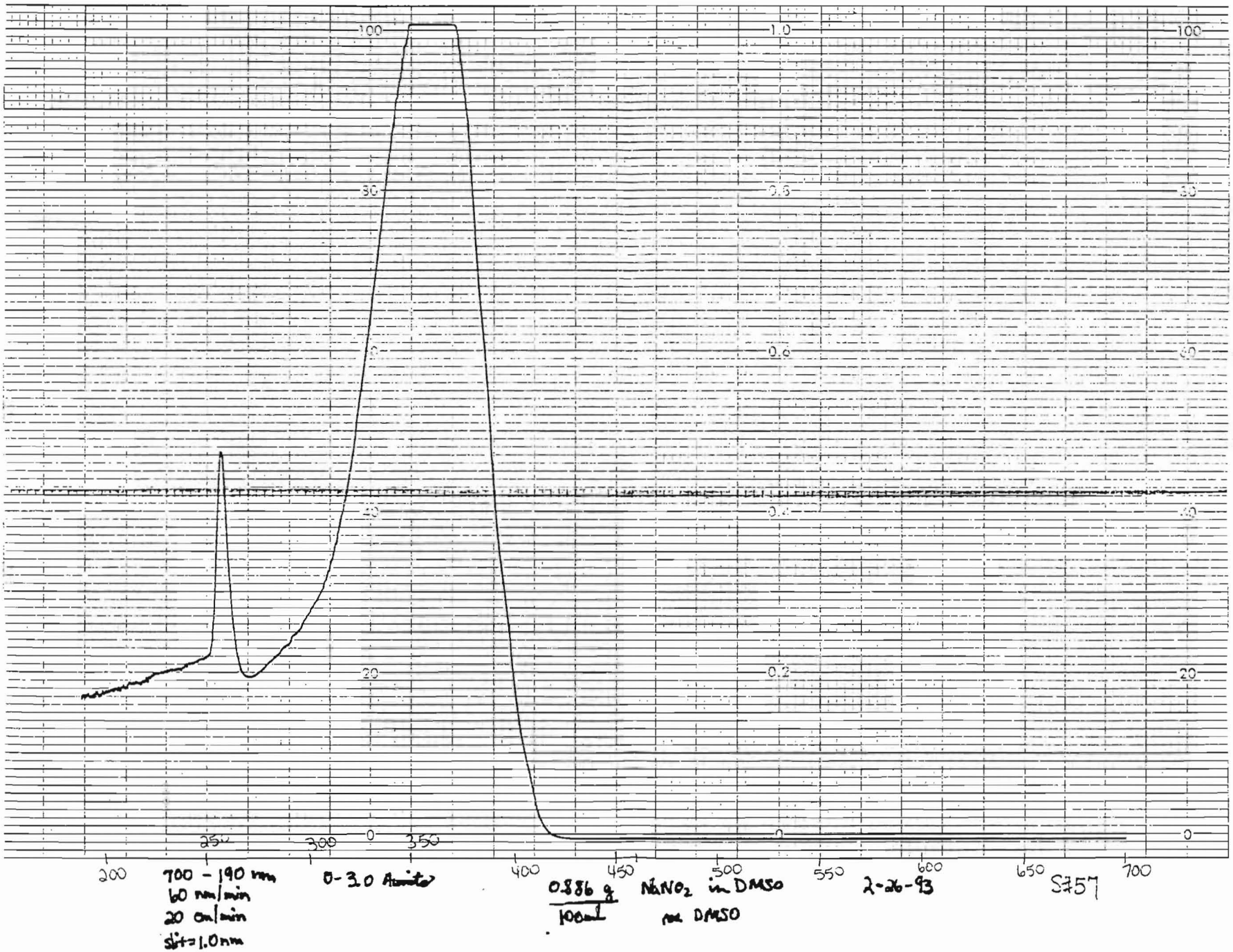
100
30
40
20
0
1.0
0.6
0.4
0.2
0
100
30
40
20
0
200
250
300
350
400
450
500
550
600
650
700
700 - 190 nm
60 nm/min
20 cm/min
slit=1.0nm
0-3.0 Abs
0.886 g / 100ml NaNO2 in DMSO
DMSO
2-26-93
S757

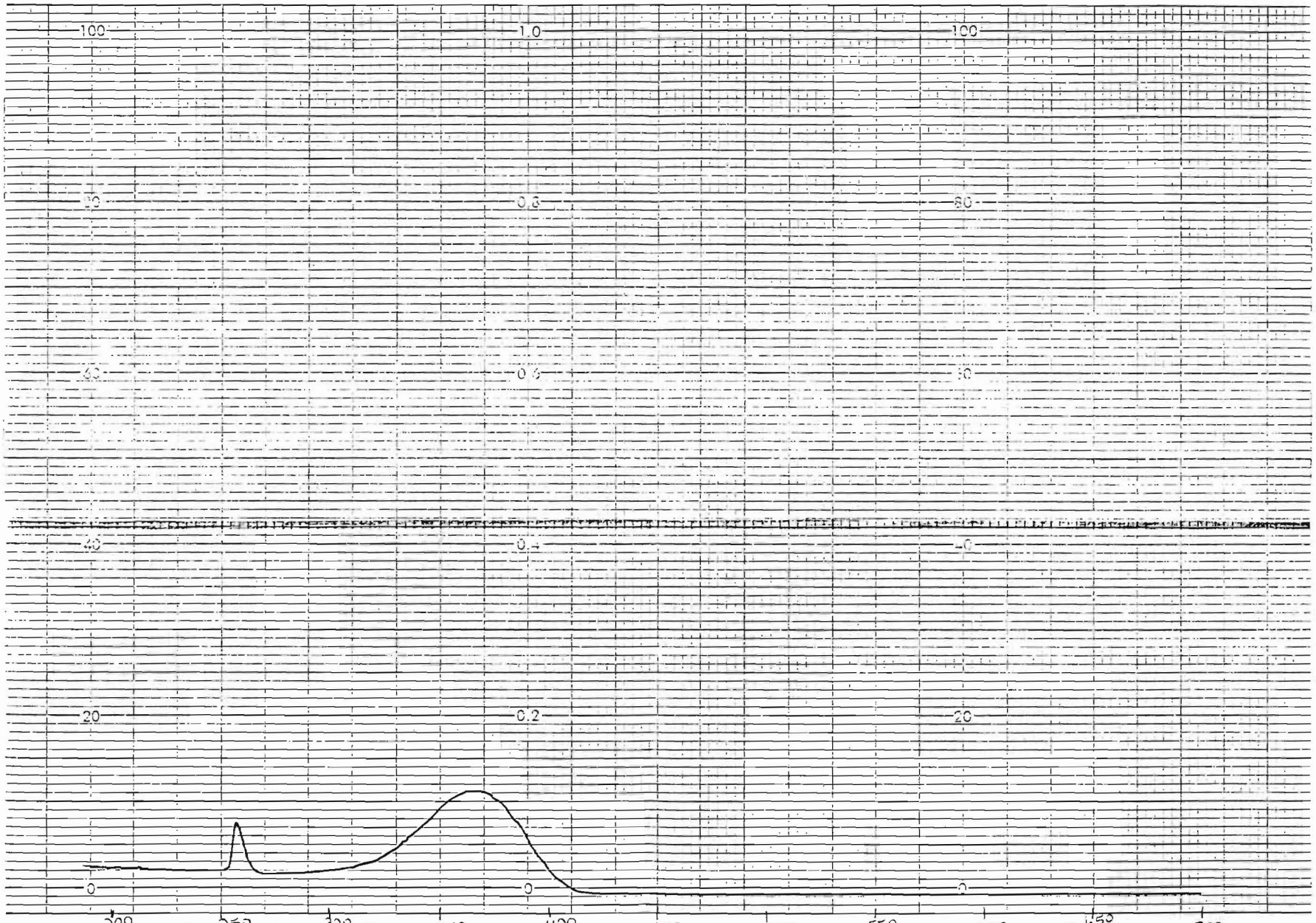
100
80
60
40
20
0
1.0
0.8
0.6
0.4
0.2
0
100
80
60
40
20
0
300
350
400
450
500
550
600
650
700
700 – 190nm
60nm/min
20 nm/cm
slit = 1.0nm
0-3 Aunits
1/10 dilution
0.886 g/100ml NaNO2 in DMSO
2-26-93
S#57

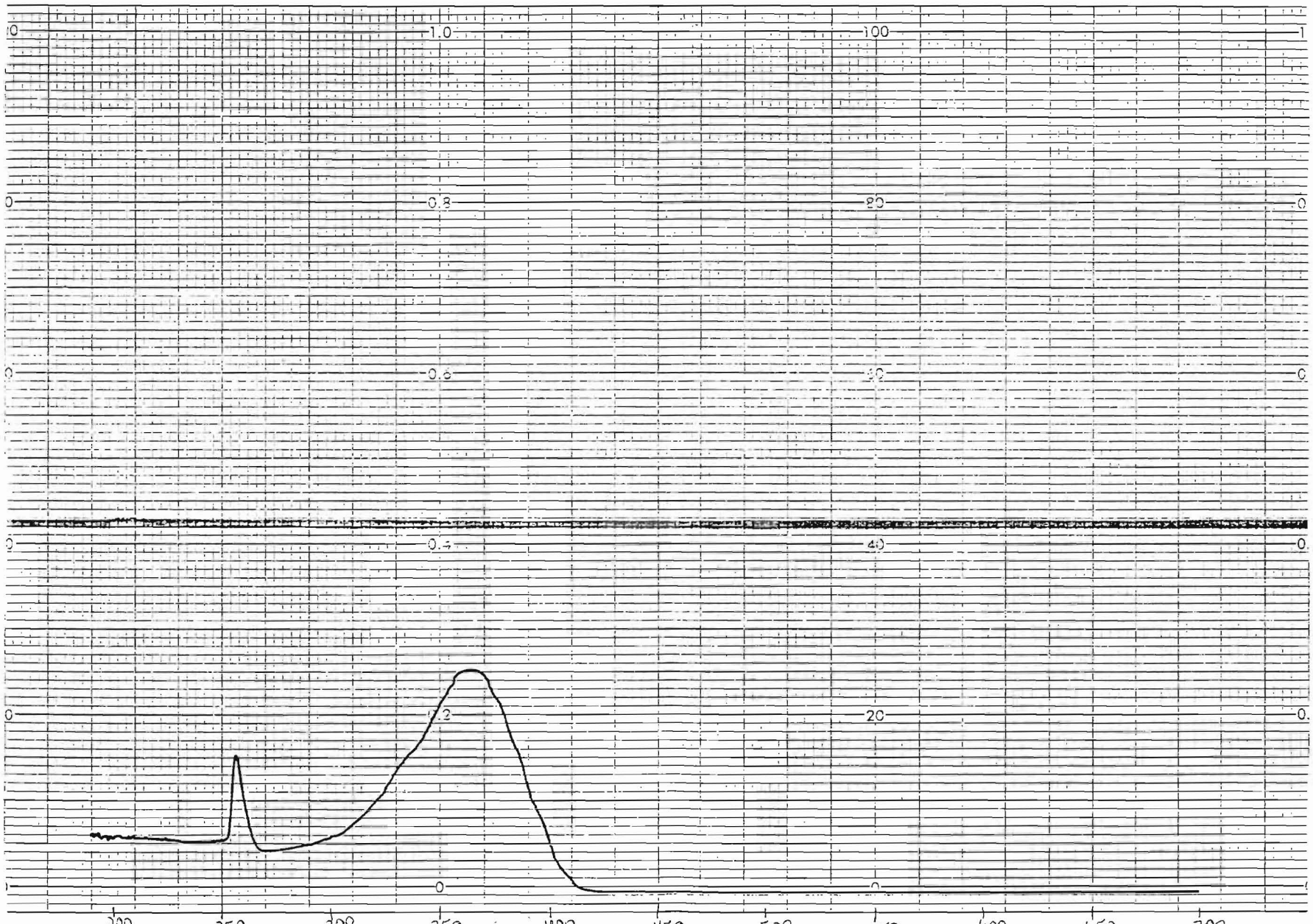
1.0
0.8
0.6
0.4
0.2
0
100
80
60
40
20
0
200
250
300
350
400
450
500
550
600
650
700
700 - 200 nm
60 nm/min
20 nm/cm
slit = 1.0 nm
0-3 Absorbs
1:10 dilution
1.880 g/100mL
NaNO2 in DMSO
2-26-93
S#59

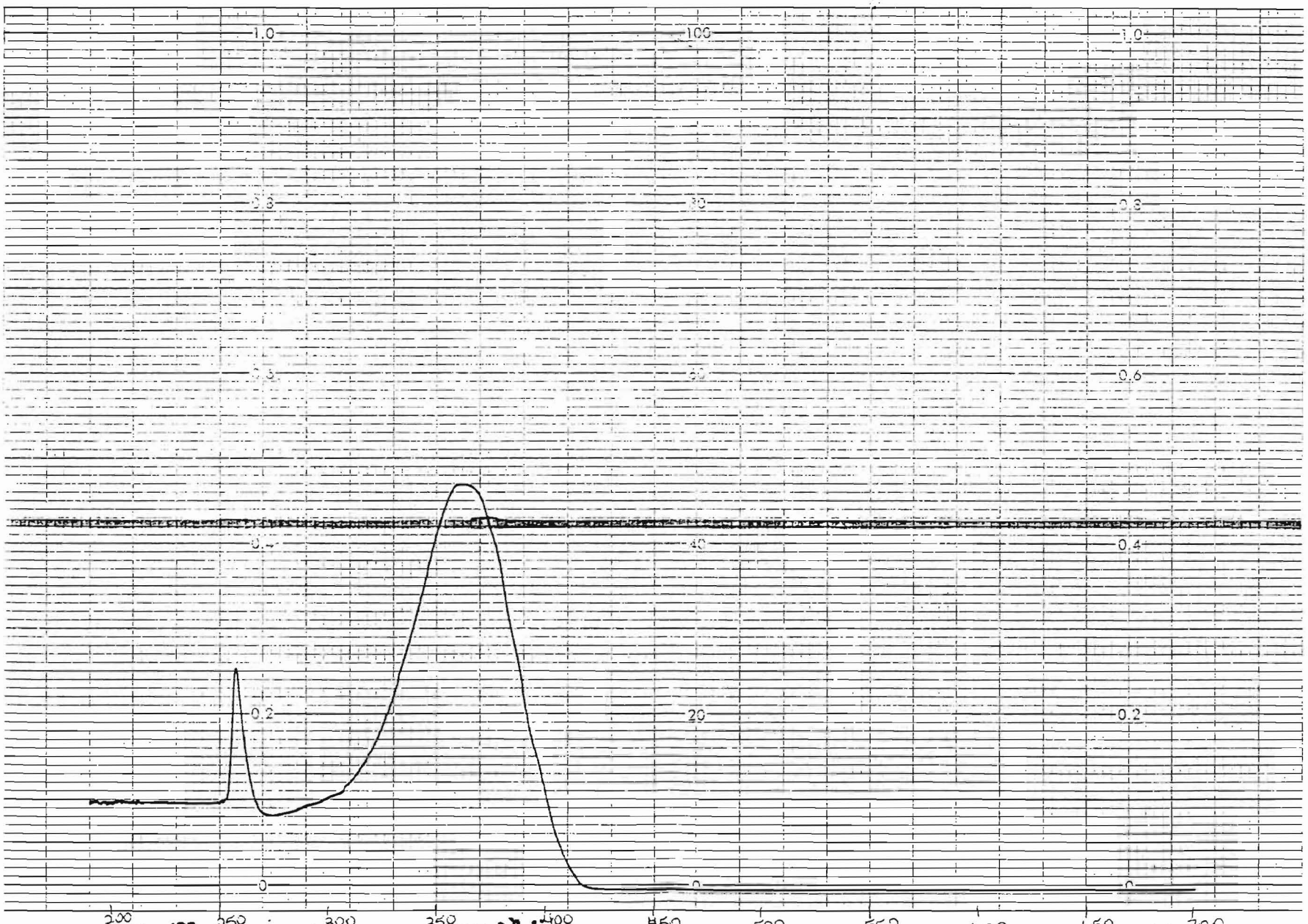

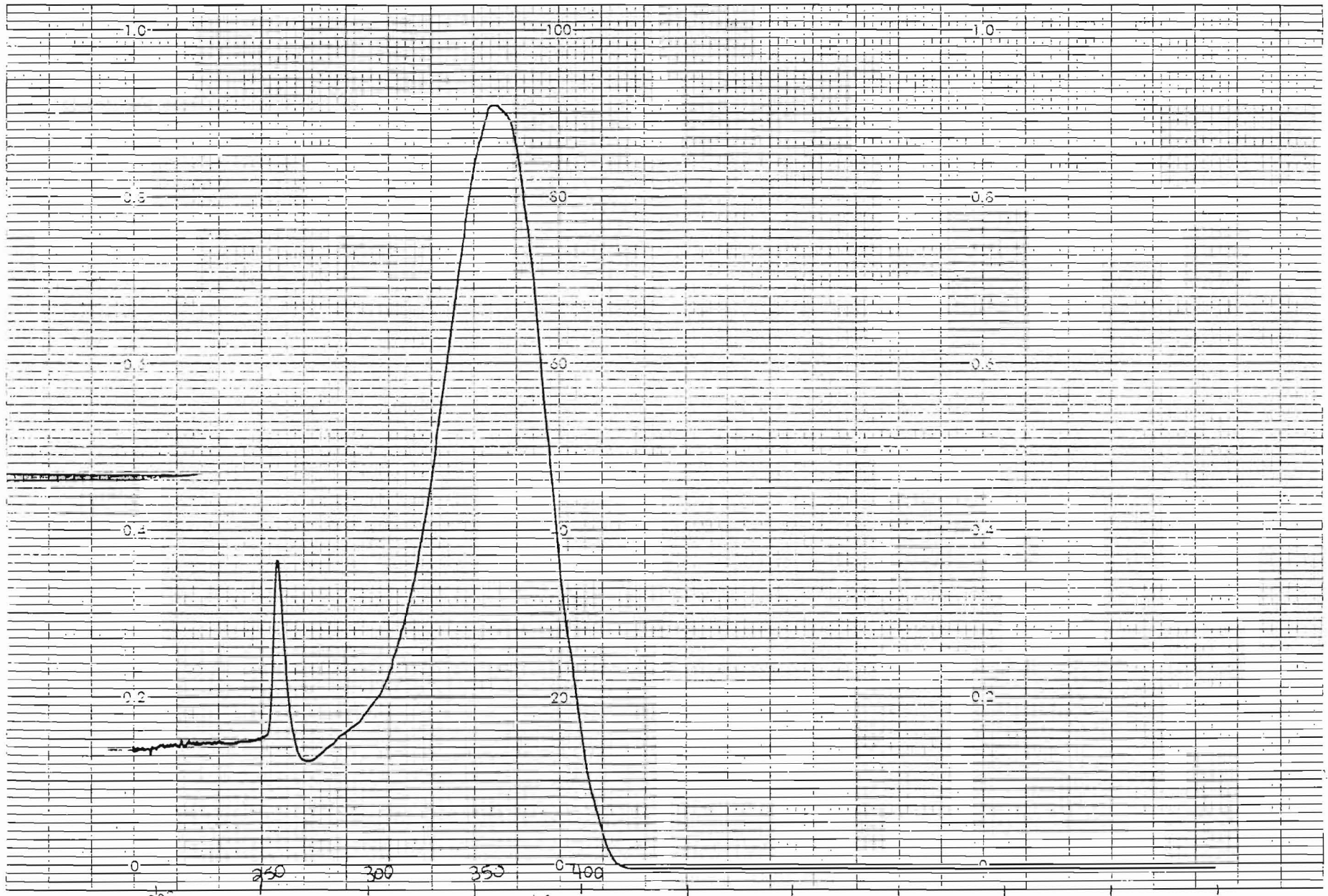
1.0
0.8
0.6
0.4
0.2
0
100
80
60
40
20
0
250
300
350
400
450
500
550
600
650
700
200
700 - 190 nm
60 nm/min
20 nm/cm
slit = 1.0 nm
0-3 Aunits
1:10 dilution
6.919 g/100mL
NaNO2 in DMSO
2-26-93
S#61

S#74

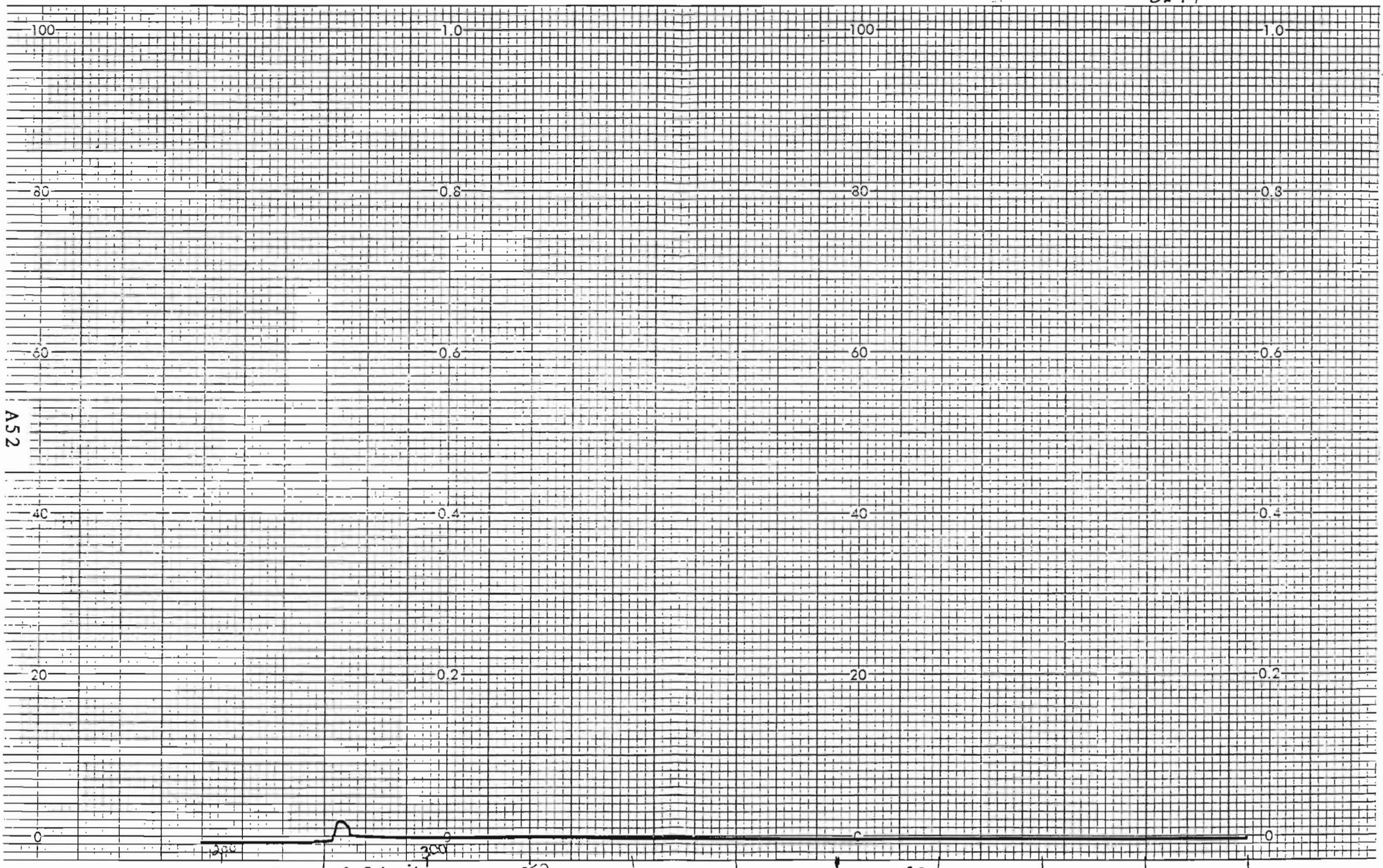

PART NO. PR 093925

S#75

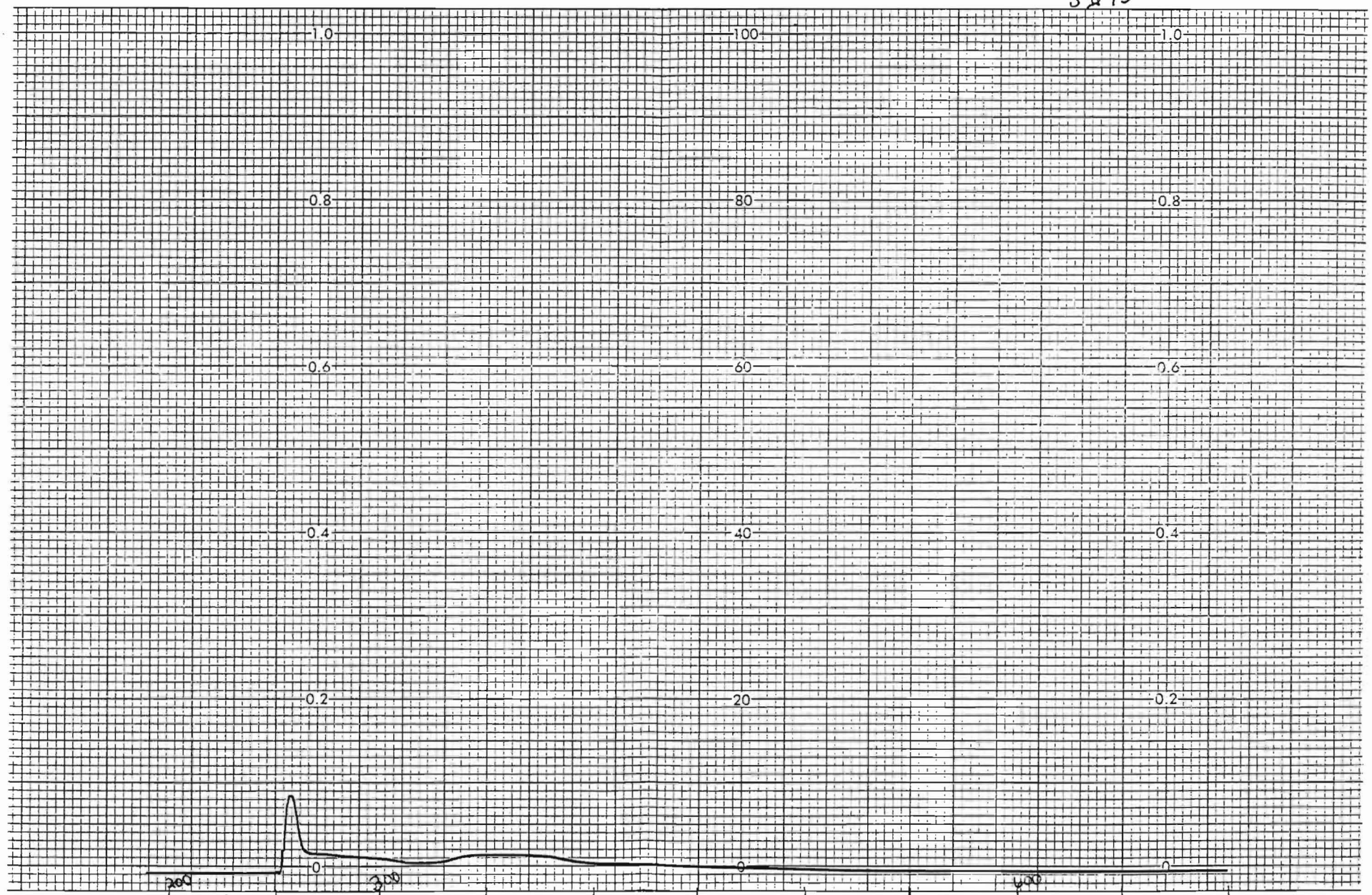
1.0
0.8
0.6
0.4
0.2
0
100
80
60
40
20
0
1.0
0.8
0.6
0.4
0.2
0
200
250
300
350
400
450
500
550
600
650
700
700-190nm
60nm/min
20nm/cm
slit= 1.0nm
0-1 Aunit
DMSO
photolyzed 15min.
3-23-93

A53

S# 76

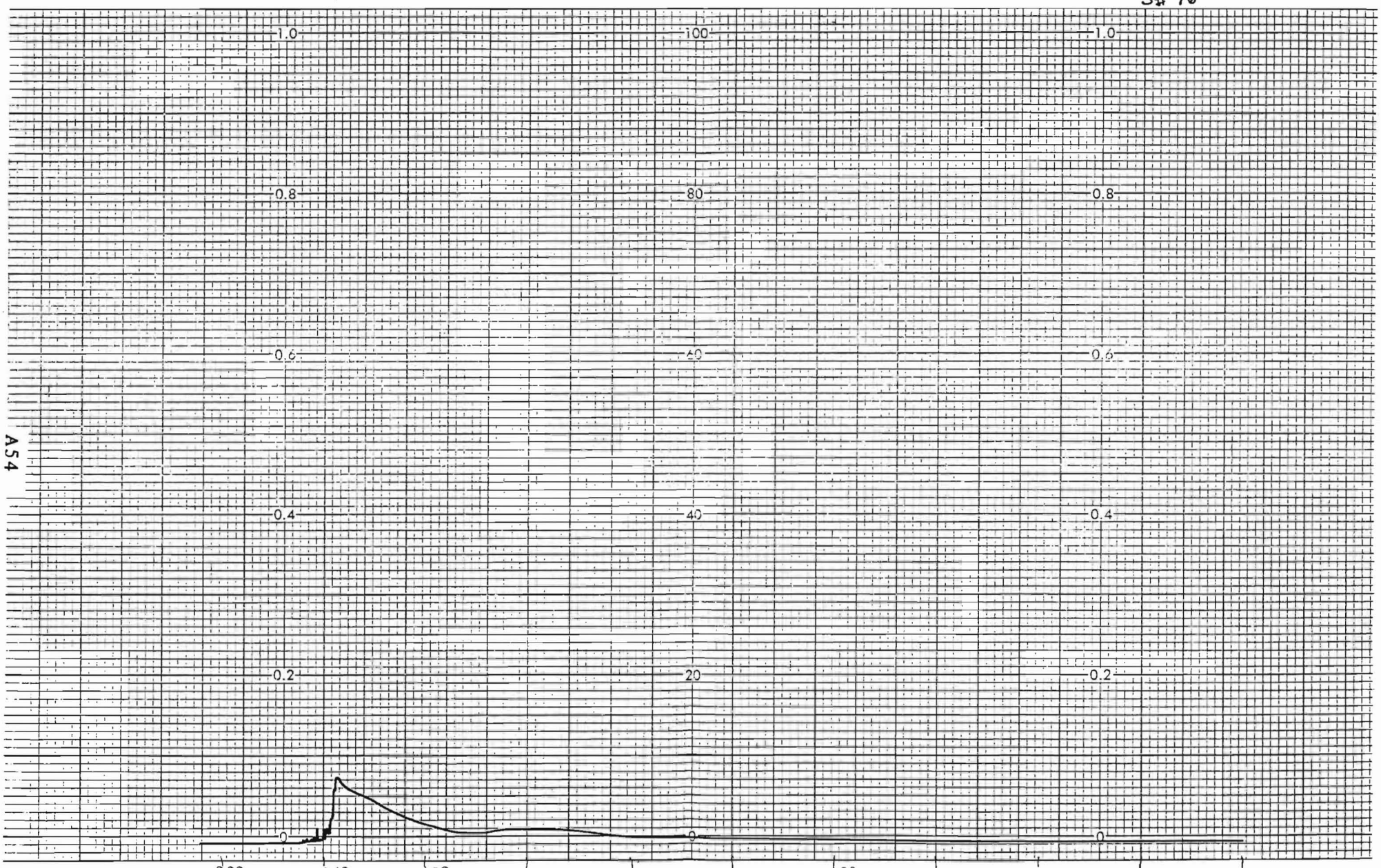

A54

S#77

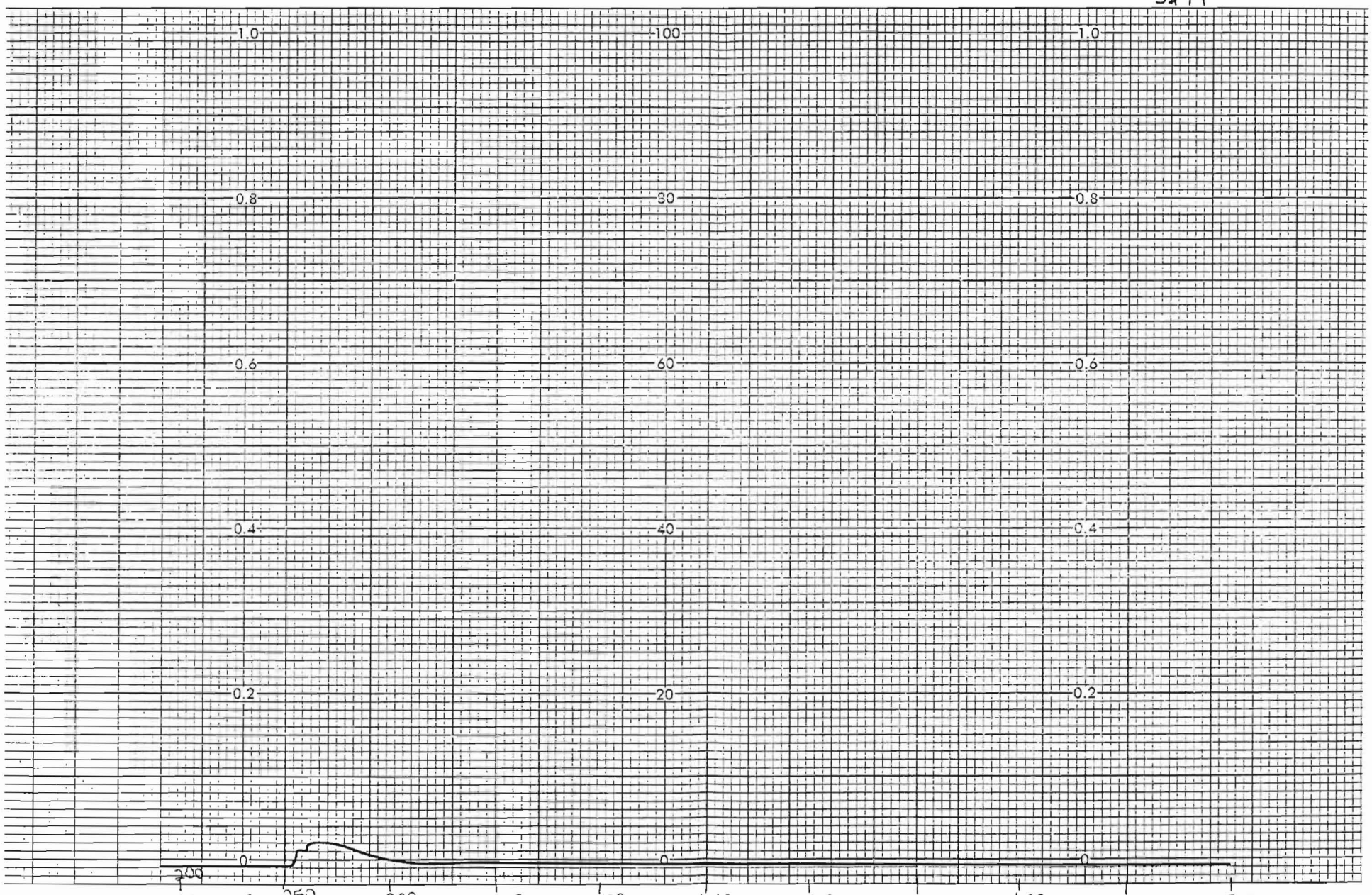

A55

PART NO. PR 093925

S#78

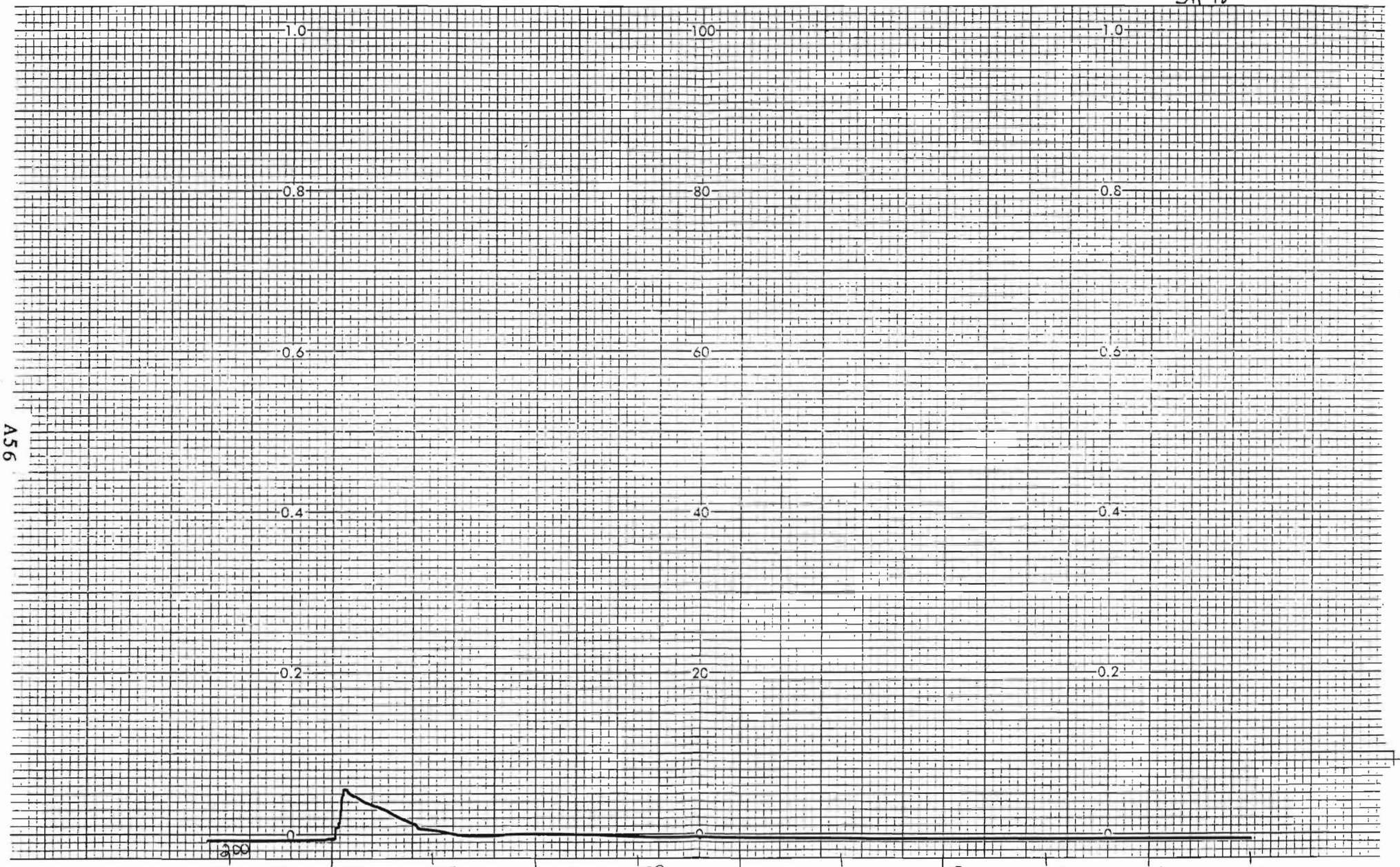

A56

700 - 190nm
60 nm/min
20 nm/cm
Slit = 1.0nm

0-1 Aunit

DMSO
photolyzed 60 min.

3-28-93

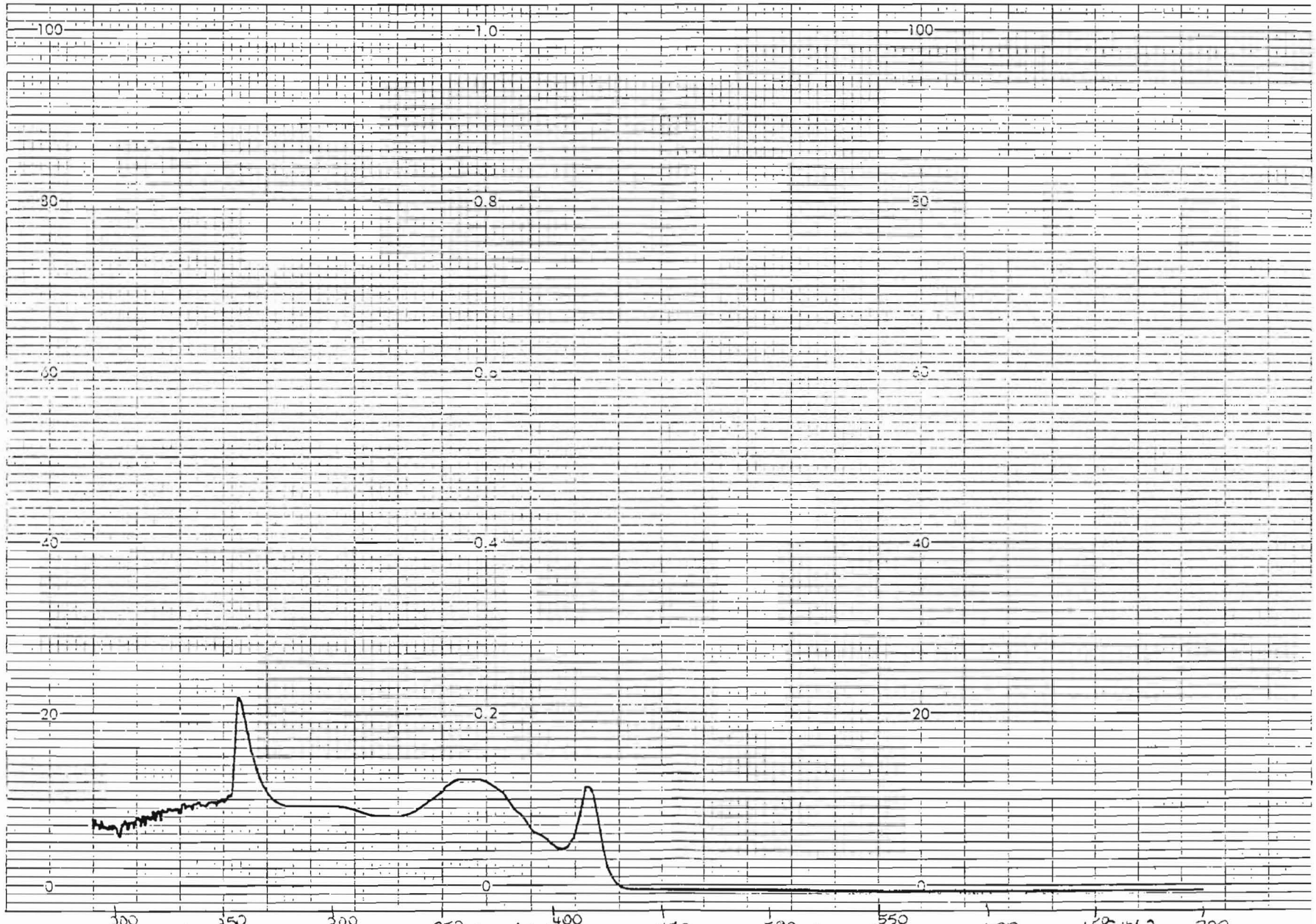
100
80
60
40
20
0
1.0
0.8
0.6
0.4
0.2
0
100
80
60
40
20
0
200
250
300
350
400
450
500
550
600
650
700
700 – 190 nm
60 nm/min
20 nm/cm
slit = 1.0nm
0 – 3 Aunits
1:10 dilution
0.886 g NaNO2 / 100mL DMSO
Photolyzed 60 min.
3-3-93
S#62

A57

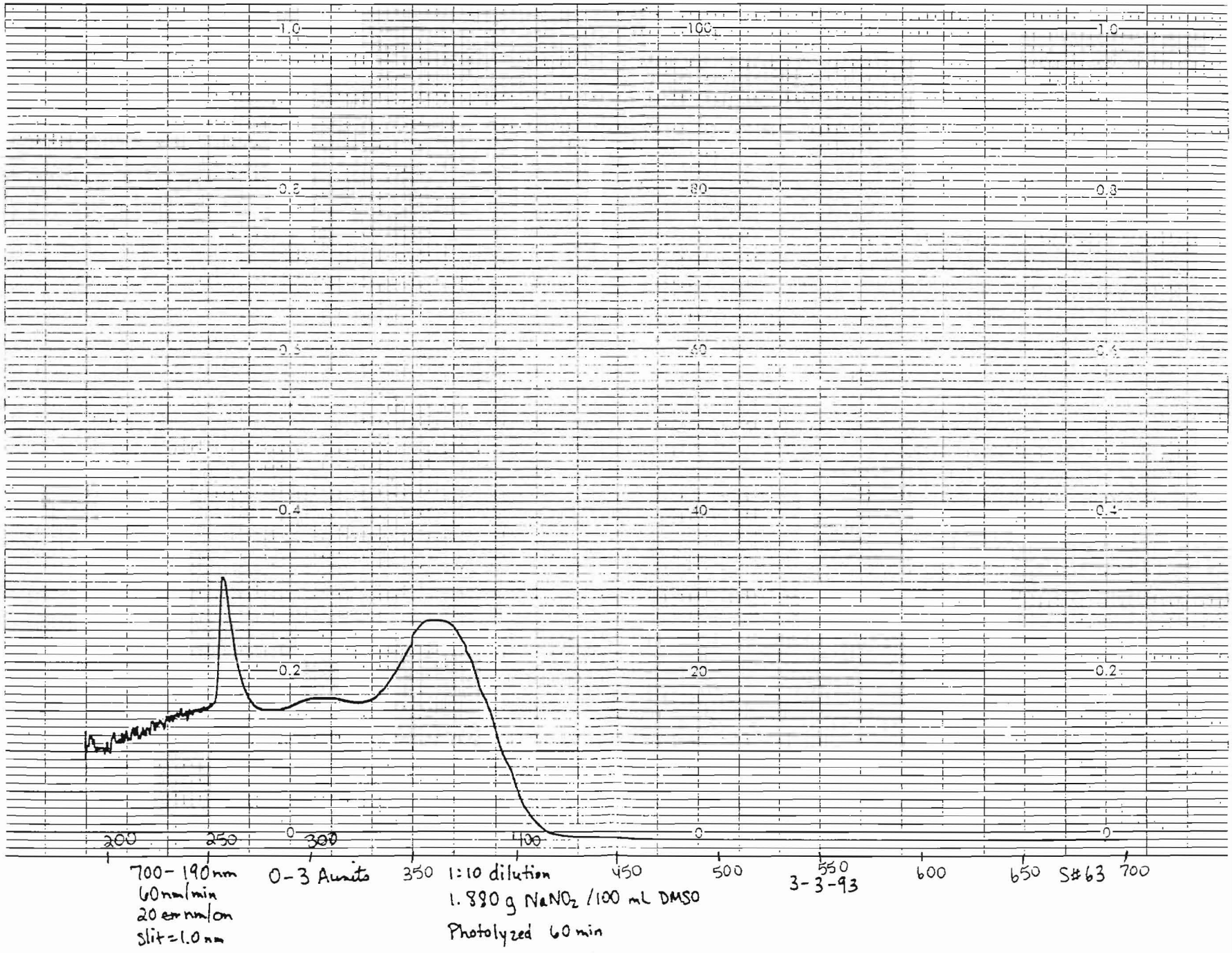
1.0
0.8
0.6
0.4
0.2
0
100
80
60
40
20
0
200
250
300
350
400
450
500
550
600
650
700
700-190nm
60nm/min
20 cm nm/cm
slit=1.0 nm
0-3 Aunits
1:10 dilution
1.880 g NaNO2 /100 mL DMSO
Photolyzed 60 min
3-3-93
S#63

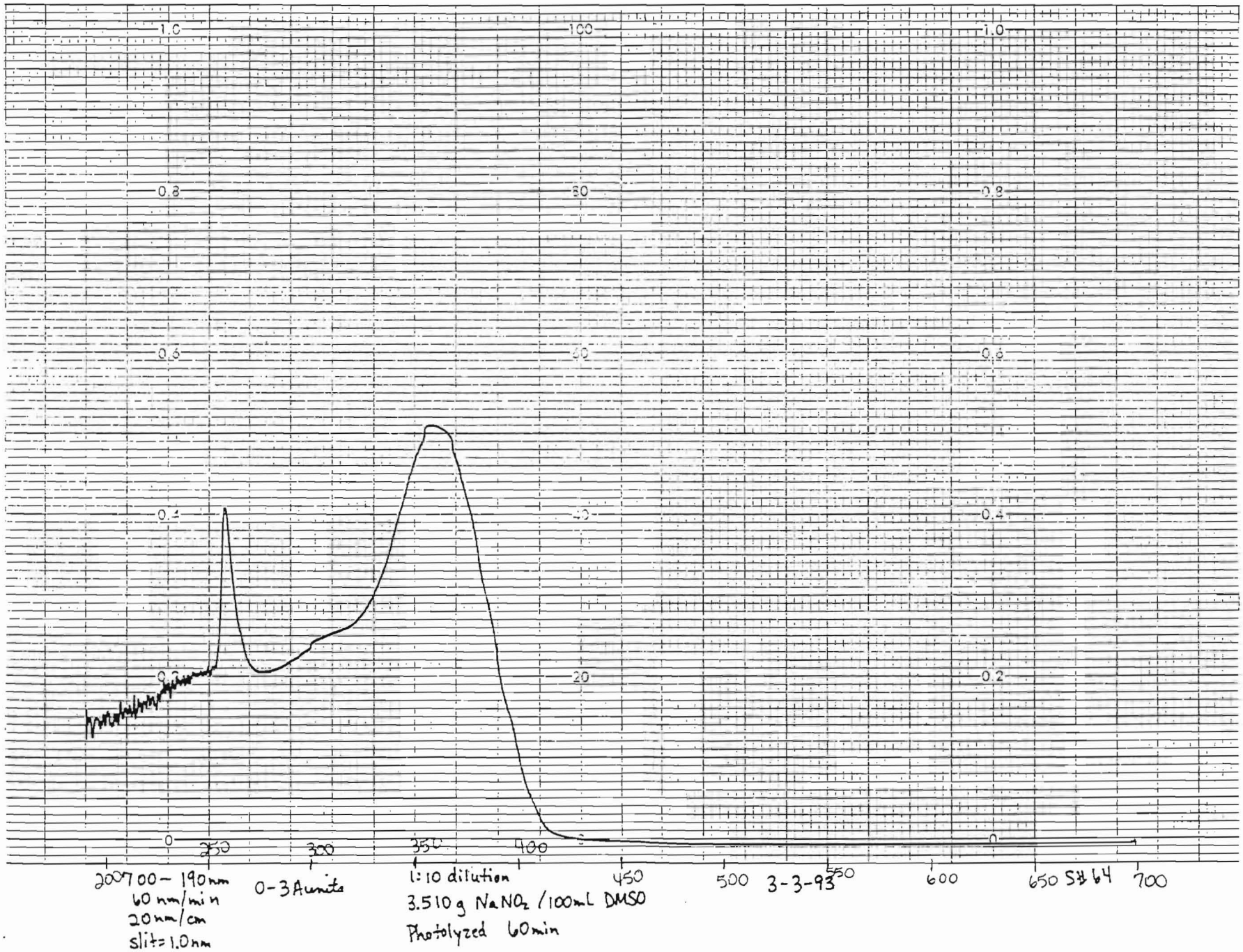
1.0
0.8
0.6
0.4
0.2
0
100
80
60
40
20
0
250
300
350
400
450
500
550
600
650
700
200
200 – 190nm
60 nm/min
20nm/cm
slit=1.0nm
0-3Aunits
1:10 dilution
3.510 g NaNO2 / 100mL DMSO
Photolyzed 60min
3-3-93
S#64

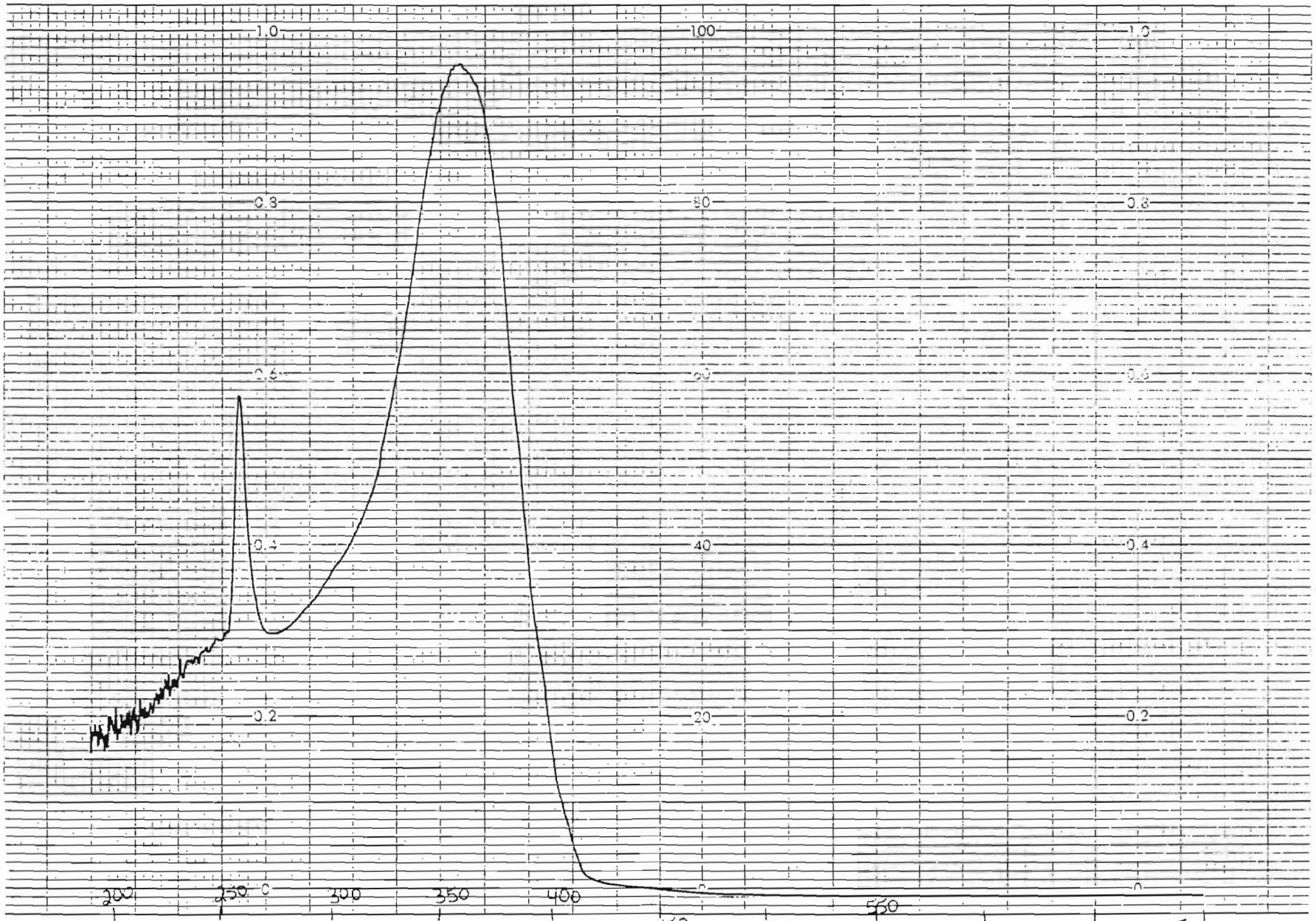
1.0
0.8
0.6
0.4
0.2
0
100
80
60
40
20
0
200
250
300
350
400
450
500
550
600
650
700
700-190 nm
60 nm/min
20 nm/cm
slit = 1.0 nm
0-3 Aunits
1:10 dilution
6.919 g NaNO2 / 100 mL DMSO
Photolyzed 60 min
3-3-93
S#65

S# 68

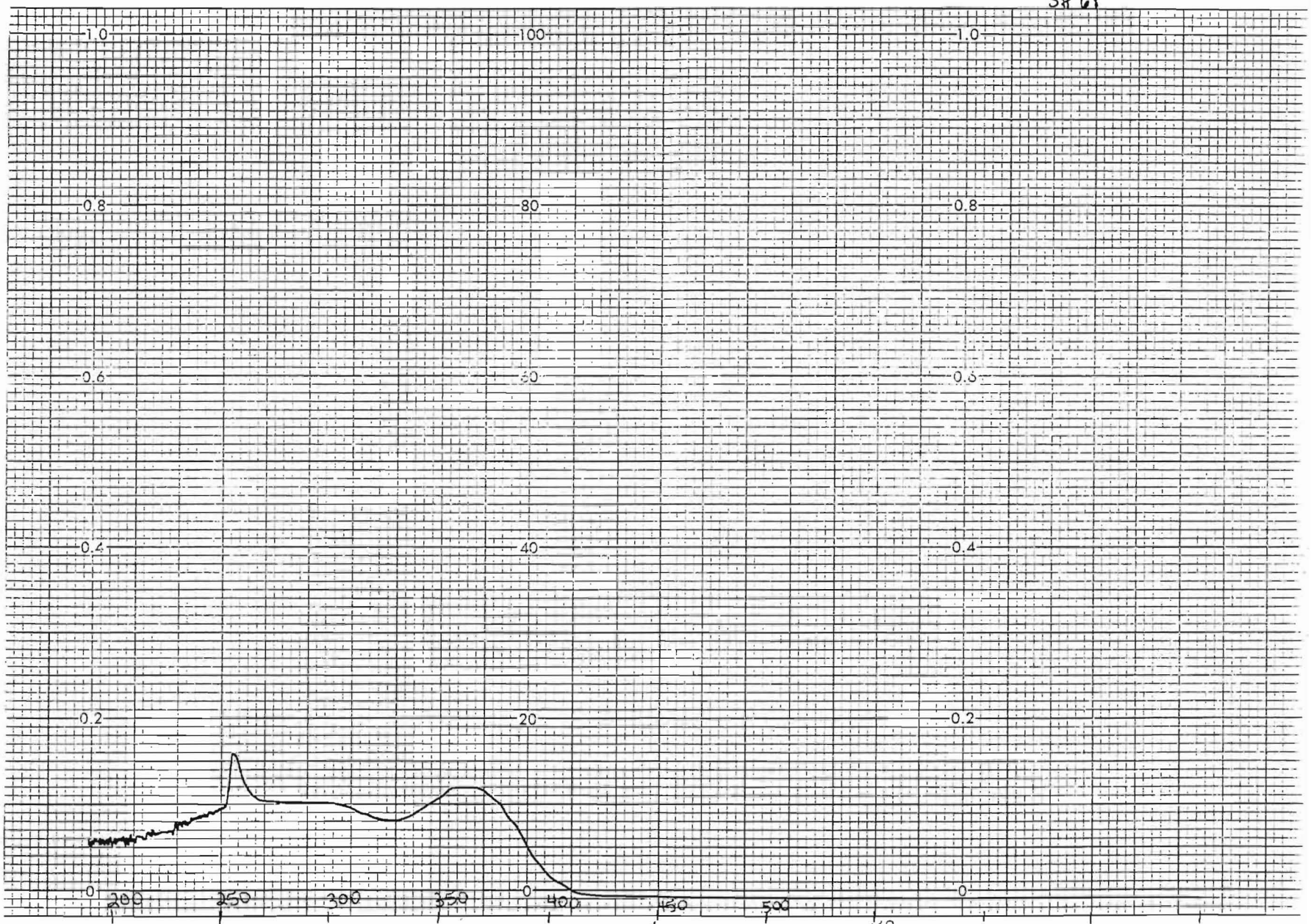
1.0
0.8
0.6
0.4
0.2
0
100
80
60
40
20
0
200
250
300
350
400
450
500
550
600
650
700
700-190 nm
60 nm/min
20 nm/cm
slit = 1.0 nm
0-3 Aunits
0.886 g NaNO2 / 100 mL DMSO
2nd Photolysis 60 min
1:10 dilution
3-17-93

A61

S#69

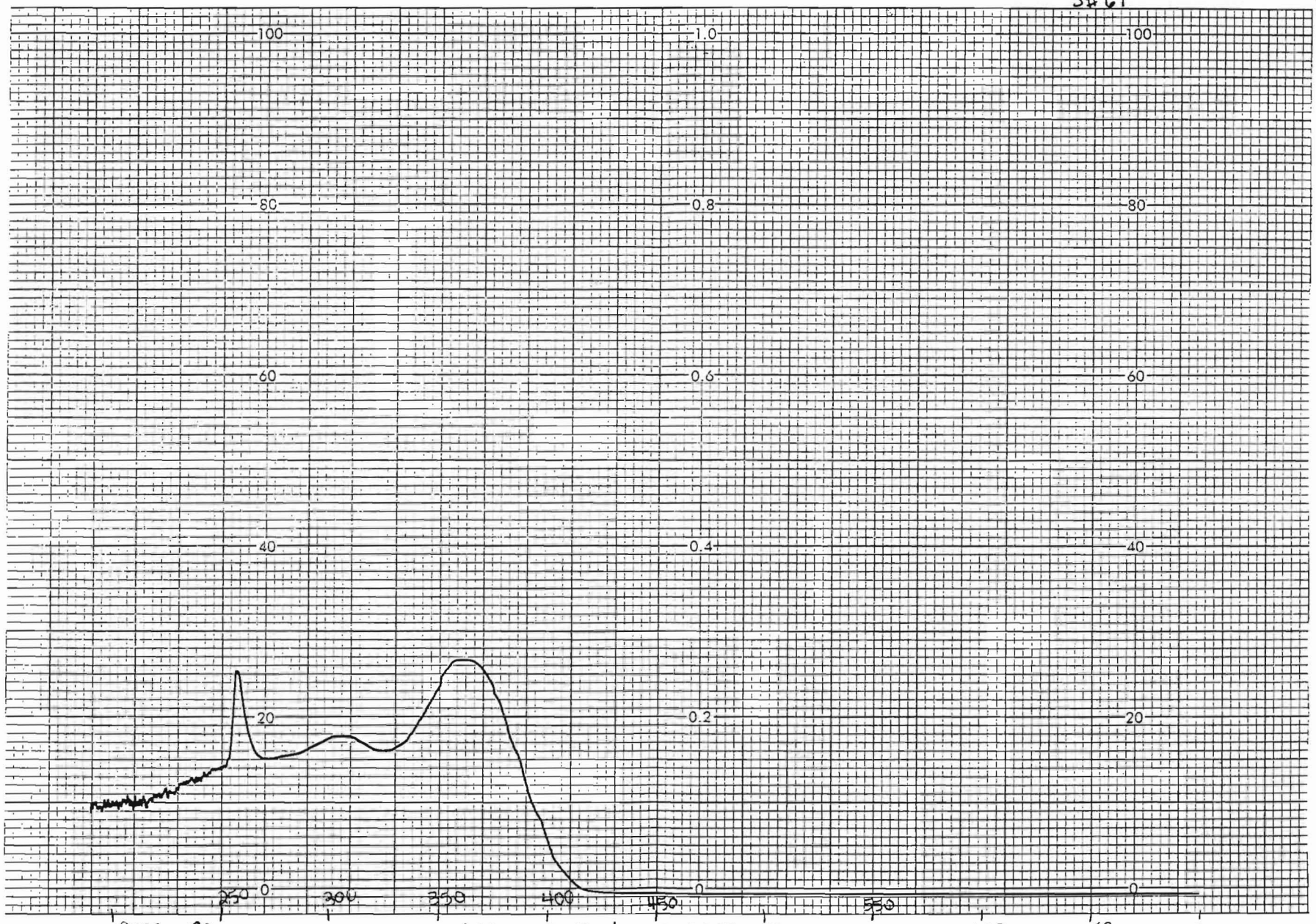

200-700 - 190 nm
60 nm/min
20 nm/cm
slit = 1.0 nm

0 - 3 Aunits

1.880 g $NaNO_2$ / 100 mL DMSO 3-17-93
2nd Photolysis 60 min
1:10 dilution

A62

RATION BUFFALO NEW YORK

S#70

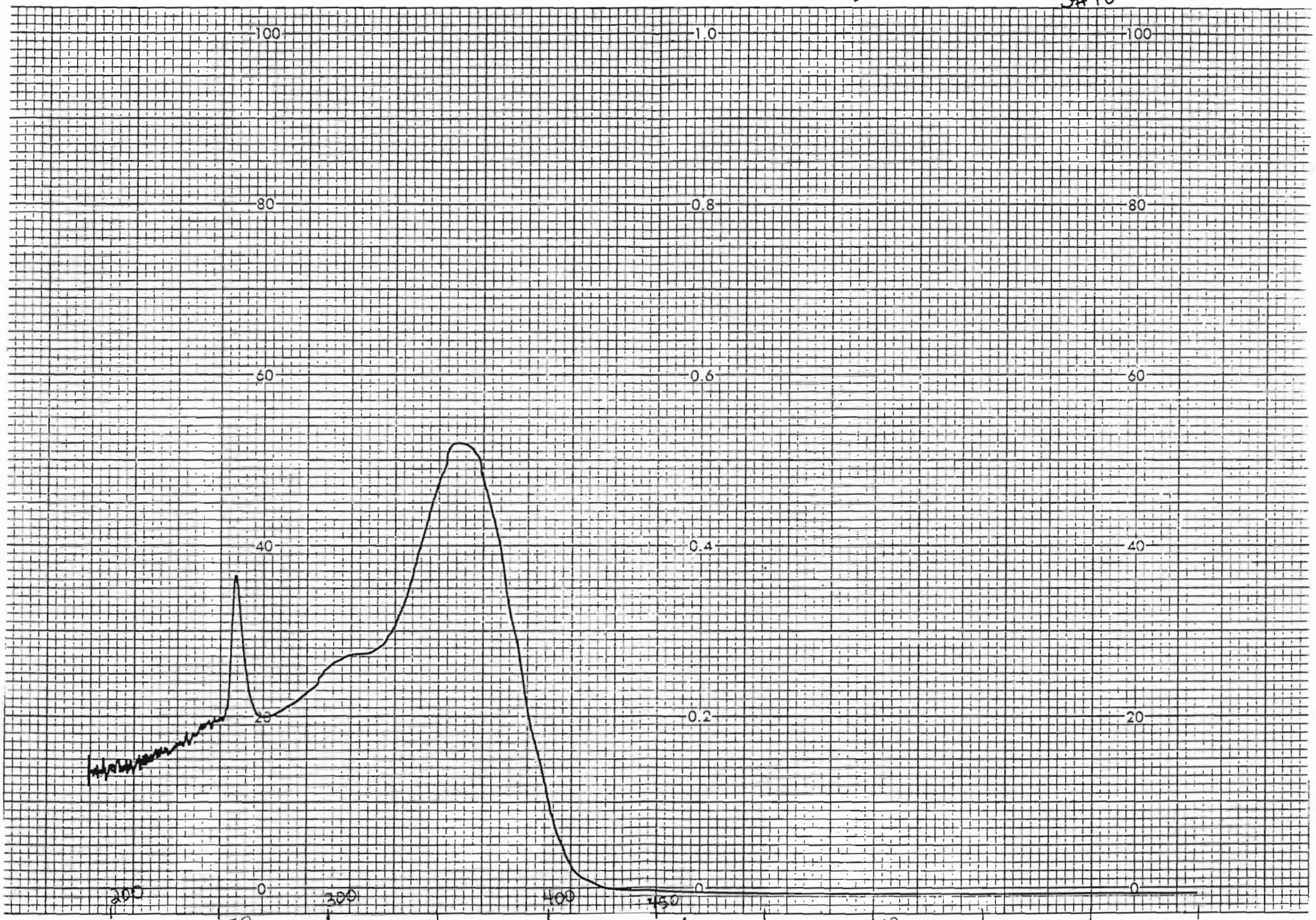
100
80
60
40
20
0
1.0
0.8
0.6
0.4
0.2
0
200
250
300
350
400
450
500
550
600
650
700
700 - 190 nm
60 nm/min
20 nm/cm
Slit = 1.0 nm
0 - 3 Aunits
3.510 g NaNO2 / DMSO
2nd Photolysis 60 min
1:10 dilution
3-17-93

A63

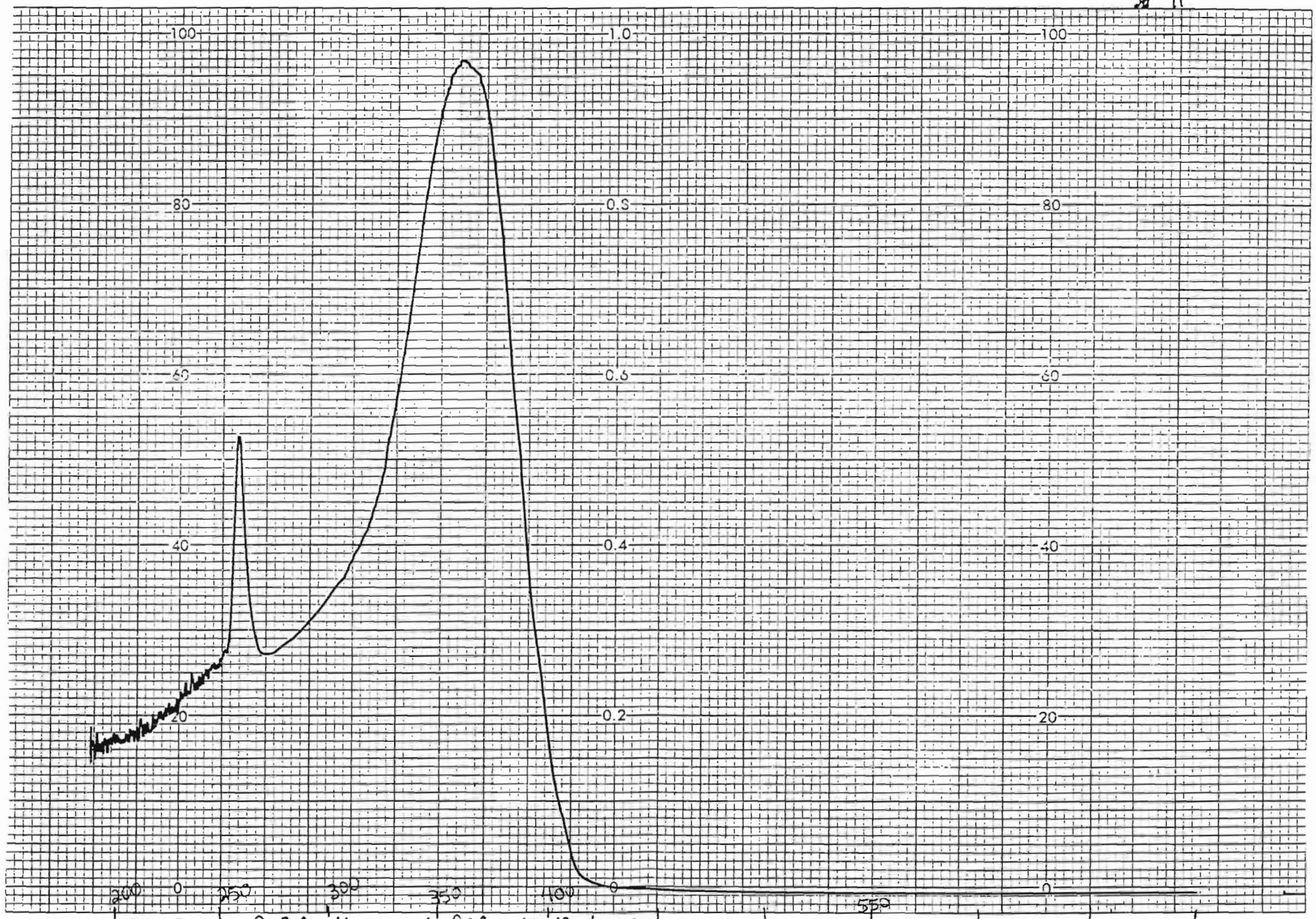
100
80
60
40
20
0
1.0
0.8
0.6
0.4
0.2
0
200
250
300
350
400
450
500
550
600
650
700
700-190nm
60nm/min
20nm/cm
slit = 1.0nm
0-3 Aunits
6.919 g NaNO2/DMSO
2nd Photolysis 60min
1:10 dilution
3-17-93

S#41

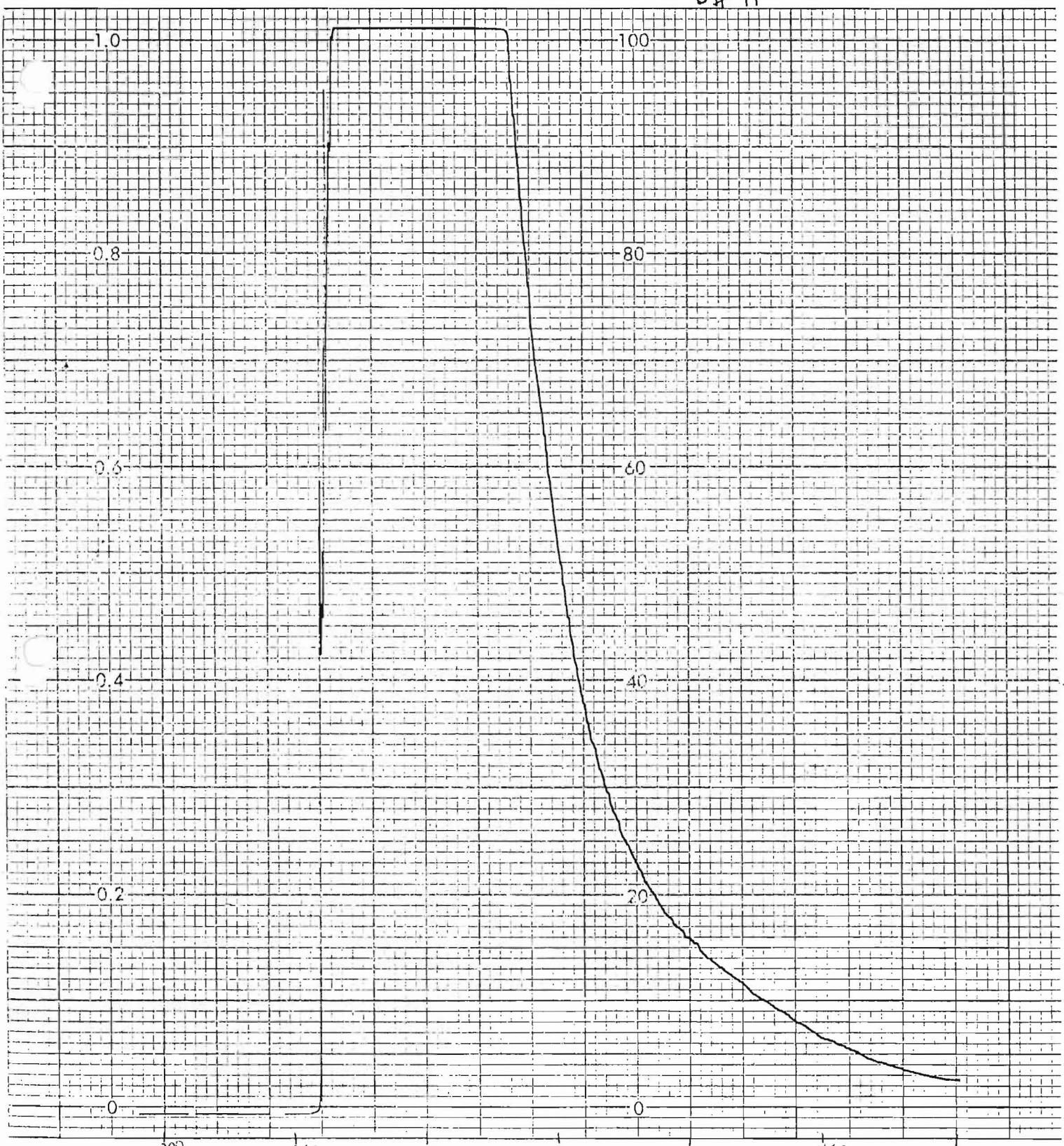

500 - 190 nm
60 nm/min
20 cm/min
slit = 1.0 nm

0 - 1 Aunit

11 - 24 - 92

thermolyzed DMSO
vs. non - thermolyzed
DMSO

S#42

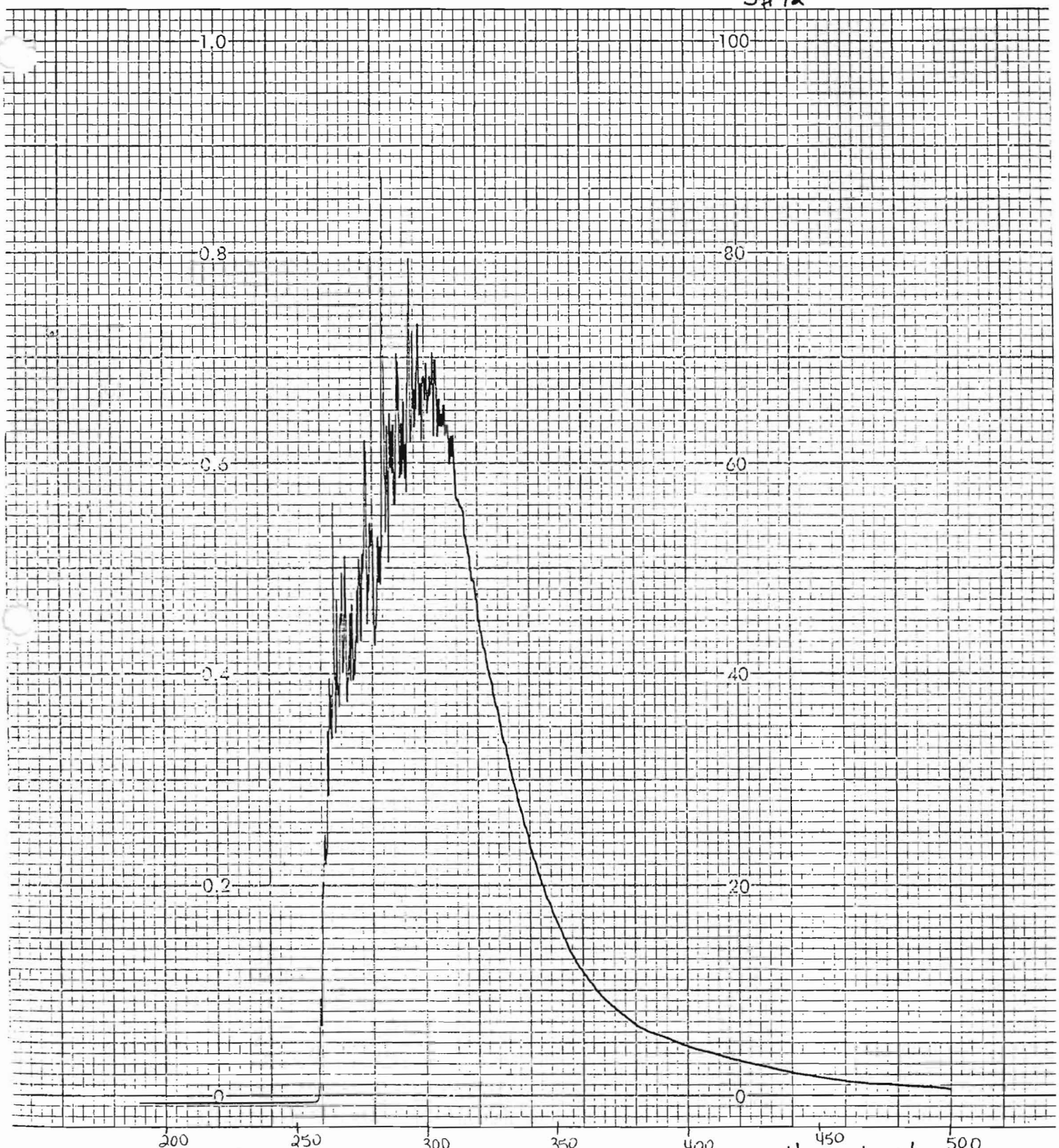

500 - 190 nm
60 nm/min
20 cm/min
Slit = 1.0 nm

0 - 3 Aunit

11 - 24 - 92

thermolyzed DMSO

S#43

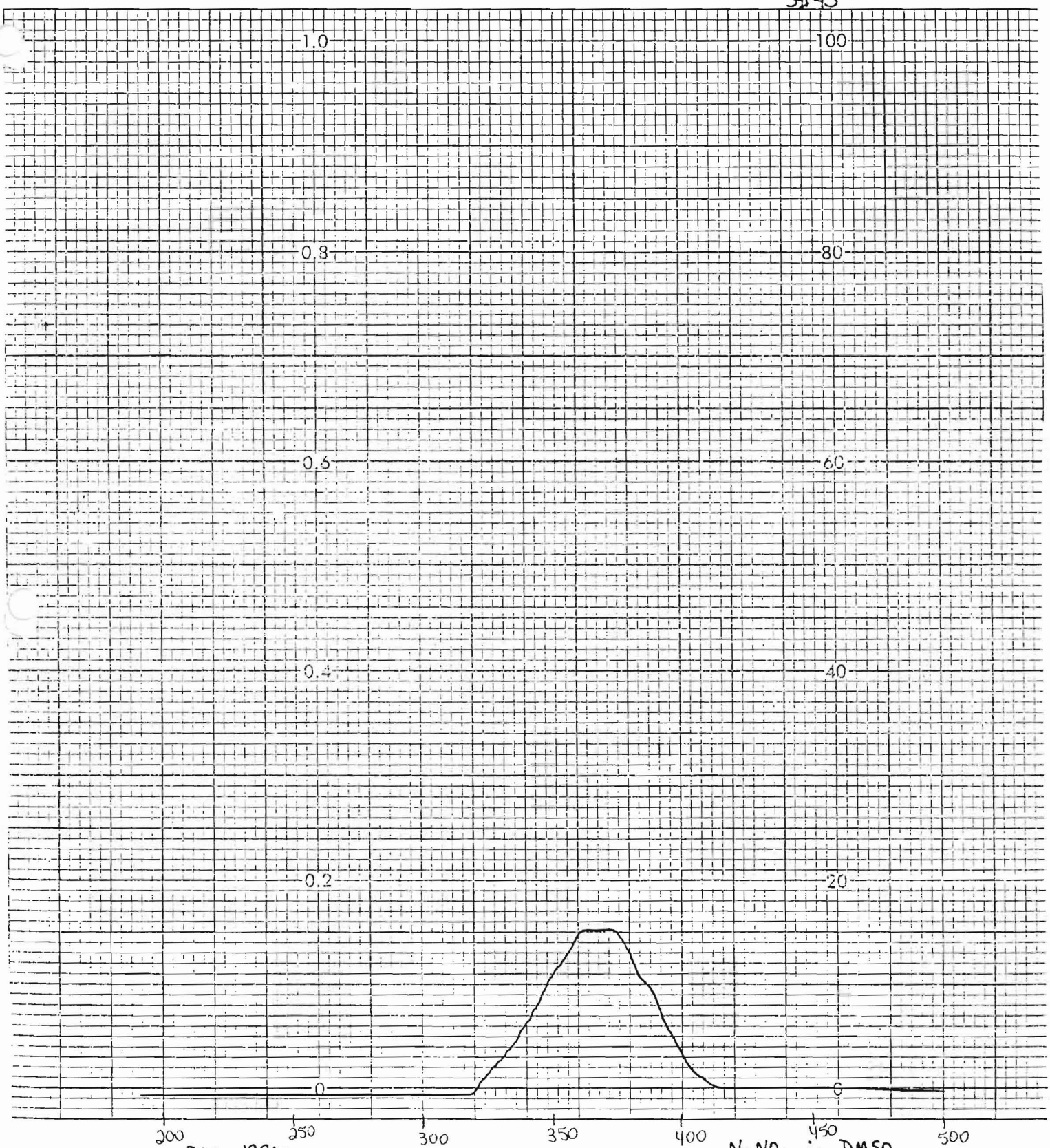

500 - 190 nm
60 nm/min
20 cm/min
slit = 1.0 nm

0-3 Aunit

11-24-92

$NaNO_2$ in DMSO
thermolyzed

S#44

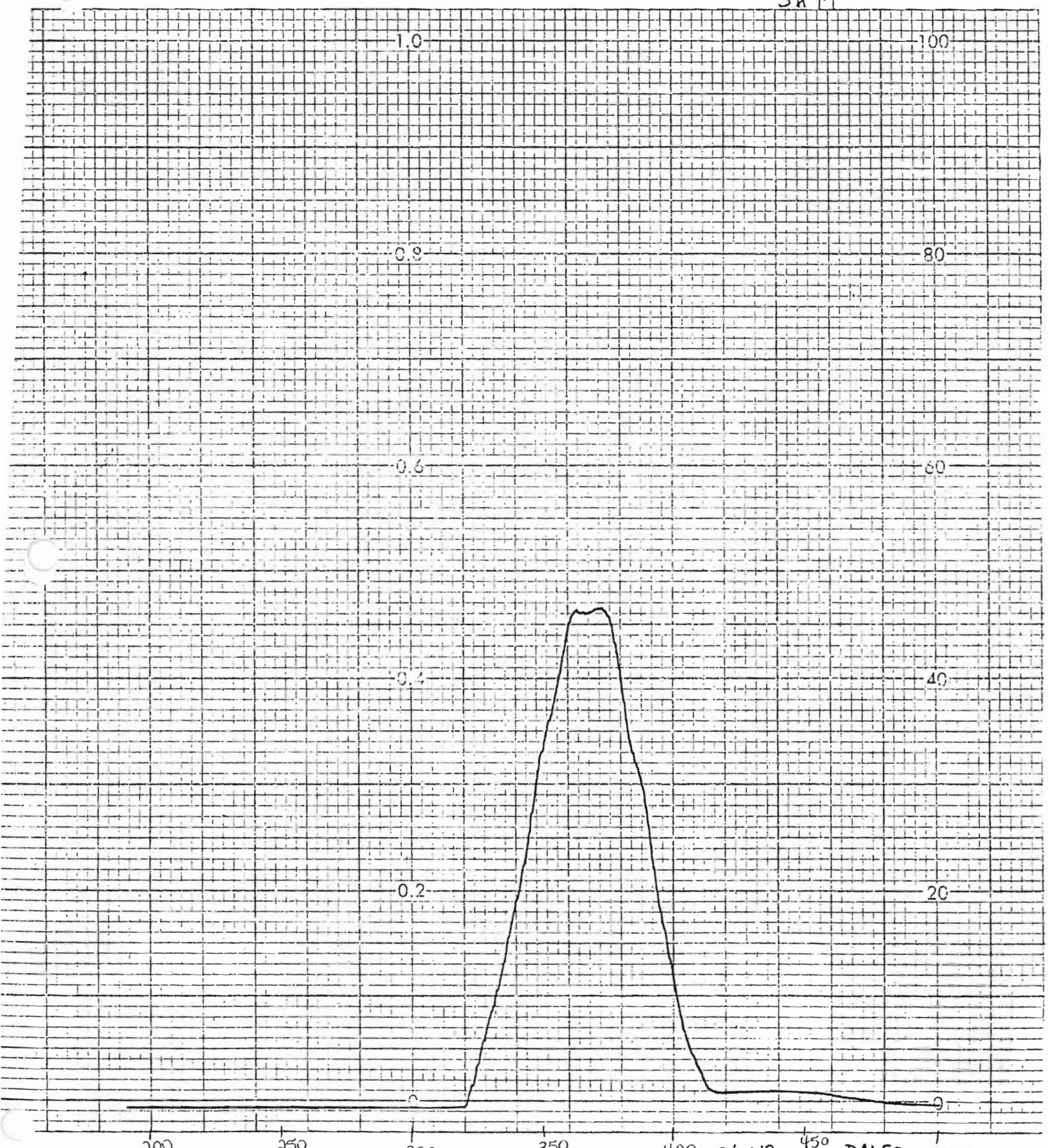

$NaNO_2$ in DMSO
thermolyzed

500 - 190 nm
60 nm/min
20 cm/min
slit = 1.0nm

0 - 1 Aunit

11-24-92

S#45

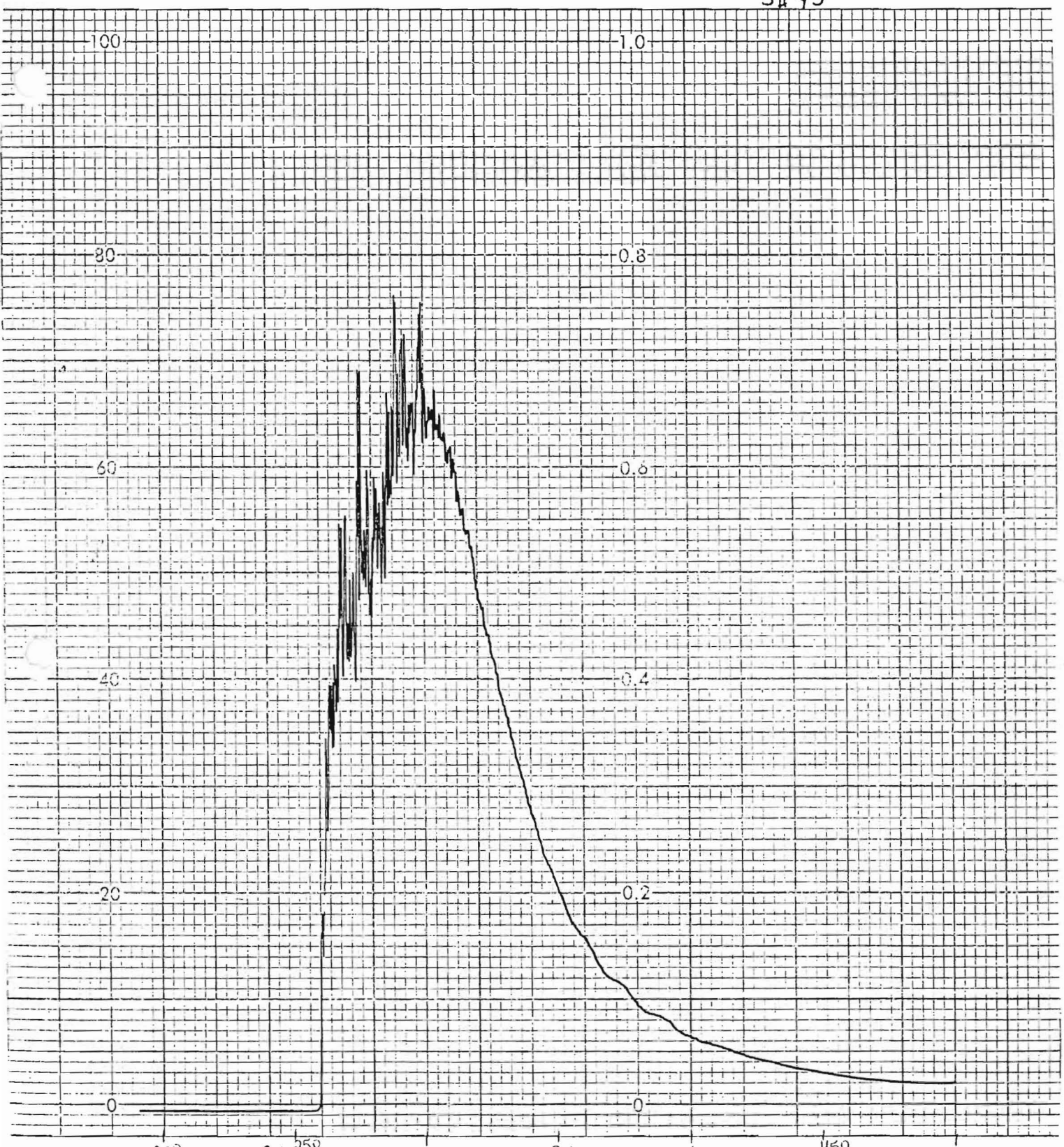

500 - 190 nm
60 nm/min
30 cm/min
slit = 1.0 nm

0 - 3 Aunit 11-24-92

thermolyzed
DMSO
bubbled with
N_2

S#46

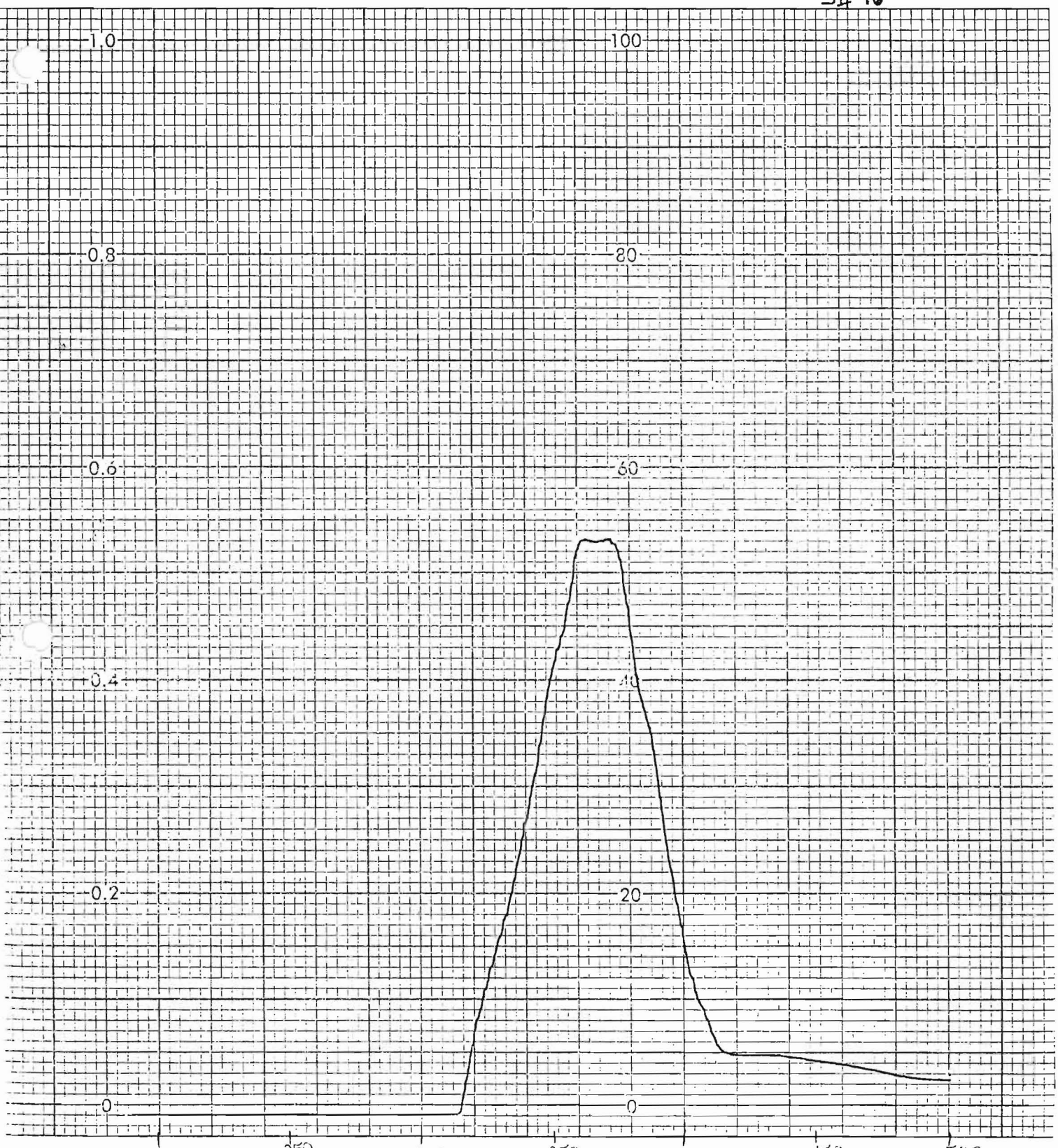

500 - 190 nm
60 nm/min
20 cm/min
Slit = 1.0 nm

0 - 1 Aunit

11-24-92

$NaNO_2$ in DMSO thermolyzed bubbled with N_2

S#79

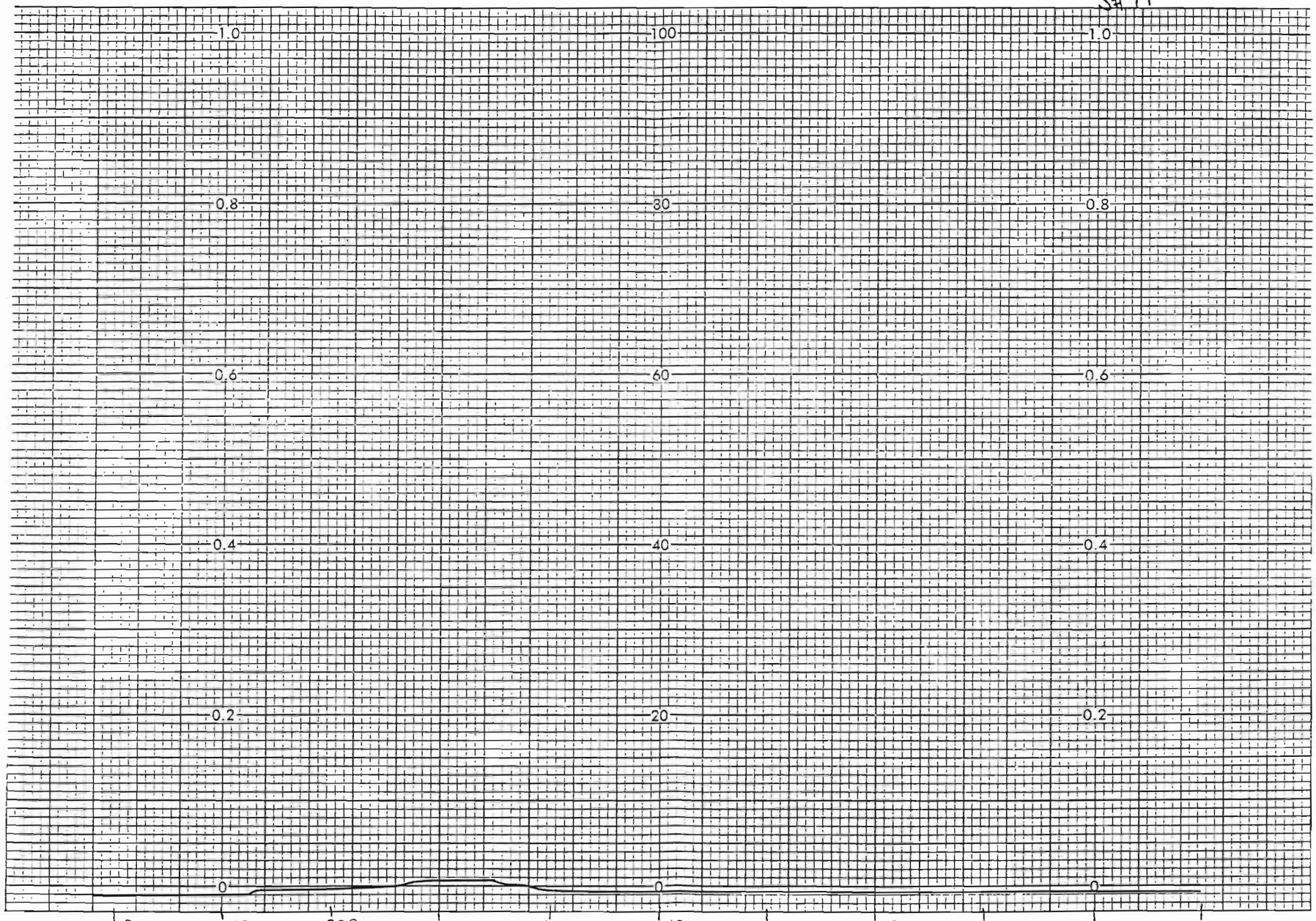
1.0
0.8
0.6
0.4
0.2
0
100
80
60
40
20
0
1.0
0.8
0.6
0.4
0.2
0
200
250
300
350
400
450
500
550
600
650
700
700 - 190nm
60 nm/min
20 nm/cm
slit = 1.0nm
0-3 Aunits
thermolyzed DMSO in N2
vs. DMSO
60 min at 60°C
4-7-93

A71

S#80

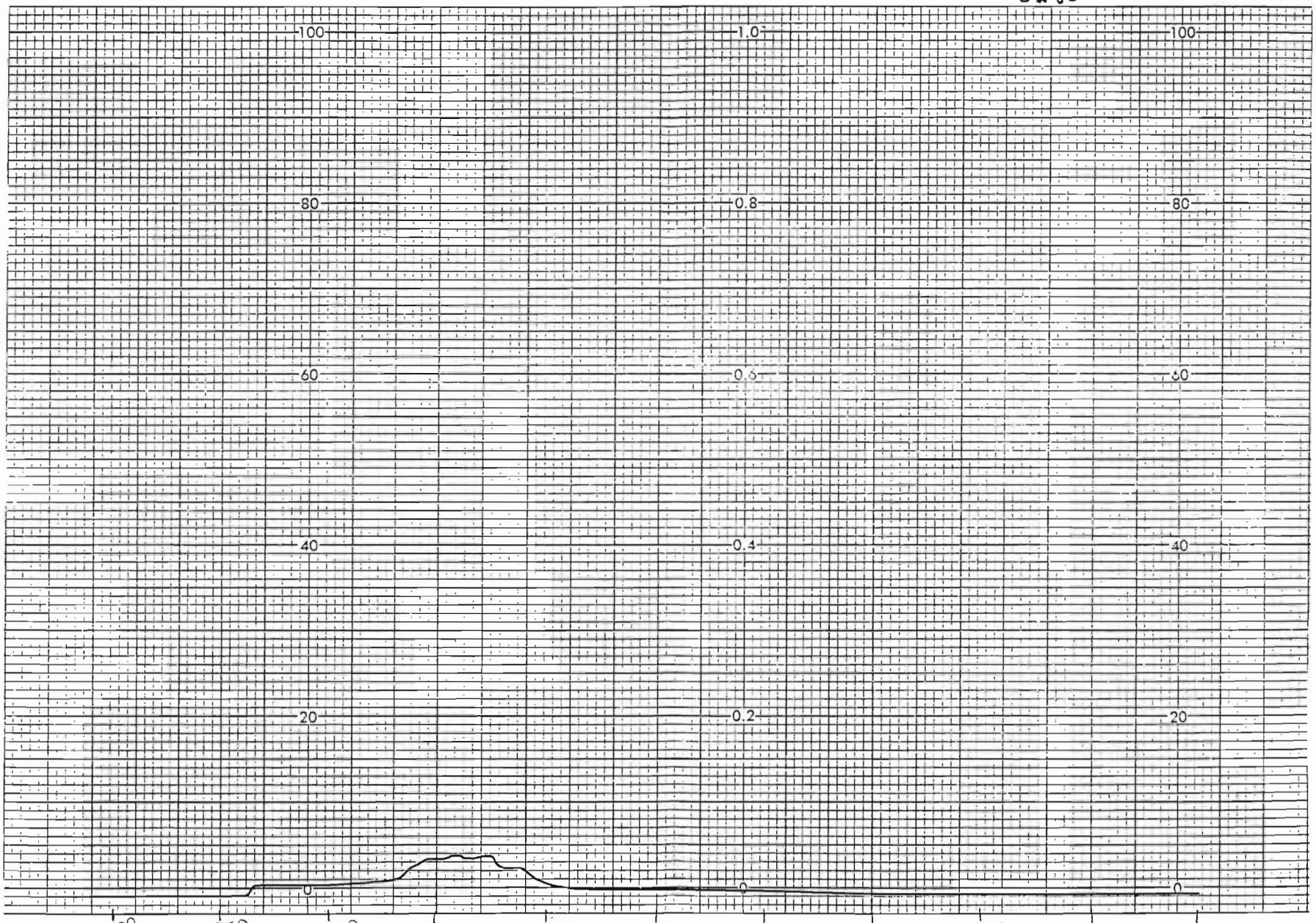

700-190nm
60 nm/min
20nm/cm
Slit=1.0nm

0-1 Aunit

thermolyzed DMSO in N_2 vs. DMSO

4-7-93

60min at 60°C

A72

S#81

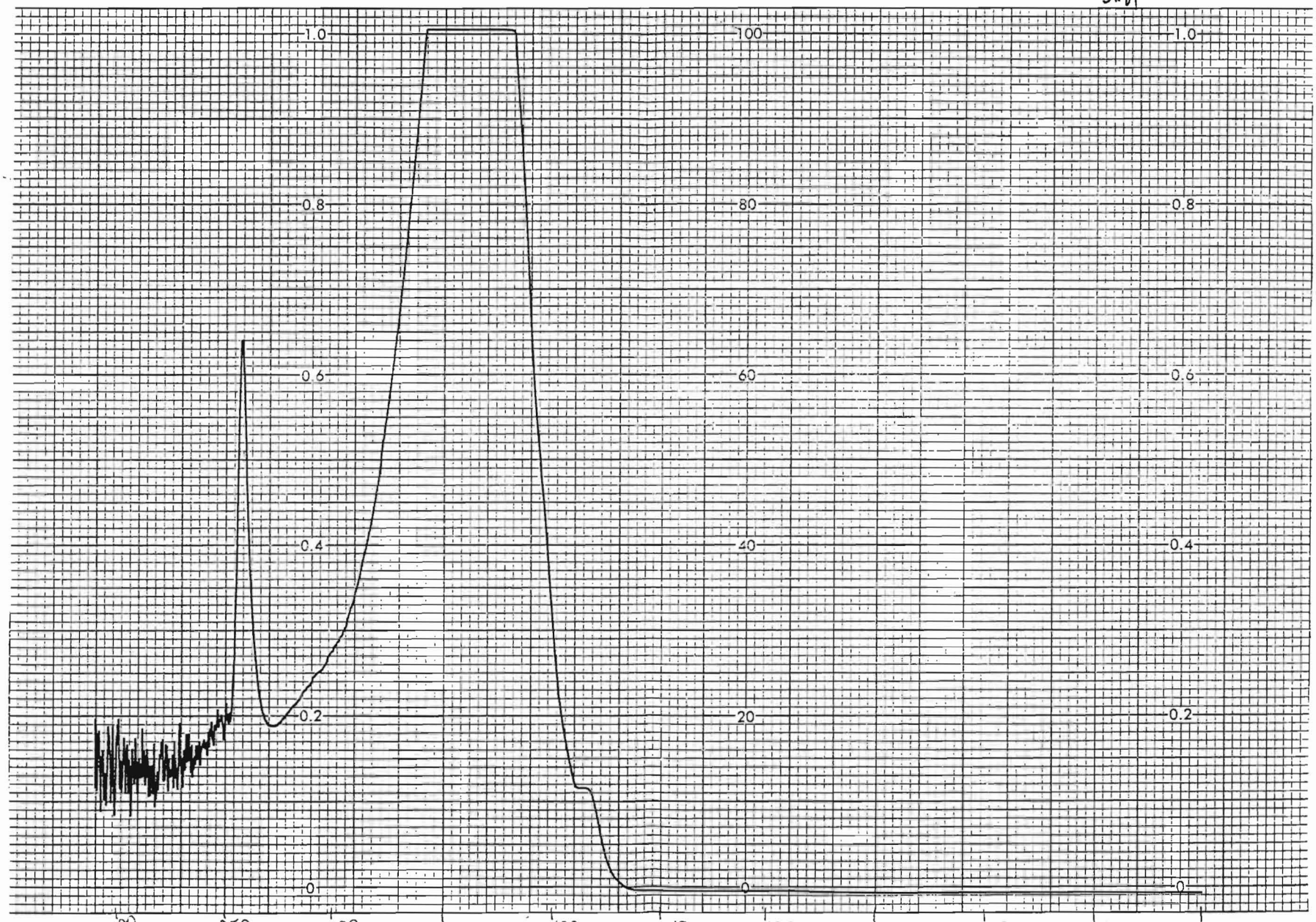
1.0
0.8
0.6
0.4
0.2
0
100
80
60
40
20
0
200
250
300
350
400
450
500
550
600
650
700
700 - 190nm
60 nm/min
20 nm/cm
slit = 1.0nm
0 - 1 Acunit
in N_2
$NaNO_2$ in DMSO
thermolyzed
60 min at 60°C
vs. DMSO
4-7-93

A73

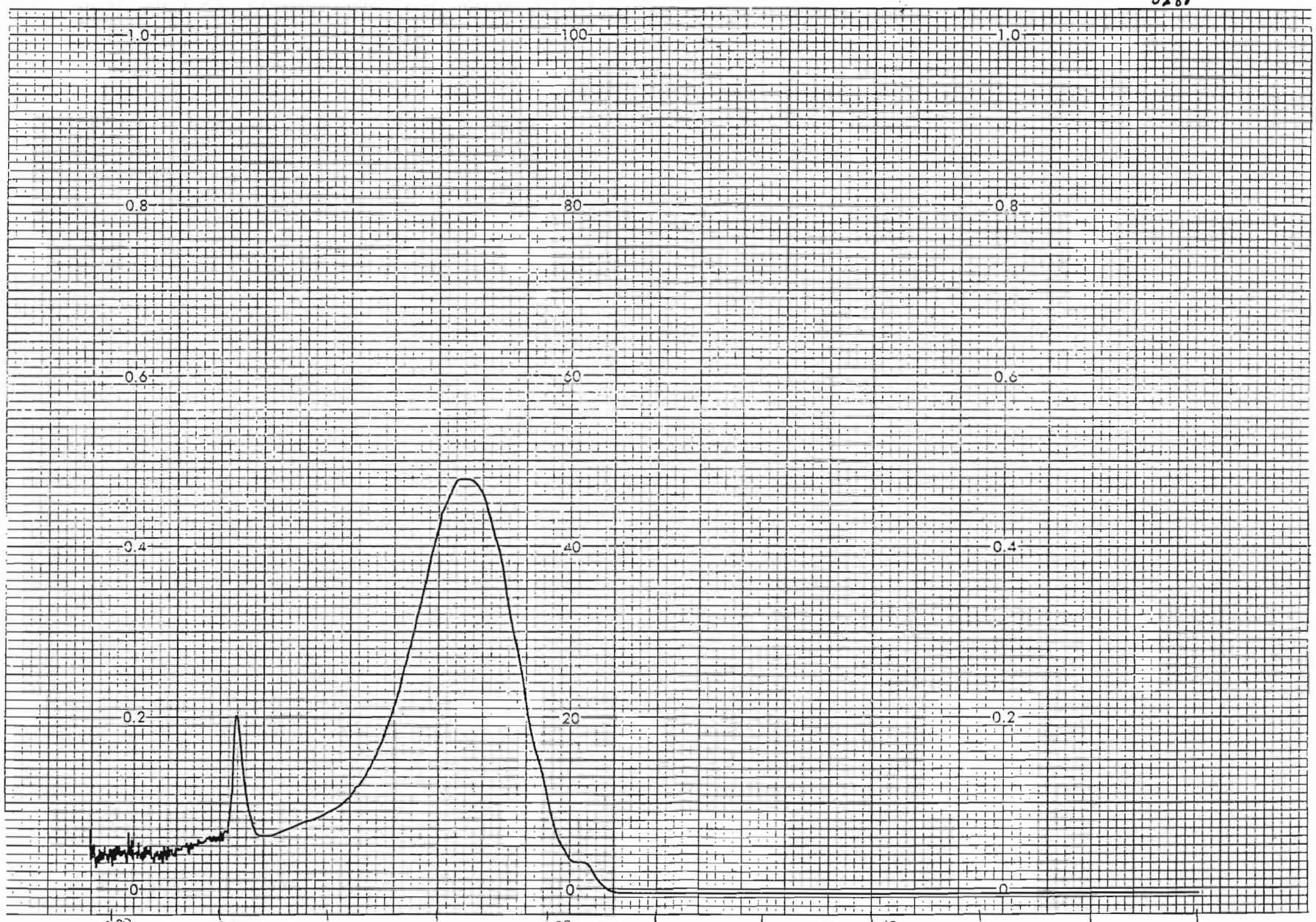

S#83

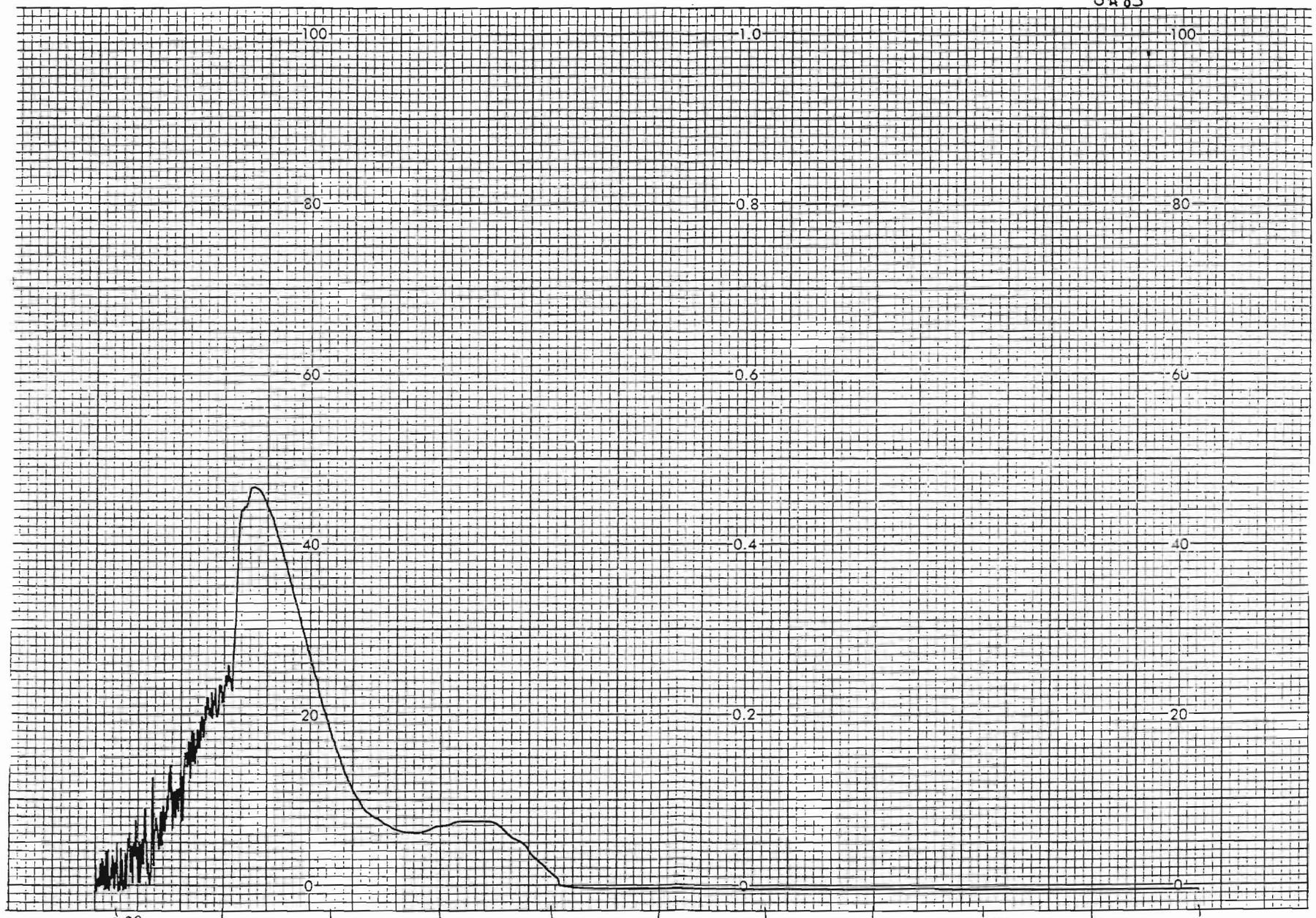

700- 190nm
60 nm/min
20 nm/cm
slit = 1.0nm

0 - 1 A unit

DMSO in O_2 vs. DMSO
thermolyzed
60 min at 60°C

4-7-93

A75

PART NO. RR 003826

S#84

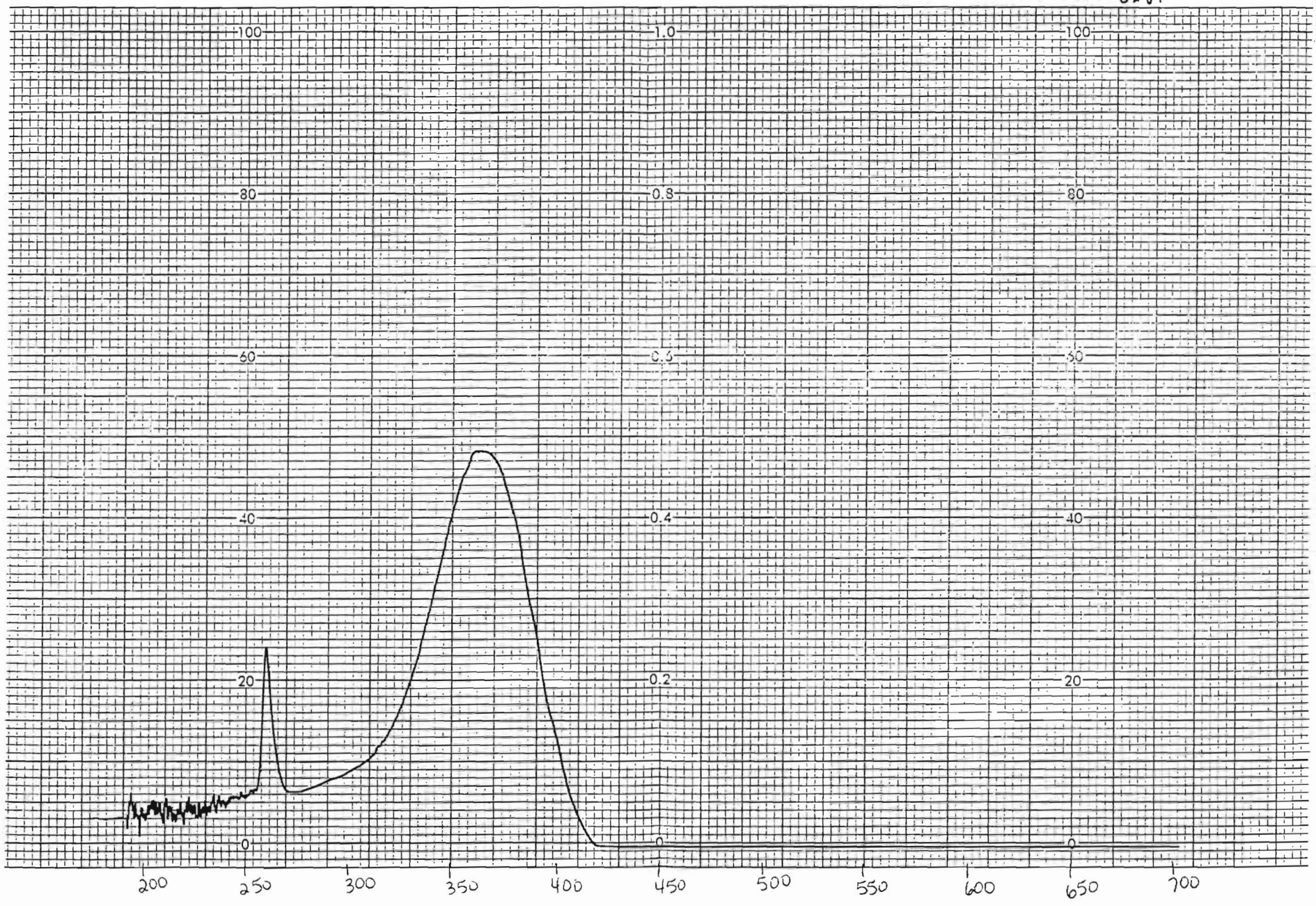

1:10 dilution

$NaNO_2$ in DMSO thermolyzed vs. DMSO

0-3 Aunit

700-190nm
60nm/min
20nm/cm

slit = 1.0nm

A76